DESIGN, IMPLEMENTATION AND EVALUATION OF A PASSIVE THRUST AUGMENTATION DEVICE FOR THE SR-30 TURBOJET

research paper
(Studienarbeit)
by
cand. aer. Donald Riedeberger

conducted at
Institute of Aircraft Propulsion Systems (ILA),
Stuttgart University, Stuttgart, Germany
and
Department of Aerospace Engineering,
The Ohio State University, Columbus, OH, USA

Columbus, June 2010

Research paper
for
Mr. cand. aer. Donald Riedeberger

Design, implementation and evaluation of a passive thrust augmentation device for the SR-30 turbojet

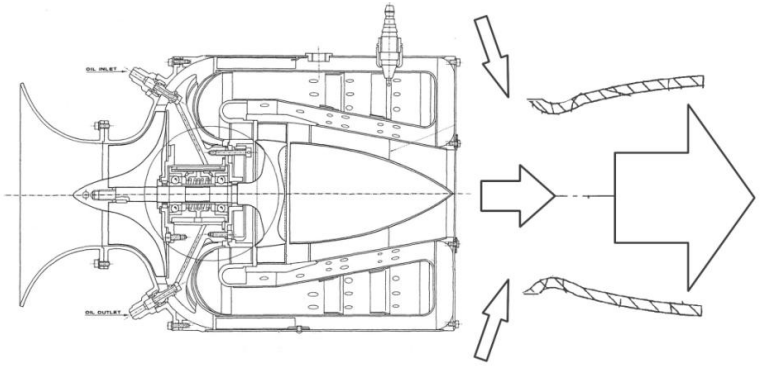

Thrust augmentation of jet engines have been in use for some time. Besides afterburners, a method of increasing the thrust is through devices that mix ambient air into the exhaust gas stream. The mixing decreases the temperature of the main jet exhaust, but increases the temperature of the entrained air from which an overall increase of thrust results.
Issues in passive thrust augmenters that have to be evaluated closely are the mixing paths, heat exchange and the overall geometry of the device that the exhaust jet flows through.

The department of Aerospace Engineering at The Ohio State University, Columbus Ohio is in possession of a SR-30 Turbo Jet engine as part of a Mini Lab made by Turbine Technologies LTD. The jet engine is completely instrumented with pressure and temperature sensors, at key positions throughout the engines, as well as with a thrust measuring device. Its operation is completely automated with push button start and stop functions. In addition a PC operated data acquisition systems allows for recording all important engine functions. The objectives are:

1) To fully chatacterise the engine performance before any changes are made.

2) To design, construct and test a passive thrust augmenter that will be added to the engine.

To meet the research objectives, a Matlab based post-processing script will be developed to evaluate engine performance.

The work on the thesis includes the following points:

- Familiarization with the SR-30 Mini Lab and passive thrust augmentation devices (engine operation, literature search)
- Writing a Matlab script to evaluate the acquired data and plot engine performance
- Design of the thrust augmentation device
- Implementation of the thrust augmenter into the engine cycle
- Evaluation of the performance data for the augmented and un-augmented cases
- Documentation of results

Mentoring (OSU): Associate Professor Dr Joseph H. Haritonidis
Mentoring (Stuttgart University): Dipl.-Ing. Alexander Klötzer

Statement of Originality

This research paper has been performed independently with support by my supervisor. It contains no material that has been accepted for the award of a degree at The Ohio State University, Stuttgart University or any other university. To the best of the candidate's knowledge and belief, this paper contains no material previously published or written by another person except where due reference is made in the text.

Erklärung

Hiermit versichere ich, dass ich diese Studienarbeit selbstständig mit Unterstützung des Betreuers angefertigt und keine anderen als die angegebenen Quellen und Hilfsmittel verwendet habe. Die Arbeit oder wesentliche Bestandteile davon sind weder an der Ohio State University, noch an der Universität Stuttgart, noch an einer anderen Bildungseinrichtung bereits zur Erlangung eines Abschlusses eingereicht worden.

place, date, signature

Abstract

The SR-30 turbojet engine has been equipped with a passive thrust augmenting device consisting of an inlet bell mouth and constant area mixing chamber. A secondary to primary flow ratio close to unity - $\alpha = 1.318$ - was investigated and length to diameter ratios of $L/D = 7$, 3.5 and 1.75 have been picked to evaluate the performance behavior for different ejector lengths. Due to practical application the mixing chamber entrance was offset by 5 in from the exhaust nozzle of the primary jet of the SR-30 engine. The thrust augmentation was determined experimentally for the different lengths of mixing chamber and compared with theoretical predictions of 1D flow analysis of a non-displaced ejector. The results were deviating from optimum performance predictions due to the displacement from the nozzle exit resulting in higher drag on the ejector inside walls and reduced pressure on the engine back face. For the given case the augmenter with a ratio of $L/D = 3.5$ resulted in recognizable augmentation of thrust up to about 4 % in the displaced arrangement.

Acknowledgments

The academic year spent by the author at The Ohio State University was financially possible due to the obtained scholarships from the German-American Fulbright Commission and the Hermann-Reissner-Stiftung e.V.. Furthermore the solid support of the Department of Aerospace Engineering at OSU as well as the Institute of Aircraft Propulsion Systems (ILA) at Stuttgart University built the basic opportunity to pursue this research objective.

Contents

List of Figures

List of Tables

Nomenclature

Latin Letters

A	Area of a cross section	m^2
a	Sonic velocity of a fluid	$\frac{\mathrm{m}}{\mathrm{s}}$
C_f	Friction coefficient, used in definition of ζ	-
c_p	Specific heat capacity for constant pressure of a fluid	$\frac{\mathrm{J}}{\mathrm{kgK}}$
D	Mixing chamber diameter of the ejector	m
d	Diameter of the primary flow nozzle	m
F	Force of a fluid or part exerted on another surface or point	N
f	Fuel to air ratio, $f = \frac{\dot{m}_{\mathrm{fuel}}}{\dot{m}_{\mathrm{air}}}$	-
$f(L/D)$	Friction loss factor used in figure 13	-
h	Specific enthalpy of a fluid	$\frac{\mathrm{J}}{\mathrm{kg}}$
H_i	Lower heating value of the fuel	$\frac{\mathrm{J}}{\mathrm{kg}}$
$\frac{L}{D}$	Mixing chamber length to diameter ratio	-
L	Mixing chamber length of the ejector	m
$\dot{m}$	Mass flow of a fluid	$\frac{\mathrm{kg}}{\mathrm{s}}$
M	Mach number of a flowing fluid	-
n	Spool speed	$\frac{1}{\mathrm{min}}$
p	Pressure of a fluid	Pa
r	Secondary inlet half circle radius used in appendix F.3	m
R_{s}	Specific gas constant of dry air, $R_{\mathrm{s}} = 287$	$\frac{\mathrm{J}}{\mathrm{kgK}}$
T	Temperature of a fluid	K
u	Velocity of a fluid	$\frac{\mathrm{m}}{\mathrm{s}}$
$\dot{V}$	Volume flow of a fluid	$\frac{\mathrm{m}^3}{\mathrm{s}}$
w	Work delivered by a process	J

Greek Letters

α	Ejector area ratio, $\frac{A_\mathrm{s}}{A_\mathrm{p}}$	-
β	Non-uniformity parameter of the velocity profile used in equation 12	-
Δ	Difference operator	-
η	Efficiency either of a component or process	-
γ	Specific heat ratio of a fluid, $\gamma = \frac{c_p}{c_v}$	-
λ_E	Entrance loss factor used in figure 13	-
Φ	Free thrust augmentation ratio of an applied ejector, $\Phi = \frac{F_\mathrm{ejector}}{F_\mathrm{nozzle,amb}}$	-
Π	Pressure ratio	-
ρ	Density of a fluid	$\frac{\mathrm{kg}}{\mathrm{m}^3}$
τ	Shear stress	Pa
ζ	Coefficient used in equation 12	-

Subscripts

0	Ambient condition
1...9	International standard notation for engine stages (exception in chapter 1.4 where 1 entrance, 2 exit of the ejector)
air	Relation to air properties
calc	Calculated value
comb. ch	Relation to the combustion chamber
comp	Relation to the compressor
dynamic	Dynamic condition of a fluid property
fuel	Relation to fuel properties
measure	Measured value
μ	Relation to shear stresses used in chapter 1.4
net	Relation to the net value (as opposed to gross value)
nozzle	Relation to the nozzle

p	Value related to the primary flow entering the ejector
R	Relation to restraining force used in chapter 1.4
is	Isentropic process
SP	Relation to static pressure force used in chapter 1.4
static	Static condition of a fluid property
s	Value related to the secondary flow entering the ejector
th	Relation to the thermodynamic value
turb	Relation to the turbine
t	Total condition of a fluid property

Abbreviations

CFD	Computational Fluid Dynamics
HP	Horse Power
MED	Mixer-Ejector-Diffuser
OSU	The Ohio State University
RPM	Rounds Per Minute, min^{-1}
SCFM	Standard Cubic Feet per Minute
TSFC	Thrust Specific Fuel Consumption
USB	Universal Serial Bus
V/STOL	Vertical/ Short Take-Off and Landing

1. Introduction

Being able to equip an existing propulsion device with the capabilities to deliver a higher thrust without the cost and weight intensive scaling of the engine itself has been of interest to engineers since the first take off. As opposed to afterburners that burn additional fuel downstream the turbine and thus increase the net thrust, also a passive way (i.e. without additional fuel) to augment the thrust of a turbojet engine exists. This way of augmentation is most commonly done by applying jet ejectors. Rather than using the high temperatures and remaining oxygen in the exhaust to facilitate a second combustion process those ejectors use the exhaust's kinematic energy - and thus high dynamic pressure - to entrain additional air, increase mass flow, facilitate a mixing process - and thus a pressure rise downstream - and create low pressure around the inlet contour of the entrained air resulting in a net forward force.

In the application of a jet ejector after the exhaust of an air breathing propulsion device of an airplane three resulting benefits are visible that relate to the main effect of such an ejector: delivering a lower speed, higher mass flow exhaust at the exit from a high speed jet at the inlet. Those beneficial results are:

- augmenting the thrust at low forward speeds [16] [13],
- suppress the noise of the exhaust jet [20] and
- reduce the average exhaust temperature (and thus infra red signature) [51].

While the augmentation objective and reduction in thermal radiation was dominated by the application to vertical/short take-off and landing vehicles (V/STOL) [5] [42] in the second half of the 20th century the recent development in air traffic and related regulations switched the interest more to the noise suppression of passenger aircrafts including the advantage of the thrust gain in some conditions of the flight path as well [24].

The rather low complexity of jet ejector devices - compared for example with forced flow control via actuators or synthetic jets - verifies the significance of this topic and their application in the reduction of jet noise and therefore for further studies in this field as a complement to other approaches. In addition to the outlined research applicability the simplicity of jet ejectors also shapes passive thrust augmentation to be a desirable topic to the educational field of fluid dynamics and propulsion in aerospace engineering. The effects of normal (pressures) and shear stresses (friction) in a flow field and the resulting forces out of the momentum equation can be studied on such an ejector in a manageable intricacy and nevertheless with practical impact.

1.1. Motivation

The department of Aerospace Engineering at The Ohio State University (OSU) is in possession of a SR-30 Jet Engine as part of the Minilab (figure 1) by Turbine Tech-

nologies™integrated into their educational framework in undergraduate studies. This

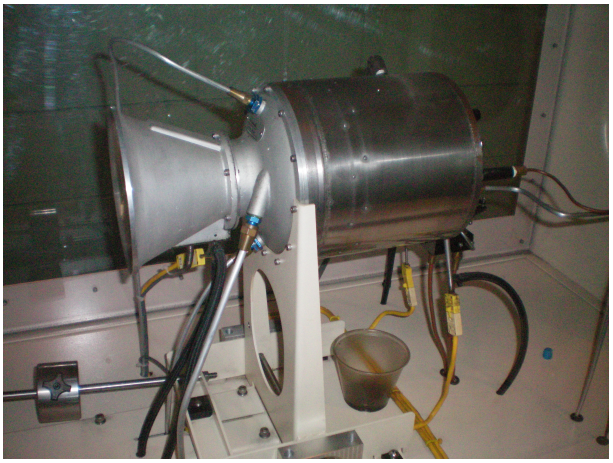

Figure 1: The SR-30 equipped in the MiniLab at the OSU department

laboratory is self contained with an automatic push-button start and a data acquisition process to capture the temperature and pressure probe data at key locations within the engine. Initially, this engine laboratory has been unused since it has been purchased. To make valuable use in undergraduate education at the department the SR-30 had to be brought into service and its performance had to be evaluated. An integration into laboratory experiments conducted by senior students was intended and a suitable experimental outline together with a performance analysis had to be created.

To make further investigations on the performance of the engine setup the implementation of a passive thrust augmenting device was seen to be a favorable addition to the analysis and also to the undergraduate education. As will be outlined in the literature review the current status of the research in passive thrust augmentation delivered several approaches for an augmenting device ranging from rather low complex forms [16] up to state-of-the-art, short mixer-ejector-diffuser (MED) systems [21].

As the present work focuses on applications to the SR-30 gas turbine as part of an educational jet engine laboratory both the evaluation of the basic engine performance as well as the thrust augmenting procedure are in context of an educational use. Therefore an intrinsic theme within this thesis will be to aim for educational use of both the jet engine setup, its performance evaluation and the implementation of the thrust augmenter.

Therefore the motivation is to apply a rather low-complexity device for thrust augmentation of the SR-30 jet engine that enables to focus on the understanding of the flow patterns, mixing process involved and the resulting thrust gain of a jet ejector. This will be complemented by collection of data sets and the post-processing to comment on the overall effect of the thrust augmenter and the engine performance itself.

1.2. Literature review

The literature search captured two different fields of interest. First of all, the available publications on the use of the SR-30 were evaluated to gain an understanding about the performance envelope of this jet engine and what values can be expected. Secondly, the vast publications on passive thrust augmentation were investigated. Out of those reports the fundamental knowledge for preliminary performance prediction, design and process analysis on an applicable thrust augmenter for a small turbojet engine was gained.

In addition to this conventional literature research, valuable information was also gained due to simultaneously ongoing studies (partially conducted by the author in team work) at the department of Aerospace Engineering at OSU. Necessary conclusions and results from this work are also given within this chapter to complement the overall information taken into account here.

While a summary is given in the following paragraphs on the literature search, an extensive chronological and commented list of the reviewed articles and reports can be found in Annex F. The interested reader is referred to use this as a starting point for any further literature research related to the topics discussed.

1.2.1. SR-30 MiniLab

The MiniLab by Turbine Technologies™has been in use world-wide, mostly in U.S. American colleges for about ten years prior to this study resulting in related reports from about a dozen universities. Different work has been conducted using the SR-30 ranging from pure educational use [34], over adaptations to the measurement capabilities [6] [29] up to exhaust gas analysis and biofuel utilization [9]. Valuable information for first run preparations, technical draw backs of the sensor equipment and especially the expected performance [32] [15] [43] [34] can be drawn from some of those reports .

The findings of a detailed review of related reports in Appendix F can be summed up as the following:

- There are valuable *comparative data sets* (tables 8 - 11) from educational uses of the SR-30 MiniLab available [32] [15] [43] [34]. These data sets - although sometimes negligent in stating all necessary operating conditions of the acquired data - offer the possibility to compare achieved results within this work.

- There are at least two *different versions of the SR-30 engine* itself - one early version equipped with few sensors (e.g. a higly constraint thrust measurement) [6] and another one with fully equipped measurements [15] [43] [15] [14]. The later one is used at OSU. Therefore a comparison of the given measurement data, although all related to the same jet engine type has to be undertaken with this knowledge in mind.

- The *single point* instrumentation of the respective cross sections puts severe constraints on obtaining accurate results in performance analysis. This is similar to

the fact of assumed one-dimensional flow with fully developed and constant velocity distribution.

- The exact lateral position of the *adjustable probes*, especially for the temperature at the compressor exit, is crucial and can deliver compromising results [43].
- Although some reports use different classification (static or stagnation) [32] of the probe values in contrast to the manufacturer [47] the measured values capture the *stagnation properties* for most of the cross sections except for the inlet dynamic pressure (also see table 1).
- The unshielded temperature probe at the exit and the pitot-static probe at the inlet can deliver *inaccurate measurements* and yield results in conflict with real values [15].
- There is a *time dependency* in the development of steady state behavior concerning the temperature measurements that vanishes after approximately 10 minutes of initial run-time [43].

Summarizing the research on the operation of the SR-30 engine consistent data (within most points) was found to provide a basis and reference point for the setup and run of the SR-30 in the laboratory at OSU. Also emphasis has been put on equipment of probes and measurement capabilities in a second version of the SR-30 Mini Lab after a first product launch by the manufacturer. This circumstance should prepare one to expect results within the precision of a 1D analysis of the engine process and create awareness of an expected error range.

1.2.2. Passive thrust augmentation

Any research on passive thrust augmentation is primarily focusing on the utilization of the ejector principle applied to a fluid jet. The majority of the literature on such devices is in the second half of the 20th century and continues up to the present. Chronologically one can see a development in addressing more and more complex flow phenomena and loss influences included into undertaken analyses and experiments. Theoretical analyses started from a simplified 1D flow [49] that built the base of understanding. These were complemented by in depth analysis of various parameters governing the ejector process [1] [2] and continued up to investigations using computational fluid dynamics (CFD) [31]. Empirical studies proved the general applicability of ejectors for augmentation purposes and also proposed preliminary design and performence criteria in the 1960s [16]. Enhanced experimental studies of different influential factors on the augmentation process within jet ejectors followed, supplying the research community with a broad range of experimental data [28] [25][48].

Also noticeable in the history of publication on this topic is a shift in application of the ejector principle. While the first decades in research were in search for applicable

augmenters for V/STOL applications [5] [42] the recent two decades delivered research leading to a broad range of civil aircraft applications primarily focusing on noise suppression purposes [24]. For the present work, the literature reviewed delivered all the necessary information to apply a jet ejector for passive thrust augmentation to a small scale jet engine - as the SR-30 is. The knowledge needed for proceeding with a design is outlined broadly in annex F and can be summarized as follows:

- In an ejector the thrust augmentation is achieved due to a *low pressure region along the inlet contour*. The low static pressure is caused by accelerated ambient air entrainment resulting from a pressure drop at the inlet of the mixing chamber which is associated with a pressure rise due to viscous mixing downstream [16] [40].
- An ejector for subsonic, static conditions should be designed using a setup of *inlet contour* preceding a constant area *mixing chamber* followed by a *diffuser* [16] [2].
- *Circular* (axisymmetric) ejectors have proven to reduce losses associated with 3D flow structures at the inlet of rectangular ejectors [25].
- The value of an *augmentation ratio* Φ can be defined in different ways [19]. The practically most relevant is the free augmentation ratio $\Phi = F_{\mathrm{ejector}}/F_{\mathrm{nozzle,amb}}$ comparing the sum of the overall forces of the ejector setup with those forces of the primary nozzle exiting to ambient conditions [16] [25].
- The augmentation ratio Φ is primarily a *function of the ratio of secondary to primary flow crossection* $\alpha = A_{\mathrm{s}}/A_{\mathrm{p}}$ as can be seen in figure 2 [49] [16] [13].

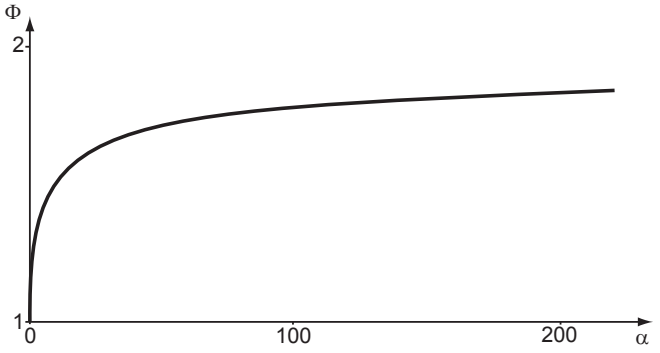

Figure 2: Augmentation ratio for ejector without diffuser as function of secondary to primary flow area ratio - $\Phi = f(\alpha)$ [16]

- For ideal augmenters (i.e. neglecting flow losses) without diffusers the augmentation ratio Φ is *bounded* by a value of 2 as also visble in figure 2 [16].

- Most experimental research has been *focussing on rather high area ratios* α whereas application to area ratios close to unity are rather rare [11].
- *Optimized designs exist* for each operational condition of an ejector [2].
- The *completeness of the viscous mixing process* in the mixing chamber is crucial for the performance of the thrust augmenting ejector and mixing chamber length to diameter ratios L/D of 6 - 7 showed optimal results in augmentation for a single centered nozzle setup [16] [36]. Augmentation ratios dropped significantly due to friction for larger L/D ratios. Smaller ratios enforce incomplete mixing and thus raise the skewness of the exit velocity profile β leading to lower augmentation as well [22].
- *Enhancement of mixing* (pursued by multiple primary nozzles or hyper mixing, lobed primary nozzles) can achieve thrust augmenting ejectors of significantly *reduced length* (down to $L/D = 0.25$) and high augmentation ratios Φ [23] [22] [20] [21] [24] - diffuser wall separation is also reduced [8].
- Primary flow ingestion using a single, centered nozzle at the inlet of the mixing chamber (as opposed to annular nozzles or Coanda nozzles) facilitates *separation in diffusers* [37].
- *Diffusers* can add a high amount of *losses* to the overal ejector process if they are poorly designed [19].
- Increasing *forward speed* within the subsonic free stream causes augmentation ratios to significantly drop and drag becomes dominant especially for values of Mach numbers exceeding 0.6 [51] [24].
- Under static (no forward movement) and subsonic conditions (cruise) and given similar working fluids in primary and secondary flow (being ambient air) *effects of pressure, density and temperature* of the primary gas are negligible to the basic performance behaviour of the thrust augmenting ejector [36] [22].

The above information will be used as design criteria and for predicting the thrust augmentation for the applied thrust augmenting ejector for the SR-30 turbojet engine as outlined in the following chapters.

1.2.3. Simultaneous studies at The Ohio State University

During the work on this project the author has also been involved into research connected to this topic at the Department of Aerospace Engineering at OSU. On the one hand a CFD course dealing with *Systems Integration* was attended. In a group work with three additional students the commercial code Fluent by Ansys was used to address some aspects of the application of the thrust augmenter design to the SR-30 jet

engine. Insight to the effects of mixing chamber length and displacement of the ejector from the exhaust jet plane was gained and results [38] delivered helpful hints for the present work. A summary of the reported achievements can be seen in Appendix F and the main conclusions of the CFD results for the undertaken investigation of this work are as follows:

- A small area ratio, simple ejector design of circular inlet and constant area mixing chamber with $L/D = 7$ delivers a *thrust gain* within range of simple theoretical predictions [16] [38] but is trending lower than predicted. A 2 % thrust gain was found for this setup.
- Reduction of *mixing chamber length* below the suggested optimum value of $L/D = 7$ to a value of $L/D = 3.5$ showed significantly increase in thrust gain [38] to above 4 % other than expected from simplified flow analysis [16].
- *Displacement* of mixing chamber entrance downstream of the primary jet exit by 3 in lead to significant decrease in thrust [38]. Reason for this was increased drag due to internal wall friction facilitated by the initial spread of the jet between exhaust nozzle and ejector entrance. Furthermore the displacement supported the rise of a low pressure region on the backside of the engine due to entrained ambient air flowing around the engine body (see pathlines on figure 3). Both effects lead to a thrust loss of about 4 % in the practical application of the ejector after the engine body.

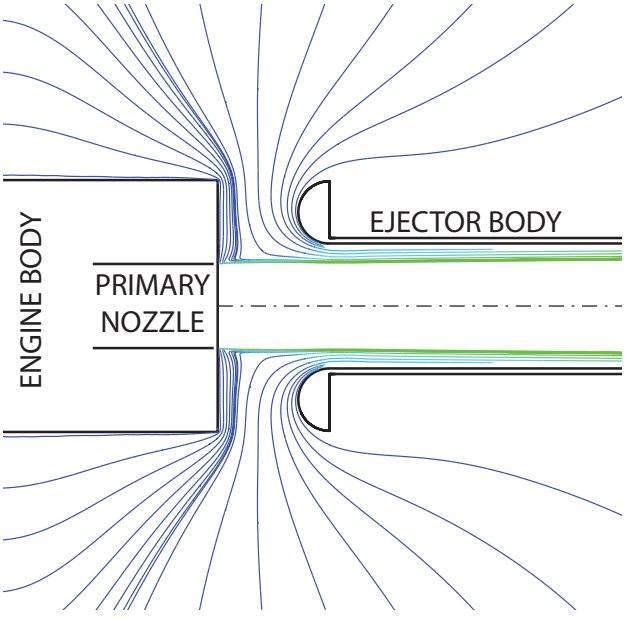

Figure 3: Entrained ambient fluid pathlines around engine and ejector body [scale of velocity magnitude: blue = 0 m/s, green = 125 m/s] [38]

Additionally a team of nine undergraduate students participated in a competition initiated and funded by the U.S. Air Force. The competing teams from different research universities within the USA aimed for designing an afterburner for the Jet-Cat P80-S jet engine. The preliminary design and knowledge of parts of this report were incorporated into early tests of the team that were conducted with a thrust augmenting ejector applied after the $d = 1.94\ \mathrm{in}$ nozzle. A bell mouth of $8\ \mathrm{in}$ outside diameter with a lemniscate lip was applied to the ejector which had an area ratio of $\alpha = 2$ and length to diameter ratio of $L/D = 7$. The experiments delivered a thrust gain of about $6\ \%$ [3] whereas the prediction using the loss incorporating nomographs by Huang [16] assumed a value of around $9\ \%$ - a comparably close match. Furtermore in varying the displacement of the ejector 2, 2.75 or $3.5\ \mathrm{in}$ after the nozzle the thrust gain showed an optimum for 2.75 in offset [3].

The conclusion of this team's findings for the work on the augmenter for the SR-30 adds to the result of the displaced study of the CFD case mentioned before. The fact that there exists an optimum in the displacement of the ejector downstream of the nozzle exit has to account for a compromise in the losses associated to the low pressure region acting on the back of the engine (more severe the closer the ejector is) and the increased drag due to the jet spread (more severe the further apart the ejector is placed). Again this rises the attention that results for augmentation will trend lower than theoretically expected for the practical application of an augmenter after the SR-30 exhaust nozzle.

1.3. Jet ejectors - physical background

In a jet ejector, as depicted in figure 4, a high momentum primary jet entrains ambient air [16]. The ejector consists of an inlet followed by a constant area mixing chamber and an optional diffuser.

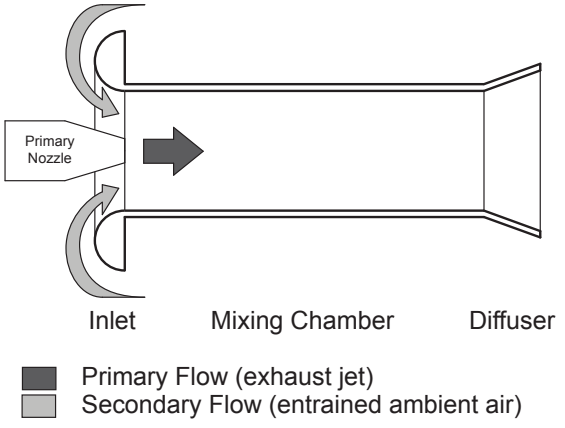

Figure 4: Jet ejector - components and flow pattern

Between the primary flow discharged into the mixing chamber with high velocity and the initially resting fluid a shear layer arises. Viscous shear stresses cause the fluid sur-

rounding the primary jet to move downstream and the created motion causes a static pressure drop at the inlet. As a result, the secondary flow is supported to built up. Downstream, in the mixing chamber, energy is transferred from the primary to the secondary flow due to turbulence and viscosity. A completed flow mixture exhausts to a back pressure at the end (or regains some kinetic energy as static pressure in an attached diffuser). Additionally this mixing process of the two fluids causes the pressure to rise and as the back pressure is fixed to ambient at the exit the consequence is a drop of static pressure on the inlet plane of the mixing chamber and thus the secondary flow mentioned before is sustained [40]. As an overall result - adding the effect of the low pressure region around the inlet and the higher mass flow at the exit - the momentum of the ejector exceeds that of the primary nozzle flow exhausting to ambient. A thrust augmentation is the consequence. The detailed root of the resulting force will be outlined in the following chapter.

1.4. Control volume analysis

As with every jet propelled engine the result of Newton's third law of motion is that the momentum of a mass flow of air at the exhaust exerts a force opposite in direction to the exiting gas and thus accelerates the engine forward. If one draws the reasonable control volume around an engine and applies the necessary pressure, friction and momentum forces it is quickly seen that the high velocity exit momentum overcomes the comparable slow entraining mass stream at the inlet and delivers a net force forward - the reader is referred to standard propulsion books [41] [30] to refresh this definition of thrust. In the case of an analysis of ejector flow patterns the momentum balance has to be drawn in a similar fashion [20]. Figures 5 to 7 show the respective control volumina that will be used to apply the momentum balance equations to an ejector without diffuser.

For the ejector control volume it is

$$
\begin{aligned}
F_{\text{momentum}} &= F_{\text{body}} + F_{\text{pressure}} && (1)\\
-(\rho u_s^2 A_s + \rho u_p^2 A_p) + \rho u_2^2 A_2 &= F_{\text{R}} - F_{\text{SP}} + \sum pA && (2)\\
-(\dot{m}_s u_s + \dot{m}_p u_p) + \dot{m}_2 u_2 &= F_{\text{R}} - F_{\text{SP}}, && (3)
\end{aligned}
$$

where F_{R} stands for the restraining force of the ejector that will be forcing on the support mechanism and F_{SP} sums up the shear stress and pressure forces on the outside contour. For the first assumption the pressures on the outsides are supposed to be atmospheric and thus $\sum pA = 0$.

For the internal control volume the difference in momentum between inlet and exit can only be attributed to frictional losses (neglecting other losses in this regard) and as a result it is

$$
\begin{aligned}
-(\rho u_s^2 A_s + \rho u_p^2 A_p) + \rho u_2^2 A_2 &= -F_\mu + \sum pA && (4)\\
-(\dot{m}_s u_s + \dot{m}_p u_p) + \dot{m}_2 u_2 &= -F_\mu. && (5)
\end{aligned}
$$

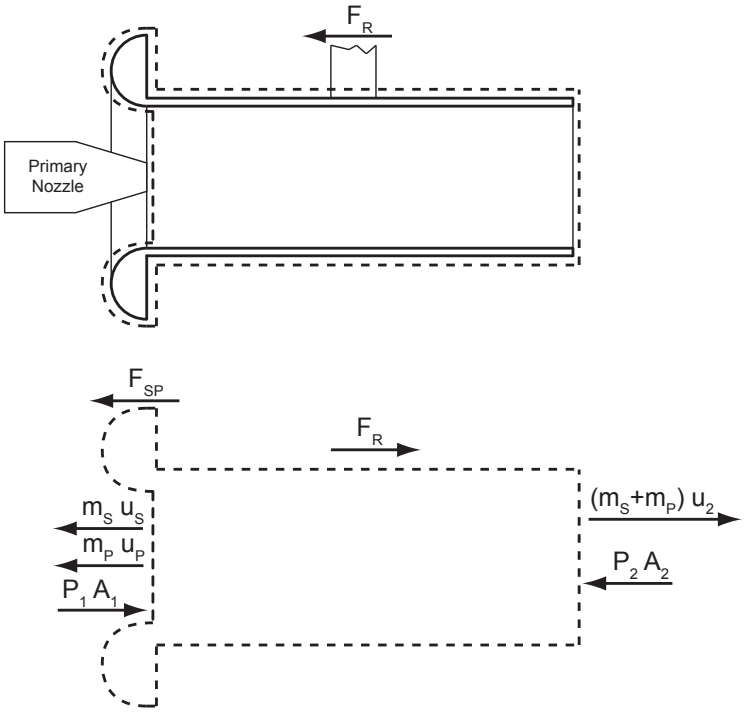

Figure 5: Ejector control volume

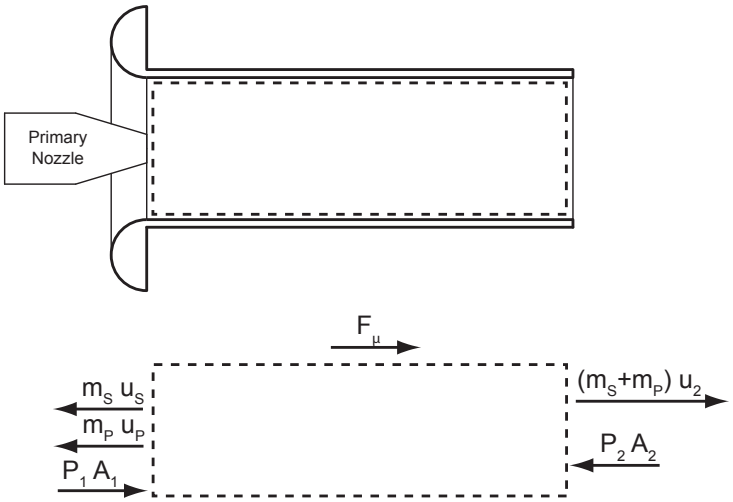

Figure 6: Mixing chamber internal control volume

Here, F_μ is the force due to friction on the internal walls. If both above equations are combined it becomes visible that the body force and therefore the thrust gain of the ejector only originates from the entrained secondary flow that creates a significantly lower pressure distribution along the inlet contour:

$$F_{\mathrm{R}} = F_{\mathrm{SP}} - F_\mu. \tag{6}$$

Apparently, the pressure forces on the inlet and the frictional losses inside of the ejector counteract each other - this reasons the previously mentioned fact that ratios of L/D greater than a specific optimum will automatically result into reduced thrust [16] [36].

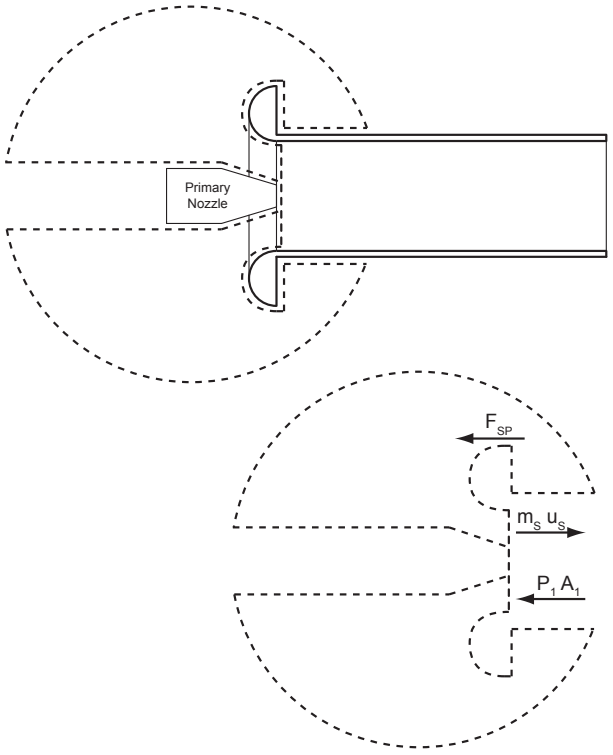

Figure 7: Secondary flow inlet control volume

The inlet control volume, assuming ambient pressure and zero velocity on the circular boundary - applying Bernoulli's equation - will give the relation between secondary mass flow and pressure force on the inlet contour as

$$
\begin{aligned}
-\rho u_s^2 A_s &= -F_{\mathrm{SP}} - (p_0 - p_1)A_s && (7)\\
-\dot{m}_s u_s &= -F_{\mathrm{SP}} - (\frac{1}{2}\rho u_2^2)A_s && (8)\\
F_{\mathrm{SP}} &= \dot{m}_s u_s - \frac{1}{2}\dot{m}_s u_s && (9)\\
F_{\mathrm{SP}} &= \frac{\dot{m_s}^2}{2\rho A_s}. && (10)
\end{aligned}
$$

Summarizing we get

$$F_{\mathrm{R}} = \frac{\dot{m_s}^2}{2\rho A_s} - F_{\mu}. \quad (11)$$

It is obvious now, that the effective thrust caused by an ejector is primarily a function of geometry (i.e. secondary flow crossection) and entrained fluid mass flow counteracted by losses inside the ejector. A vital understanding of this relation is of great help as it is the theoretical core for the following work and its practical application. To emphasize the impact of this very basic first analysis of the problem the following facts can be derived directly from this point of knowledge:

- The thrust gain will be highest for the static condition and negligible for cruise as the streamlines cover less inlet surface area the faster the secondary mass flow entrain [51] [24].
- The inlet design needs to assure proper entrainment without separation to reduce any losses associated [25] [20].
- The geometry factors of secondary flow cross section at the inlet (respectively area ratio α) and mixing chamber length - respectively L/D that influences the associated drag and mixing completeness - are the basic design parameters [16].

It remains to deliver a thorough analysis of the internal control volume of the mixing chamber and to apply conservation of mass, momentum and energy to derive a closed formulation of the thrust gained as a function of secondary to primary area ratio at the inlet. As outlined by Presz [22] the entrained mass flow at the secondary inlet can be related to the primary mass flow by the equation

$$0 = \left(\frac{\dot{m}_{\mathrm{s}}}{\dot{m}_{\mathrm{p}}}\sqrt{\frac{T_{\mathrm{t,s}}}{T_{\mathrm{t,p}}}}\right)^2 \left(\zeta + \frac{1}{2}\left(1 - \frac{A_{\mathrm{p}}}{A_{\mathrm{s}}}\right)^2\right) + \left(\frac{\dot{m}_{\mathrm{s}}}{\dot{m}_{\mathrm{p}}}\sqrt{\frac{T_{\mathrm{t,s}}}{T_{\mathrm{t,p}}}}\right) 2\zeta + \left(\zeta + 1 + \frac{A_{\mathrm{p}}}{A_{\mathrm{s}}}\right)^2 . \quad (12)$$

Here $\zeta = -\beta(\frac{C_f}{2}\frac{L}{D} + 1)$ accounts for the effects of frictional losses at the walls and the losses associated to incomplete mixing and $C_f = \tau/(0.5\rho_2\beta\bar{u_2}^2)$ is a friction coefficient

defined for the ejector [22]. In this formulation it is $\beta = \int \frac{u_2^2 dA_2}{\bar{u_2^2}}$ the non-uniformity parameter for the velocity profile at the exit. As velocity profiles at both primary and secondary stream inlet are supposed to be uniform - an assumption reasonable for small area ratio ejectors especially [16] - it is the skewness of the velocity profile at the exit of the ejector that can significantly decrease the effectiveness of the thrust gain by the ejector. The shorter the ejector is, the less complete the mixing process is and the higher the skewness becomes (rising above the ideal value of unity) resulting in a lower performance of the thrust augmenter [35]. It is also noted that the assumption of density ratios of primary to secondary flow close to unity have been considered ($\rho_p/\rho_s \approx 1$) and that the parameter $\left(\frac{\dot{m}_\mathrm{s}}{\dot{m}_\mathrm{p}}\sqrt{\frac{T_\mathrm{t,s}}{T_\mathrm{t,p}}}\right)$ collapses the data for various densities and temperatures into one pumping curve - i.e. density and temperature problems drop out of the formulation [23]. The result of the above formulation - obtained for assuming incompressible flow but holding similarly for compressible fluids - shows that the ejector pumping rate is not influenced by the pressure ratio of the primary flow and that the resulting pumping parameter depends only on the effectiveness of mixing and ejector area ratio $\alpha = A_\mathrm{s}/A_\mathrm{p}$ [20]. Similar analysis of the flow patterns available in the literature resulted in the same appointment of the pumping rate to be the dominating parameter for thrust augmentation of the ejector [13] and this pumping rate is related to geometry as presented above.

Given the additional assumption that completeness of mixing and thus uniform velocity profile at the exit of the ejector is given (assured by the definition of an optimal ejector length ratio of $L/D \approx 7$ [16]) the analysis can be adapted to deliver a closed form solution for the augmentation ratio as a function of ejector area ratio - i.e. $\Phi = f(\alpha)$. This formulation is further neglecting flow losses in the ideal analysis and accounts for real flow phenomena by applying loss factors as outlined later. Formulating the so called *free augmentation ratio* as the relation between the force of the whole setup with equipped ejector F_ejector to the force of the sole nozzle exhausting to ambient conditions $F_\mathrm{nozzle,amb}$ [16] [25] it is

$$\Phi = \frac{F_\mathrm{ejector}}{F_\mathrm{nozzle,amb}} \tag{13}$$

and the analysis is carried out [16] incorporating the equations for continuity, momentum and energy conservation yielding the equations for the mass entrainment and augmentation ratio to be

$$\frac{\dot{m}_\mathrm{s}}{\dot{m}_\mathrm{p}} = \frac{(\alpha-1)\left[-(\alpha-1)+\alpha\sqrt{2\alpha}\right]-(\alpha^2+1)}{\alpha^2+1}, \tag{14}$$

$$\Phi = \frac{(\alpha+1)(-(\alpha-1)+\alpha\sqrt{2\alpha})^2}{(\alpha^2+1)^2-(-2\alpha+(\alpha+1)\sqrt{2\alpha})^2}. \tag{15}$$

As already noted, the effects of non-uniformity of velocity profiles, losses at the inlet and drag on the internal walls are taken into account at this analysis by further applying reduction factors who are obtained from graphical plots representing results from nu-

merical iterations over the full equations governing the flow. The use of those factors will be shown later in the performance prediction of chapter 2.3.1.

As for the concern of the control volume analysis it has been clearly shown that the augmentation - i.e. the additional force acting on the ejector - results from the pumping of ambient fluid through the secondary flow inlet caused by the primary flow. This pumping is subject to mixing completeness and friction but mainly relates to the geometry of the ejector and thus the ejector area ratio α. Overall, an ideal analysis based on assumptions concerning the fluid properties and flow patterns leads to a closed formulation for the augmentation $\Phi = f(\alpha)$ and account for losses due to non-uniformity of the flow and due to mixing and friction is taken via correction factors.

2. Experimental Preparation and Procedure

The central work within this project addresses two objectives. First to run and evaluate the basic engine performance of the SR-30 MiniLab and apply it into the educational framework. Second to design, build and apply a thrust augmenting ejector to the SR-30 and evaluate the performance under those circumstances. It will be outlined in the following how the SR-30 was brought into service after resting for a long time. Details will be given on encountered problems in the setup and after this the data collection and post processing will be presented. Also the necessary documentation for the application of the SR-30 within a senior students study laboratory will be given. In addition, the design criteria for the passive thrust augmenter using a jet ejector will be given followed by the documentation of the building and assembly process of the ejector and the attachment to the engine.

2.1. The SR-30 jet engine MiniLab

The SR-30 is small scale, single-spool turbojet engine. No air is bypassing the core. The design of the components is typical for a jet engine of this compact size as it incorporates a radial compressor and has a change in flow direction in the annular, reverse flow combustion chamber. In streamwise order the engine components can be listed as an inlet bell mouth, a radial compressor, an annular reverse flow combustion chamber, an axial turbine and a converging exit nozzle. A basic cutaway picture of the engine is shown in 8. The gas turbine process can be sketched in a block diagram. The international standard notation is applied and the process of the SR-30 jet engine can thus be depicted as in figure 9.

For measurement purposes the engine has been equipped with 13 sensors [47] at key locations. Both pressure and temperature is measured at five different places. Within the inlet, shortly before the compression stage a pitot-tube measures the dynamic pressure and a total temperature is taken. Total values of pressure and temperature are recorded at the cross sections after the compressor, at the end of the combustion chamber, after the turbine stage and at the nozzle exit. In addition to those thermodynamic measurements three other parameters are possible to record. The spool speed n is taken from a tachometer in the hub of the engine. Furthermore, the flow of fuel in the supply system is recorded using a pressure measurement in the reflow system. Also, the support mechanism that the engine body is resting on is pivoting around a bearing and pushing on a load cell at the base of the test cell. Given the pre-calibration by the manufacturer to apply the moment law this setup allows direct measurement of the net thrust (i.e. the gros thrust of the nozzle reduced by the inflow momentum of the inlet). The location of the probes is given in table 1 following the international standard notation. In addition to this also the cross sections of the stages in the turbine that the fluid flows through are given by the manufacturer [45] and are listed in table 2.

The test bed in which the SR-30 is embedded supplies the engine with fuel and oil

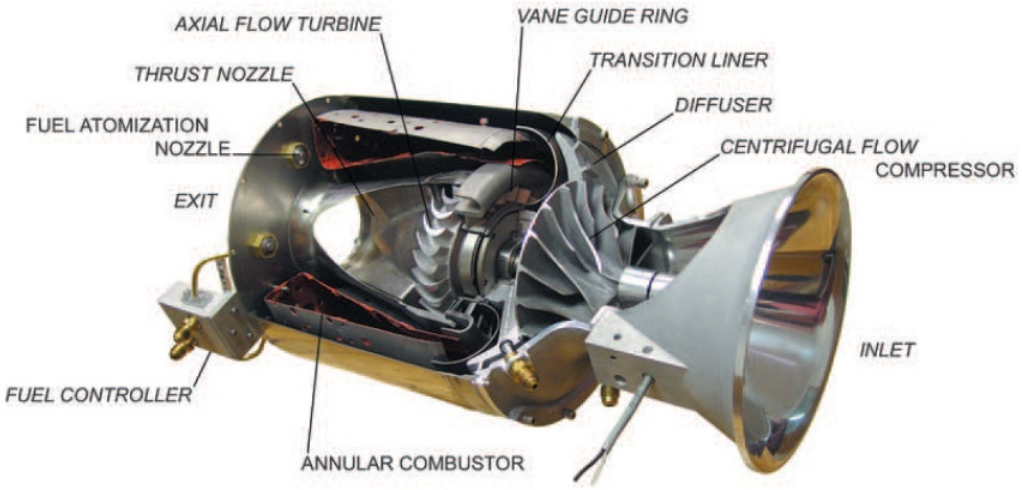

Figure 8: SR-30 cut away impression with labeled components [47]

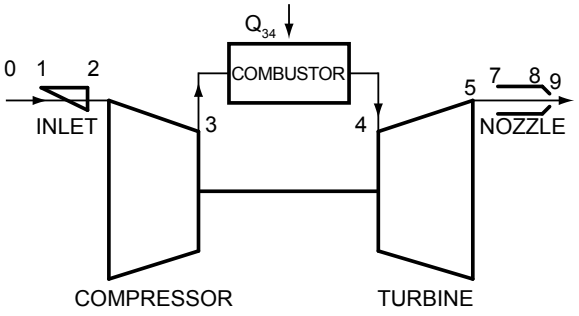

Figure 9: Cycle schematic of a single spool turbojet engine (no bypass air, no second combustion) in international standard notation

	Stages					
Physical Value	2	3	4	5	9	overall
Pressure	p_{dyn}	p_t	p_t	p_t	p_t	
Temperature	T_t	T_t	T_t	T_t	T_t	
Spool Speed						n
Thrust						F
Fuel Flow						$\dot{m}_{\mathrm{fuel}}$

Table 1: Measured sensor data from the SR-30 sorted by stages

Stage Nbr.	A [in^2]
2	4.75
3	1.23
4	2.08
5	2.14
9	3.88

Table 2: Cross sections of the SR-30 engine stages [45]

for lubrication out of two separate containers and pumping systems. The fuel is pumped into the engine and a lever, operated manually, controls the amount of fuel that is allowed to reflow into the reservoir. A spark plug system assures ignition and pressurized air of 100-120 psi (690-830 kPa) [47] has to be provided externally to initially drive the turbine and deliver the work to start the engine process. All of the system controls are on the operator panel (figure 10) where the engine can be started by a single push button. This panel also monitors the values of turbine inlet temperature $T_{\mathrm{t},4}$, exhaust gas temperature $T_{\mathrm{t},9}$ and spool speed n is monitored. In addition the pressures in the air, fuel and oil supply are measured and compressor exit pressure is indicated.

Figure 10: Operator panel of the SR-30 MiniLab

During the startup process the electronic control unit will supply the pressurized air to the turbine stage until a sufficient spool speed is reached. Fuel is sprayed into the combustor via eight nozzles and ignited by a single arc of the spark plug. The combustion process starts (visible by a flame out of the exhaust nozzle) and the spool speed is regulated to idle conditions. Approximately 25 seconds pass for this automatic start procedure.

In operational condition the engine performance envelope can be accessed from idle up to 87,000 RPM [47] by adjusting a lever that increases the amount of fuel that goes

into the combustion process. A IOtech Personal Daq/56 USB module is equipped to the before mentioned sensors. Through a USB interface and a personal computer program the sensor data can be monitored and recorded. For this purpose the program IOtech's Personal DaqView that is delivered with the MiniLab is utilized. A calibration file for the sensors has been made available by Turbine Technologies™.

Just like the start up, the shut down process is facilitated by a one button procedure on the operator panel as well and if necessary a cool-air-flush procedure of five seconds can be applied to facilitate cool down process if needed.

2.2. Evaluation of engine performance

Obtaining the performance parameters for the SR-30 jet engine is a vital part of this work. Any thrust gain possibly created by an augmenter equipped to the engine can only be evaluated if the base line performance of the engine is known. Furthermore the engine should also be fully characterized to assure its use within education and research at the department.

2.2.1. Preparation and running of the SR-30

At the beginning of this work the SR-30 MiniLab has been resting for some time in a test cell within the aerodynamics laboratory of the department at OSU. After the initial purchase in 2000 it was operated some times and then sent in to Turbine Technologies™for an overhaul - basically equipping the second generation measurement capabilities as outlined in chapter 1.2.1. After it was returned it has been at rest without any startup.

In the advent of working on this paper first of all a necessary cleaning of the outside of test-bed and engine parts of the MiniLab was done. Then followed a connection of it to electrical power and auxiliary air supply. As was experienced during early runs of the first version of the engine, the in-house supply of pressurized air was not sufficient to facilitate a proper engine start up [12]. It is the understanding that the size of the in-house pressurized air system cannot deliver the necessary pressure level over the timeframe of the 25 second start up procedure. After the initial inflow of air into the engine the pressure in the system dropped too fast. The problem was addressed by using an external air compressor located close to the engine with minimized length of connection tubing. The Porter Cable Shop Boss has the performance and type specifications as given in table 3. This compressor operates in a way that makes its application to this specific problem convenient as it resumes the compression process as soon as the pressure in the reservoir drops under a chosen value.

After frequent runs of the MiniLab some attempts showed that the automatic startup procedure would fail to lead to an ignition within the combustion chamber. Two possible reasons were found to be connected to this issue. On the one hand, the spark plug, being attached to a radial hole of the combustion chamber on the top of the engine body, showed substantial covering with soot particles. The procedure of frequent cleaning of

Maximum Pressure	175 psi
Tank Size	25 gal
Running Horsepower	1.6 HP
Air Delivery @ 90 PSI ISO1217	4.7 SCFM
Electrical Power	120 V x 15 A
Valve	Adjustable

Table 3: Specifications of external compressor Shop Boss 175 psi, two-stage, 25 gal

the spark plug head with a cloth prior to engine runs (after some idle time of no runs) eliminated problems related to this issue. A more serious problem in assuring a smooth startup process was the discovery of water droplets on the compressor blades and downstream of the engine exhaust in the test chamber after unsuccessful start attempts. An investigation of the pressurized air supply revealed that water accumulated at the lowest part of the hose between compressor and MiniLab air supply as well as on the bottom of the external compressor reservoir. The generally humid climate of Ohio together with the pressurization process therefore result in a perfectly practical - and in this case disadvantageous - application of thermodynamic principles. As no conditioning (i.e. dehydration) of the air is done prior to the compression process and no additional heating is facilitated the problem of condensation in the reservoir cannot be overcome. The practical consequence taken for this setup is that of draining the compressed air reservoir after each session to minimize accumulation of water in the air supply. The problem of water droplets within the engine air stream did not reoccur and the automatic engine startup process worked in a reliable fashion ever since.

2.2.2. Adaptations to the measurement capabilities of the MiniLab

As data acquisition was addressed in later runs the recording process was found to be uncomplicated as is reported in chapter 2.2.3. The investigation of the measured values delivered some compromising results that needed to be further addressed by adaptations to the engine and the MiniLab. One of the problems was related to the thrust measurement capability using the load cell on the base of the test bed. This sensor equipment is one of the improvements to the engine's first version. As the engine has not been run between its adaptation and the start on this investigation the bringing into service of the pivoting support, the SR-30 engine is resting on, was not sufficiently documented. The result was that four block plastic cushions on the base of the engine support were not taken off and hindered completely free movement around the bearing. After removal of those transport securities pivoting of the support was freed.

Another anomalous result that was found after the first evaluations of the measured data sets was that at the idling condition of $n = 48,000\ \mathrm{RPM}$ the turbine exit temperature $T_{\mathrm{t},5} = 398°C$ was actually exceeding the turbine inlet temperature $T_{\mathrm{t},4} = 393°C$. As the turbine inlet temperature is by definition the highest process temperature in the

engine cycle at hand the problem needed to be addressed. First, from discussions with the manufacturer it was suggested that at low spool speeds the combustion process is not complete resulting in fuel still being burned within the turbine stage [46]. As the plane of the turbine exit was visibly accessible from the back of the engine similar conditions were set in idling the SR-30 but no glow or flame was seen that would indicate the combustion through the turbine stage. After this result the thermocouples at both questioned locations were more closely looked at. Detaching them from the engine and placing them together into a hot air stream showed that the data delivered by both probes was very close. Measurement offset therefore was not an issue. As radial movement of the measurement probes was reported to be of importance in some earlier investigations [43] the placement of the probe at the turbine inlet was reconsidered. Along the radial direction into the engine the wall of the reversing passage from the combustor exit to the turbine inlet hindered further insertion of the probe into the air stream. A light bending of the head of the probe made it possible to place it further in. Subsequent runs were done and the previously observed discrepancy was not encountered again.

As an overview, again the most crucial remarks on the encountered problems during the SR-30 setup and data collection are given as follows:

- in-house startup air pressure was not high enough -> implementation of external compressor
- sooth particles covering the spark plug -> frequent cleaning prior to startup
- water accumulated in the pressurized air system -> frequent draining of the reservoir
- engine support could not pivot freely leading to no thrust being measured -> removed plastic support
- turbine inlet temperature probe delivered lower values than turbine exit temperature probe -> repositioning of turbine inlet temperature probe

2.2.3. Data acquisition and Matlab post-processing

As outlined before the MiniLab utilizes a digital/analog acquisition system that processes the analogue input of the probes and passes it onto a personal computer connected to a USB port at the test stand. The thirteen probe measurements (see table 1) can be viewed in real time or recorded into different file formats, one of which is compatible with the software Matlab. The order in which the values are recorded and the range of the signal can be taken from table 4.

Following a so called 0D analysis as it is undertaken in most undergraduate courses, [41] [30] the sensor data is used to obtain the performance parameters of the engine process as well as the component efficiencies and the overall net thrust. The analysis is outlined in appendix A and has been implemented into a Matlab code as can be found in

Channel Nr.	Measured Variable	Dimension
1	$p_{\text{dynamic 2}}$	psig
2	p_{t3}	psig
3	p_{t4}	psig
4	p_{t5}	psig
5	p_{t9}	psig
6	$\dot{m}_{\text{fuel}}$	$\frac{gal}{h}$
7	n	min^{-1}
8	F	Lbs
9	T_{t2}	°C
10	T_{t3}	°C
11	T_{t4}	°C
12	T_{t5}	°C
13	T_{t9}	°C

Table 4: Channel listing of recorded sensor data of the MiniLab

appendix B. Within the calculation as presented in appendix A the assumption of ideal gas is made ($p = \rho R_{\text{s}} T$). Based on ambient pressure and temperature the air density is calculated and the gas constant is taken to be $R_{\text{s}} = 287\ \text{kJ/kgK}$. The values for the specific heat of air which is calculated for each stage and process between the stages were taken from a temperature relation [18] as

$$c_p = 1.9327 \cdot 10^{-10} T_t^4 - 7.9999 \cdot 10^{-7} T_t^3 + 1.1407 \cdot 10^{-3} T_t^2 - 0.44890 T_t + 1057.5 \quad (16)$$

The cross sections within the engine as presented previously in table 2 are utilized for calculating mass flow at the inlet and nozzle. A slight difference was observed for the inlet plane as reported by Turbine Technologies™[45]. Measurements were made to evaluate exactly the cross section of the plane at which the pressure probe in the inlet is located as opposed to approximately take the cross section at the compressor exit. For convenience and completeness the values of cross sectional area at both the inlet pressure probe and nozzle exit locations are given in table 5.

Stage Nbr.	$A\ [\text{in}^2]$
2 (probe)	5.456
9	3.88

Table 5: Corrected cross sections of the SR-30 engine stages

The Matlab code is assuring an easy post-processing of the data as recorded by the MiniLab. From the saved record from the acquisition software, the program reads in the 13 variables measured. The user inputs the ambient temperature T_0 and pressure p_0

and after this the temperature values are plotted over the time period recorded. With this graph in sight the user is asked how many steady state intervals there are in the set and if data has also been recorded for an offset time previous to the run. The process continues to ask the user to mark the beginning and end of the offset and each steady state interval and the code continues to calculate the process parameters from the mean values taken from the measurements of all sensor data. The results are printed into a text file for easy access and further use after the program has come to an end. Figure 11 shows a representative screen shot of the program in use just when the user needs to specify the beginning and end of the steady data plateaus. Representative text file outputs are given in appendix E.

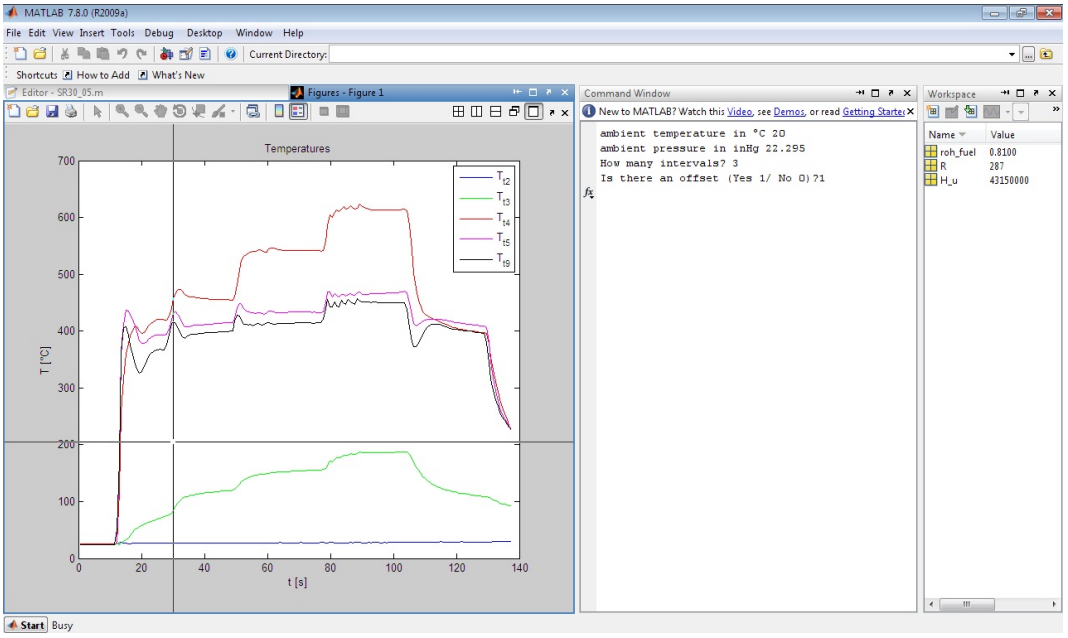

Figure 11: Screenshot of the Matlab program demanding user input on the steady data intervals

2.2.4. Senior student laboratory experiment

Due to the implementation of the SR-30 engine into the educational curriculum of undergraduate courses at the department it is the intention of this paper to also deliver a satisfactory procedure for a possible laboratory experiment regarding jet engine propulsion for senior students. Therefore the most important topics on engine performance analysis are presented and a data post-processing task as well as further tasks concerning the whole laboratory procedure are prepared and given in the annex C. Furthermore this annex also holds a step by step list for an instructor or teaching assistant on how to prepare, run and evaluate a typical experiment utilizing the SR-30 MiniLab as installed at OSU.

2.3. Design of the jet ejector

As the simplest approach the jet ejector consists of three sections as pictured previously in figure 4 namely inlet, constant area mixing chamber and diffuser. The inlet contour needs to be applied to assure proper entrainment of the secondary flow without causing separation along the walls [16]. A circular contour (rather than the optimal lemniscate shape) is picked to enable uncomplicated production. The mixing-chamber of constant diameter is chosen to assure a pressure rise over the mixing path. The diffuser is seen to be optional as a compromise has to be made between the fact that a diffuser can lower the mixing losses and the circumstance of enhancing the frictional drag [21]. Furthermore the difficulty to prevent separation around the diffuser walls in a single centered nozzle setup [37] as taken here has to be seen as a key factor. As the aim is to design a reasonably complex ejector applied to a single primary nozzle and no application of enhanced mixer lobes or an annular nozzle setup is implemented it is decided to use no diffuser rather than one whose frictional losses and separation issues cannot be addressed properly. Thus the setup for the thrust augmenting ejector is seen to consist of an inlet and constant area mixing chamber as pictured in figure 12.

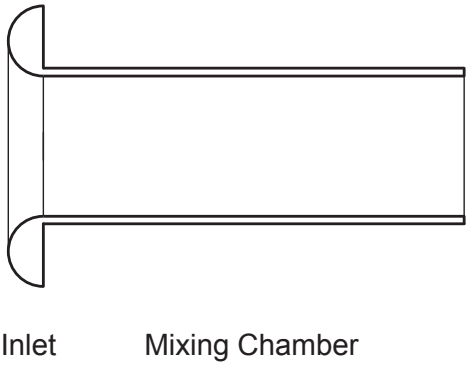

Figure 12: Jet ejector - design schematic

2.3.1. Specifications and performance prediction

The main objective of any applied thrust augmenting device is to deliver a higher thrust than the jet engine by itself. Therefore the different thrust values after equipping the device in comparison to the case of the sole ejection of the primary jet to atmosphere have to be compared quantitatively. As a measure for this thrust gain the free augmentation ratio Φ will be used in this report just as outlined before [16] [25] where in particular

$$\Phi = \frac{F_{\text{ejector}}}{F_{\text{nozzle,amb}}}. \tag{17}$$

If one takes the equations that govern the fluid flow, Bernoulli equation, equation of state and follows an analytical approach across the mixing chamber control volume and

the path from the quiescent ambient condition to the inlet for the secondary flow [16] one can obtain the following relation for ideal thrust gain based on the secondary flow to primary flow cross sectional area ratio α as

$$\Phi = \frac{(\alpha+1)(-(\alpha-1)+\alpha\sqrt{2\alpha})^2}{(\alpha^2+1)^2-(-2\alpha+(\alpha+1)\sqrt{2\alpha})^2}. \tag{18}$$

The nozzle area of the SR-30 is given with $A_\mathrm{p} = 3.88\ \mathrm{in}^2$ based on a diameter of the nozzle of $d = 2.22\ \mathrm{in}$ and it remains to determine the secondary flow area and thus the diameter of the mixing chamber. As noted before, the mixing chamber has to assure complete mixing and this is done by taking a long enough path in the mixing chamber resulting in length to diameter ratios of about $L/D = 7$ that need to be used. To keep the dimensions of the overall ejector within a practical applicable range and also because this work wanted to address area ratios close to unity a diameter of $D = 3.38\ \mathrm{in}$ was chosen. The reason for this particular value becomes evident in the production outline but it can be mentioned here that the design aimed to use commercially available material and thus utilizes standard exhaust piping that comes with specific outside diameter and wall thickness specifications.

With the above geometry data the given area ratio and then the expected ideal thrust augmentation can be calculated and yields

$$\alpha = \frac{D^2-d^2}{d^2} = 1.318 \tag{19}$$

$$\Phi_\mathrm{ideal} = 1.24, \tag{20}$$

relating to a 24 % thrust increase if losses are completely neglected.

As this value is meaningless in the practical sense, the incorporation of losses associated to wall friction along the inside of the mixing chamber as well as along the contour of the inlet need to be taken into account as outlined in the literature [16]. To account for those losses the so called *nomograph* as pictured in figure 13 shows the variety of numerical solutions to the closed analysis of the ejector flow processes[16]. Therefore the loss factor associated with the ejector has to be determined first. The friction loss factor based on the pipe surface and length is chosen to be $f(L/D) = 0.03$ which is commonly used for commercially smooth pipes and a loss factor for the circular entrance contour is taken to be $\lambda_E = 0.03$ [16].

In the plot the area ratio α is picked on the first axis and then the intersection with the respective graph for the chosen λ_E is found. Proceeding on a horizontal line the intersection with the different slopes for the various frictional loss factors $f(L/D)$ delivers a point that brings a vertical intersection with the questioned practical augmentation ratio Φ that is representing an analytical expectation incorporating losses as

$$\Phi_\mathrm{losses} = 1.06. \tag{21}$$

If we expect the analytical solution to account for most, but definitely not all present losses, one can expect that a thrust gain of 6 % has to be seen as the maximum value this

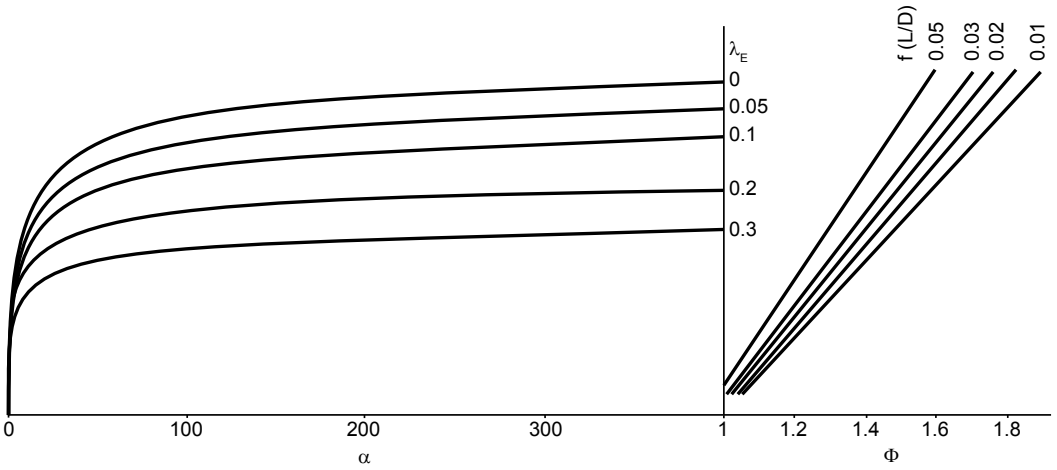

Figure 13: Nomograph to evaluate augmentation ratio for static, incompressible flow and no diffuser [16]

ejector configuration can possibly reach if placed directly at the nozzle exit of the SR-30. It is noted here that the graphically obtained expectation also includes a rather high truncation error due to the fact that the incorporation of loss factors diverses broadly for high area ratios α but is collapsing into almost one single line close to the origin for small values of α. As the installation tubing and regulators on the back of the engine hinder placing the ejector close to the exit of the nozzle it is expected that any thrust value found will be significantly lower than the expectation just put forward. This is due to the influence of higher drag due to jet spread and low pressure region on the engine back face as outlined in the literature review. It remains the effort of the experiment to evaluate to what extend the displacement of the ejector after the primary nozzle will effect the thrust augmentation objective.

2.3.2. Secondary stream inlet

In the design of propulsion devices an inlet's main function is to deliver a low-loss flow from ambient, free stream conditions to the state required at the entrance of the compression stage [30] [10]. Nevertheless, for a design point of static operation (that this project is dealing with) the concerns of specific pressure recovery, flow matching and installation drag become of secondary importance or even negligible. The main goal of an inlet for the passive thrust augmenter is to deliver a well-shaped surface for the entrained air to proceed from the resting ambient conditions to the cross section of the mixing chamber inlet.

The geometry of the inlet has been empirically shown to be important for the losses associated with the entrained secondary stream [16]. A flared inlet is superior to any sharp or rounded edge and the circular shape is a good compromise between a lemniscate and straight contour regarding complexity, overall dimensions and losses [16].

Furthermore, another constraint has to be put on the inlet geometry concerning the ratio of the entrance diameter to mixing tube diameter which should be of a ratio of 1.5 or greater to assure low loss entrainment [16].

2.3.3. Mixing chamber

The circular, constant area pipe that forms the mixing chamber is far from complex. It's specifications are derived from the mentioned restrictions from the performance prediction. Thus, the diameter is $D = 3.38\,\text{in}$ and the legth $L = 7D = 23.66 \approx 24\,\text{in}$. For the reduced length cases of half and one quarter of the initial length that will also be evaluated one gets $L = 3.5D = 11.83 \approx 12\,\text{in}$ and $L = 1.75D = 5.92 \approx 6\,\text{in}$.

2.3.4. Support and attachment mechanism

Crucial for the application of the designed thrust augmenting ejector is its implementation on the SR-30 engine in a way that leaves the basic engine cycle untouched, utilizes the thrust measurement capabilities of the MiniLab and is easy to (dis-)assemble to assure the use of the basic engine setup and the ejector whenever one is needed without a time consuming reconfiguration. It was chosen to utilize a setup that makes use of clamping the augmentor support around the main body of the SR-30 engine using hose clamps. Three support arms that extend after the back of the engine assure a sufficient and also easy to center holding of the augmenter. A slight bend in all of the three arms is incorporated to prevent an offset from the axis. The body of the thrust ejector, i.e. the pipe that is forming the mixing chamber, is attached to three flanges that are clamped onto its circumference. Slots in both the arms that are attached to the engines main body as well as in the flanges on the ejector make it possible to connect both parts with each other using three screws and washers. The slots assure that the support mechanism can hold different sized ejectors (also with angled walls) and that the ejector can be moved in a stream wise direction. An assembly view of the support mechanism visualizes the basic functionality and can be found in annex D in figure 25.

2.4. Production, assembly and implementation of the jet ejector

Given the previous design specifications the necessary parts for both the ejector and the support mechanism needed to be produced. The following is an outline of the augmenter construction.

2.4.1. Production

The main three components for this project that needed to be produced are the inlet, the mixing chamber and the support mechanism. For the inlet contour, as it was picked to be

circular, the commercially available velocity stacks utilized in automotive turbo chargers were seen to be very applicable. The half-circular shape and the outside dimensions of the chosen velocity stacks as seen in figure 14 matched the design requirements of this work. The outside diameter of $D = 6\,\mathrm{in}$ assured the necessary ratio to allow entrainment without separation - i.e. a diameter at the largest cross section of the inlet of at least 1.5 times the ejector diameter [16]. Furthermore it is within the limits of the bounding support mechanism which restricted the outside dimensions of the applied bell mouth.

Figure 14: Velocity stacks used for the inlet contour

Stainless steel automotive exhaust pipe $3.5\,\mathrm{in}$ in diameter with $0.060\,\mathrm{in}$ wall thickness was used for the mixing chamber. Both parts of the ejector were connected by putting the inlet on the entrance of the pipe - both of the inside diameters were matching. A small aluminum strip of the length of the circumference was put over the joining area. Both sides of the strip are then tightened onto the circumference of the inlet and pipe using hose clamps.

For the support mechanism, the raw material was a $0.2\,\mathrm{in}$ thick steel bar of $1\,\mathrm{in}$ in width. The necessary elements to build the arms and flanges of the device were cut and the slots were milled in the machine shop of the department. After that the part of the flanges that contact the circumference of either the engine body or the ejector needed to be bent along their longest axis and this was done utilizing a hydraulic press in the mechanical engineering department of OSU. The flanges for the engine body as well as for the ejector consisted of the circumferential part and a slotted arm and those were attached to each other by welding in the machine shop (see figure 15). All related

technical drawings can be found in the annex D.

Figure 15: Welded parts for the support mechanism

The overall assembly was done by clamping the parts of the support mechanism onto the engine body and the ejector circumference. The result can be seen in figure 17 after its implementation into the SR-30 setup as described in the following paragraph.

2.4.2. Implementation to the SR-30 and necessary adaptations

The practical application of the jet ejector to the SR-30 engine faced the basic challenge that the inlet plane of the mixing chamber could not placed directly in the same plane as the nozzle exit as it has been done by most of the prior research given in chapter 1.2. The main reason for this is that the SR-30 engine in its compactness totally incorporates the converging nozzle into its body and thus the engines back face is the nozzle exit. In addition to this, tubing for the fuel nozzles as well as measurement probes and the thrust lever attachment constrain access to the back plane of the engine. It was therefore necessary that some of the tubing elements supplying and recirculating fuel needed to be rearranged. Instead of two supply lines leaving the engine back plane in a stream-wise fashion, connection angles were purchased and manually adapted (re-threaded) to facilitate a lateral displacement as seen in figure 16.

As a result, the accessible region at the back of the engine could be arranged so that the possible ejector setup could be placed as close as $4.2\ \mathrm{in}$ after the nozzle exit plane which results in a displacement of the mixing chamber entrance of about $5\ \mathrm{in}$.

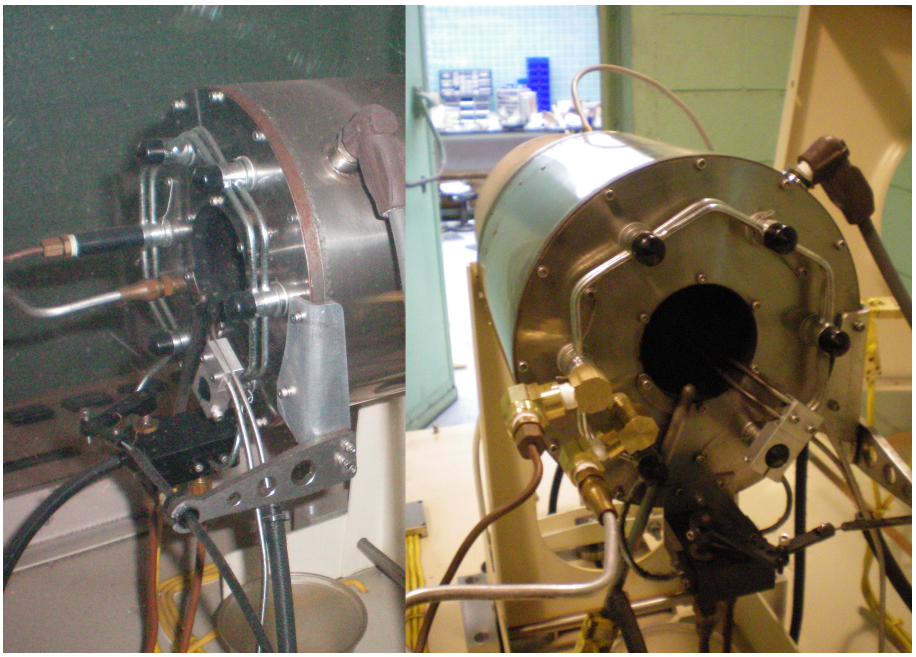

Figure 16: Tubing on the engine back side before (left) and after (right) modification

With those changes made, the support mechanism could be attached. The three flanges with the slotted arms were attached to the circumference of the engine and secured with two hose clamps. The utilization of a short pipe-element that the whole support mechanism was temporarily clamped upon was used to ease this process. The location of the three flanges around the engine body were chosen in a way so that the offset between them is at least 100° so that the MiniLab cover can still be lifted and closed.

After the support flanges were located and tightened the decision must be taken if the setup should be covered or not with the MiniLab's hood as the ejector configuration is extending the dimensions of the cover of the test stand in the downstream direction. After this the ejector could be assessed with the slotted flanges around its circumference. Tightening was also assured using two applicable hose clamps. Matching the slots on the flanges around the ejector with the slots in the support arms the whole device can be mounted applying three suitable screws and washers. Due to the three ways the ejector can slide radially on the slots of the support mechanism, the centering of the ejector is achieved easily. The support mechanism holds the ejector configuration in place and downstream displacement is applied by rearranging the ejector along the three slots of the arms on the flanges (figure 17).

Due to the substantial mass of the ejector configuration the tilting mechanism that the SR-30 is resting on needed to be balanced with a bigger counter weight than the one supplied by the manufacturer. The placement of several mass elements on the base of the pivoting frame as well as a reinforcement of the actual counterweight on its supporting

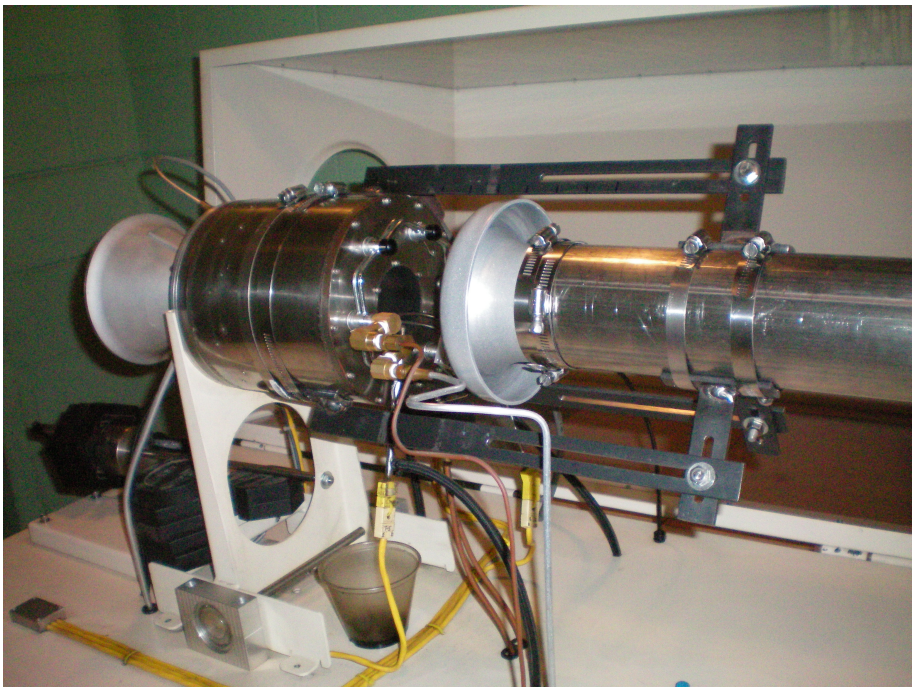

Figure 17: Ejector on the support mechanism attached to the SR-30 engine

arm solved the problem. A mass of 1 kg placed on the frame close to the load cell and an additional 5 kg mass on the lever arm together with the factory supplied weight placed the system in balance. The point of zero thrust recorded was approximately adjusted by moving the counterweight on its support arm until the data acquisition system reported a thrust value close to zero (no distinct zero needed to be achieved due to the offset subtraction in the post-processing program). As the option to run the engine without the hood of the mini lab closed was addressed previously, and since this option was taken for the pursued experiments to assure easy access for rearrangements, it was necessary to install an additional shield to the test stand protecting the operator in front of the MiniLab from any harm. A plexiglas shield (hold by an assembled frame arrangement as seen in figure 18) was placed next to the SR-30 engine and test runs could be safely conducted.

The above adaptations made it possible to further proceed with the process of running the SR-30 with the ejector applied and all measurement capabilities intact - especially the force measurement using the load cell.

Figure 18: Plexiglas shield and frame for the un-hooded test stand

3. Results

The previously predicted performance of the designed and applied thrust augmenting ejector is evaluated based on the base line engine performance of the SR-30. The obtained data from unaugmented runs and test-runs with different augmenter setups is analyzed and the results are reviewed in light of the achieved thrust augmentation. The base line performance is also characterized and compared to results obtained from the literature. Concerning the augmented cases the reason for deviation of the results from predicted values is given as well as a conclusion is drawn and an outlook for possible further investigations on the topic is given.

3.1. Review of plain engine performance

The SR-30 engine was run several times over the work on this project and, given the way of installation of the sensor equipment as outlined in previous chapters, the resulting engine performance was reproducible under all those runs. A representative set of measurements is given for the run on May 20, 2010 in the plots of figure 19 and the relating data evaluation is given in table 6 and the plots of figure 20.

As can be seen from the data records (figure 19) this run was recorded as a second acquisition after a previous run. This assures that the time dependent heating of the elements of the engine is of less impact and thus a more steady temperature state can be reached in a shorter amount of running time. Looking at the recorded data itself some conclusions can already be drawn:

- An unsteady start up phase is observed as the engine is ignited and brought to idle (around $n = 47,000\ \mathrm{min}^{-1}$) in approximately 20 seconds.
- The turbine inlet shows the highest process temperature $T_{\mathrm{t}4}$ and the other temperature probes record data as anticipated [41].
- The high pressure after the compressor and the drop over the turbine is evident.
- Both fuel consumption and net thrust show direct proportional behavior to the spool speed.

Thus it can be summed up that the given data record is a good representation of the behavior of a typical turbojet engine and that it can be considered as a good example to pursue the calculations and use the results.

Regarding the calculated performance parameters (using the Matlab code from Appendix B as outlined before) more light is shed into the engines baseline behavior. The 0D analysis of the engine yields the results as given in table 6 and the related plots in figure 20. Looking at the calculated parameters the following things can be outlined on the performance of the SR-30 engine.

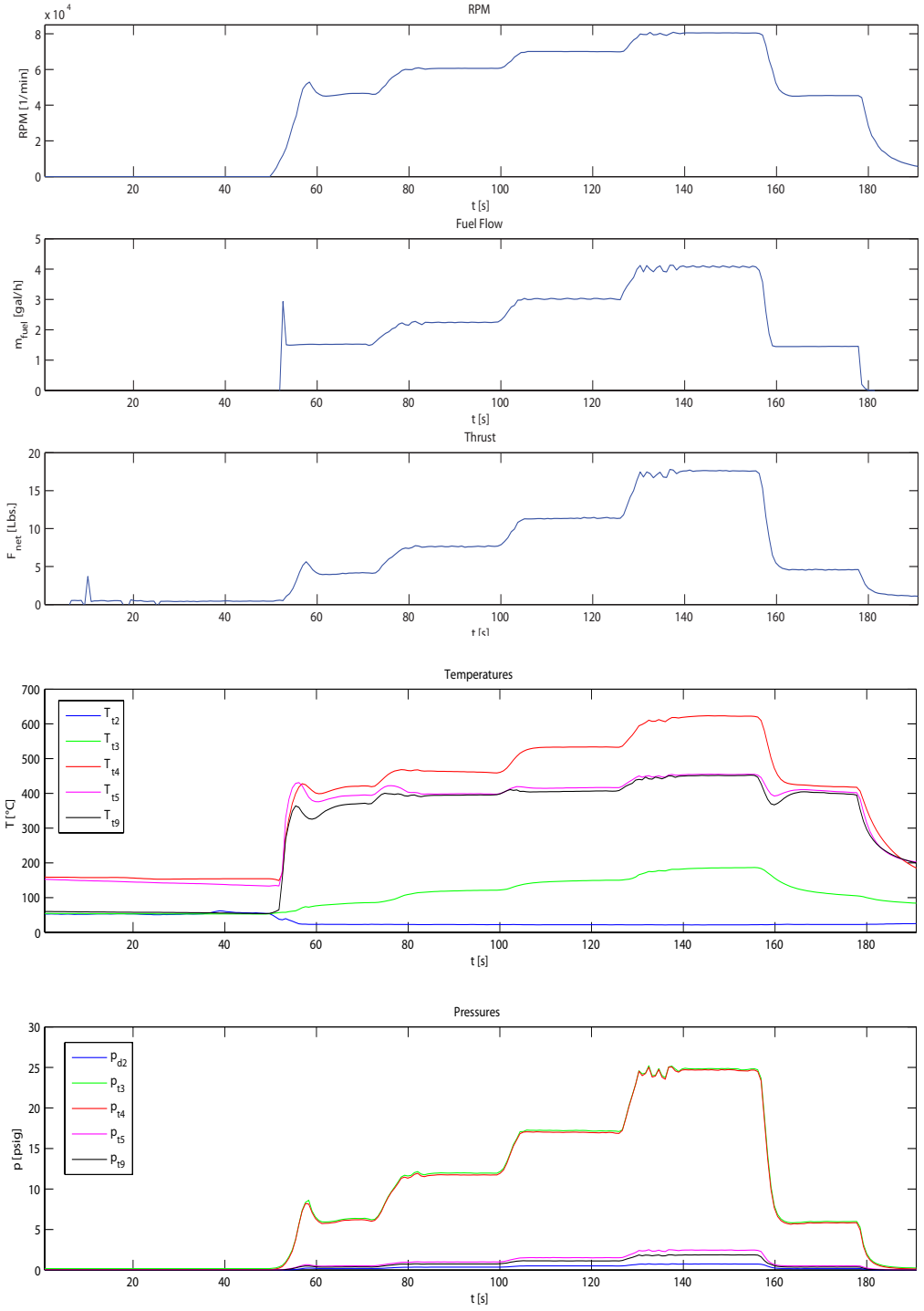

Figure 19: Time-wise sensor data from the SR-30 measured at OSU on May 20, 2010

n [1/min]	$\dot{m}_{air}$ [kg/s]	$\dot{m}_{fuel}$ [kg/s]	$f = \frac{\dot{m}_{fuel}}{\dot{m}_{air}}$ [-]
46625	0.2133	0.00131	0.00612
60656	0.2931	0.00192	0.00656
70057	0.3510	0.00259	0.00737
80496	0.4245	0.00348	0.00821
	Π_{comp} [-]	$\Delta p_{t\ \text{comb.ch.}}$ [-]	Π_{turb} [-]
	1.44	0.0081	1.38
	1.83	0.0088	1.70
	2.19	0.0066	1.97
	2.72	0.0038	2.32
	$\eta_{\text{is,comp}}$ [-]		$\eta_{\text{is,turb}}$ [-]
	0.54		0.46
	0.59		0.66
	0.61		0.89
	0.62		0.95
	$F_{\text{net, calc}}$ [N]	$F_{\text{net, measure}}$ [N]	$TSFC$ [$(\text{kg}_{\text{fuel}}/\text{s})/\text{N}$]
	17.05	16.84	$7.752{\cdot}10^{-5}$
	31.78	32.28	$5.957{\cdot}10^{-5}$
	48.15	48.90	$5.288{\cdot}10^{-5}$
	77.18	76.62	$4.549{\cdot}10^{-5}$
	u_2 [m/s]	u_9 [m/s]	M_9 [-]
	46.88	126.02	0.25
	64.42	171.72	0.34
	77.15	212.77	0.42
	93.31	272.86	0.53

Table 6: Calculated performance data for SR-30 measured at OSU on May 20, 2010

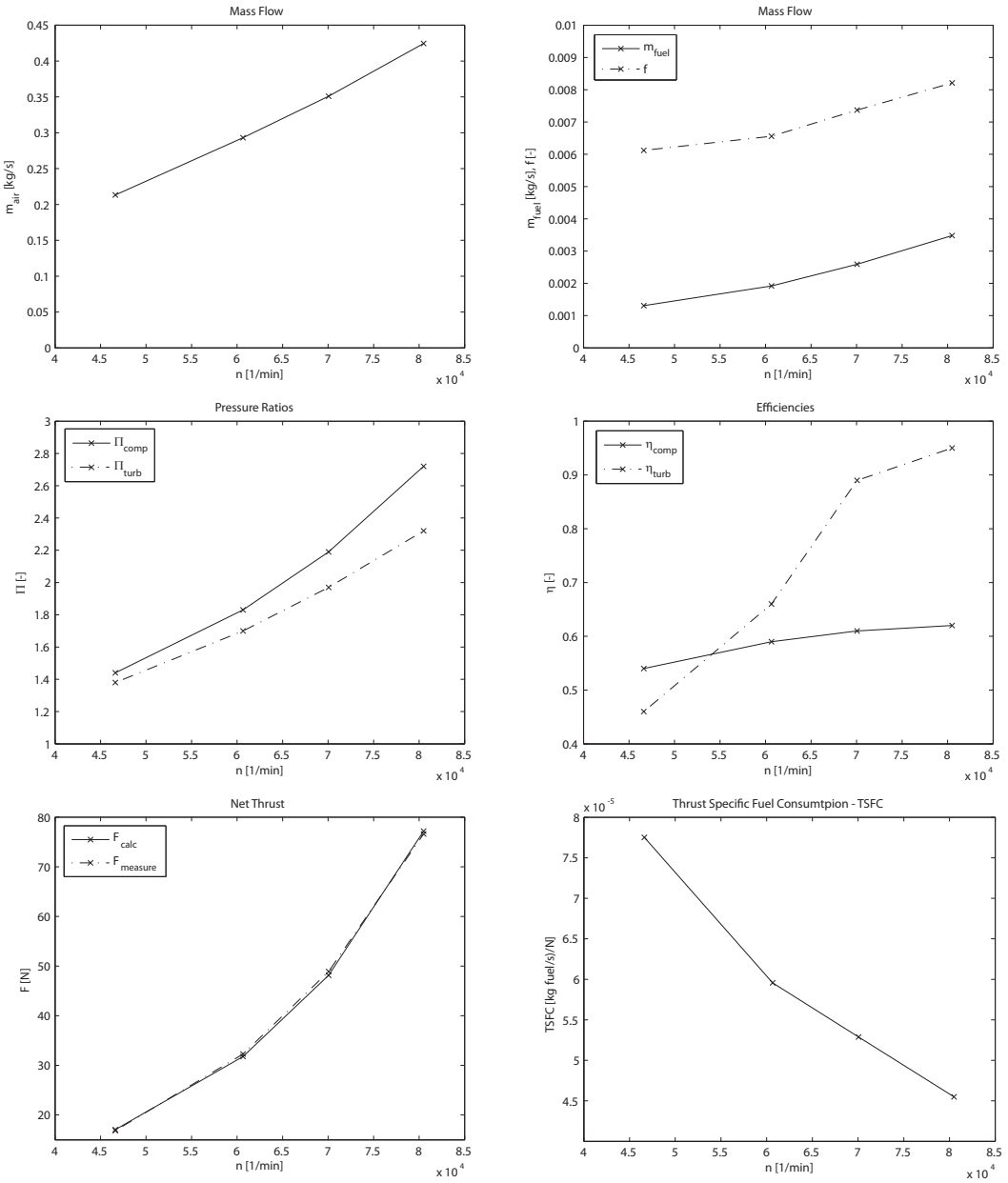

Figure 20: Plotted results of performance data for the SR-30 measured at OSU on May 20, 2010

- The engine performance is directly related to the spool speed and the components efficiencies get better at the higher levels of RPM indicating that the design spool speed is beyond $n = 80,000$ RPM.
- The mass flow of air as well as fuel is rising with spool speed going up.
- Efficiencies of both compressor and turbine are peaking at higher RPM while η_{comp} shows less variation over the range of RPM investigated.
- The net thrust rises with RPM just as TSFC falls as the delivered thrust is a direct function of the mass flow which proportionally rises with spool speed.
- The net thrust as calculated and as measured only deviate a little from each other indicating that the measured value can be used with great confidence for the evaluation of the later augmentation cases.
- The TSFC is in the anticipated range for an engine of this kind [34] [15] making the overall performance to be trustworthy.

As a final approach, the gained results will be compared to the reference tables 8 - 11in appendix F by other institutions and the following conclusions can be drawn:

- A clear dependency of engine spool speed is visible in the development of the performance parameters.
- The measured values for mass flow $\dot{m}_{air}$, pressure ratio Π_{comp}, efficiencies $\eta_{\mathrm{is,comp}}$, $\eta_{\mathrm{is,turb}}$ and $TSFC$ match the published values at similar engine speeds.
- The values for the thrust F are of similar scale and the mismatch of measurement and calculation is less than 10% as in some of the published data.
- The offset of measured and calculated thrust is accounted towards the adding up of measurement errors in the calculation - net thrust was calculated from different measurements as a result of subsequent calculations - as well as to hysteresis in the support mechanism of the engine.
- In comparison f is smaller by a factor of approximately $1/2$ than published values.

It is further noted that some calculations - e.g. for combustion chamber efficiency - were not carried out during the 0D analysis as the measured values by the equipment of the SR-30 were just not as precise to work with. Furthermore, undertaken effort to obtain a cycle efficiency was only giving plausible results for high spool speeds ($n > 70,000$) resulting in thermal efficiencies η_{th} of 3.5 to 8 %.

As seen, the resulting performance parameters are in the range of previously reported runs of the SR-30 at other institutions and also represent a typical jet engine of that scale [41]. The SR-30 is thus characterized in its performance behavior.

3.2. Review of augmented engine performance

Starting from a characterized SR-30 with given performance parameters, the thrust augmenting ejector in its different cases is attached to the engine. In subsequent runs during a time period of some few hours the data for different lengths of the ejector with a mixing chamber inlet displaced by 5 in from the nozzle exit was taken. The runs at four steady spool speeds were conducted for the $D = 3.38$ in inside diameter ejector and for the full, half and quarter length ($L = 24$ in, $L = 12$ in, $L = 6$ in). The measured value of the net thrust as well as the evaluation of the TSFC for each augmentation case is given in table 7 as well as graphically in the plots of figure 21.

n [1/min]	$F_{\text{net, measure}}$ [N]	$TSFC$ [(kg$_{\text{fuel}}$/s)/N]	Φ [−]
	$L = 24$ in		
45,479	15.76	$8.18 \cdot 10^{-5}$	0.9359
59,700	30.89	$5.93 \cdot 10^{-5}$	0.9569
70,286	47.66	$5.41 \cdot 10^{-5}$	0.9746
80,076	74.88	$4.58 \cdot 10^{-5}$	0.9773
	$L = 12$ in		
46,113	16.67	$7.80 \cdot 10^{-5}$	0.9899
60,569	33.62	$5.72 \cdot 10^{-5}$	1.0415
70,156	50.08	$5.16 \cdot 10^{-5}$	1.0241
79,878	77.20	$4.41 \cdot 10^{-5}$	1.0076
	$L = 6$ in		
45,795	15.75	$8.20 \cdot 10^{-5}$	0.9352
60,333	32.33	$6.03 \cdot 10^{-5}$	1.0015
70,294	48.89	$5.38 \cdot 10^{-5}$	0.9997
80,345	76.68	$4.52 \cdot 10^{-5}$	1.0008

Table 7: Results of augmented net thrust, TSFC and Φ for different length cases

As can be seen compared to the given baseline performance the various length cases of the ejector yield different results. Furthermore none of the cases results in the predicted performance with augmentation ratio resulting in around 6 % net thrust gain. Looking at the length of $L = 24$ in which should be the superior version of a non-displaced scenario as predicted before a visible decrease in net thrust over the whole engine speed range is obtained. This results in a augmentation ratio $\Phi < 1$ and thus a net thrust loss compared to the unaugmented case of the nozzle just exhausting to ambient conditions as in the baseline case. Observing the half length ejector of $L = 12$ in a superior thrust gain manifests itself at all engine speeds greater than idle which is also evident in the thrust specific fuel consumption for this case. The resulting augmentation ranges from

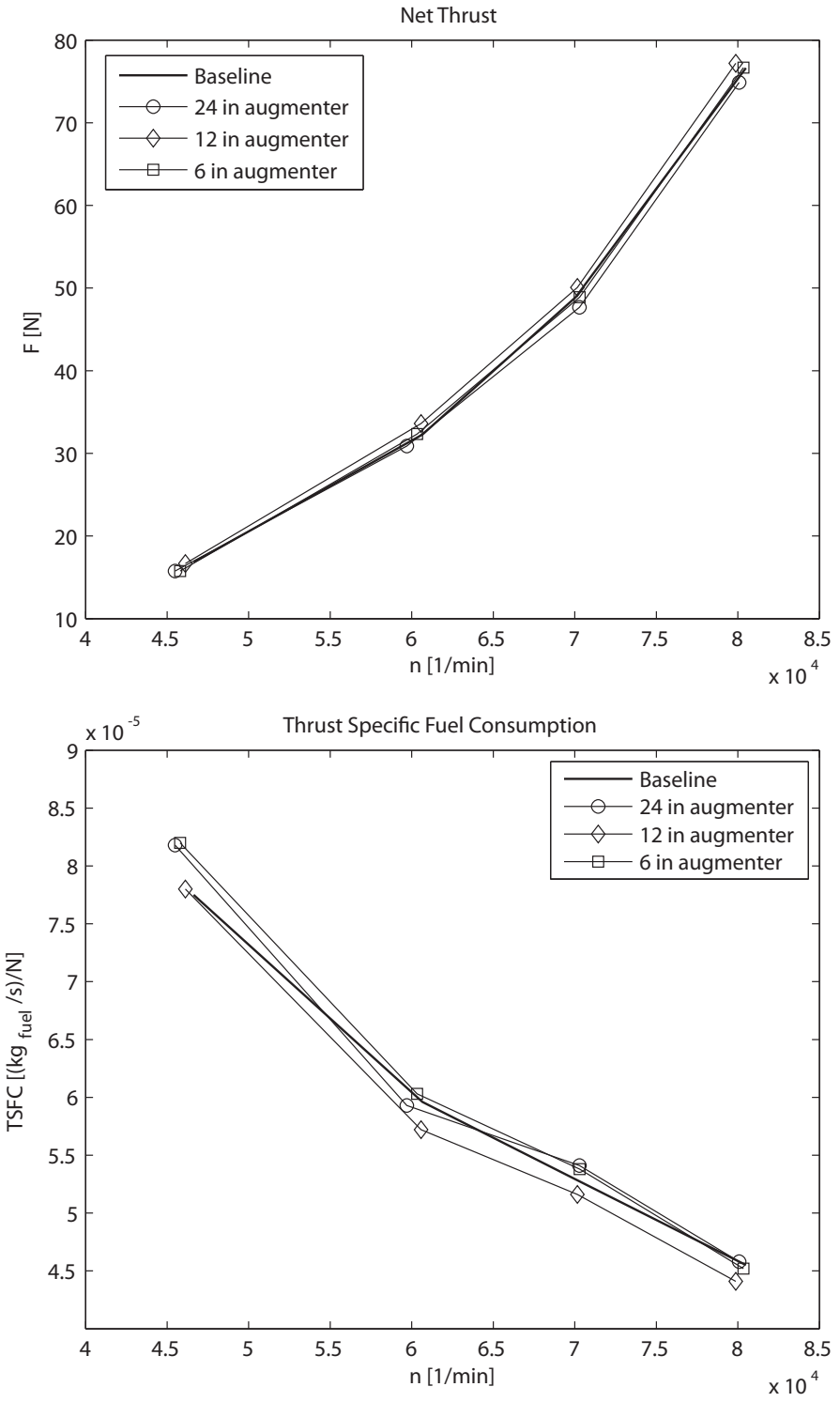

Figure 21: Plots of net thrust and TSFC for the augmented and baseline cases

around 0.75 to 4 % of the value of unaugmented thrust. Finally the quarter length ejector case with $L = 6$ in shows values of net thrust close to the base line and thus $\Phi \approx 1$ - i.e. no augmentation.

Analyzing the above observations of thrust evolution a first conclusion can be drawn that optimal augmentation is not achieved for a mixing chamber length to diameter ratio of $L/D = 7$ ($L = 24$ in) - as theoretically anticipated [16] - but for lower values. The reason for this has to be seen connected to the displacement of the ejector entrance from the primary nozzle - an obvious difference from the studies in prior literature as reviewed before. It can be anticipated, that in the span of 5 in between the nozzle exit and the entrance to the ejector, mixing processes and entrainment in the shear layer of the turbulent jet have already taken place. The resulting lateral spreading of the jet entering the mixing chamber of the ejector has the effect of more momentum that will act on the internal walls resulting in more friction compared to a non-displaced case of the same length. As wall friction is counteracting any thrust gain produced by the suction of the inflowing ambient air over the inlet contour the resulting thrust loss in a displaced case of that magnitude is evident (see section 1.4). In fact, the reduction of thrust for a displaced ejector of $L/D = 7$ has also been shown by the CFD case study done at OSU [38] with similar boundary conditions. The performance of the half length ejector ($L/D = 3.5$, $L = 12$ in) can be reasoned in a similar way as for the full length case. Assuming that mixing is completed earlier than at the location of $L/D = 7$ after the ejector entrance due to the displacement the length can be reduced and thus mixing losses prevented. Additionally, the reduction in length will result in frictional drag reduction and thus the superior result of the half length ejector is reasoned. The dropping performance of the quarter length ejector is reasoned as the length reduction gives a rise in losses due to incomplete mixing - and thus non-uniform exit velocity profile - that creates losses counteracting the further reduction of wall friction and thus the thrust augmentation is brought to a negligible amount. It is noted here that it was subjectively observed, that the radiated noise emissions standing in front of the uncovered MiniLab during all of the augmented runs have been lower than in the un-hooded run of the baseline case and thus a zero thrust gain in the case of $L/D = 1.75$, $L = 6$ in can still be considered valuable as far as noise reduction is concerned.

In the observation of the resulting performance, a second conclusion has to be drawn accounting for the fact that none of the augmentation devices reached the predicted value of 6 % thrust gain. There are various reasons that can be given for this: sup-optimal alignment of the ejector in the exhaust stream resulting in more wall friction, introduced losses at the inlet not captured by the utilized loss coefficients in the calculations, losses associated to unsteady flow phenomena due to vibration of the support mechanism and various other things. One of the more solid reasons for a reduced thrust than anticipated by the prediction for all augmenter cases is the fact of the engine backside walls being exposed to the secondary flow stream. The undertaken CFD result (see annex F.3 and figure 27) from the related case study [38] clearly shows a velocity magnitude around the engine back due to entrained ambient air. In the related discussion of the CFD results

this accounts for $F = 1.56$ in the stream wise direction which reduces the effective thurst gained [38]. As this phenomenon is present in all investigated lengths of the ejector due to the closeness to the engine back surface, the thrust as an effect of the displaced ejector is always lower than in the analysis that does not account for this effect resulting in lower overall augmentation ratio Φ.

3.3. Conclusion

Within the work of this paper the designed thrust augmenting ejector ($\alpha = 1.318$) applied to the SR-30 jet engine was able to deliver a thrust increase of up to 4 % for a 5 in displaced case of $L/D = 3.5$. A longer mixing chamber resulted in increased drag due to mixing already taking place in the offset region between nozzle and ejector entrance. Shorter ejector length resulted in less complete mixing and thus losses associated with this phenomenon. The impact on thrust reduction by a low pressure region effective on the engine backside was also noticed, resulting in augmentation ratios that trend lower than analytically predicted for non-displaced ejectors.

Overall, the application of a passive thrust augmenting device for the SR-30 based on a jet ejector was successfully achieved and results delivered further insight into the flow phenomena and practically achievable augmentation ratios as opposed to previously studied ideal setups. The experimentally observed difference of optimum performance in case of displacement of the ejector inlet plane from the exhaust nozzle (primary flow) is a valuable addition to the results obtained by theoretical analysis in the literature before. Related studies [3] also showed that there is indication for an optimal placement distance of an ejector. This is seen to be related to the fact that the effect of the low pressure region on the engine back side is more sever the closer the ejector is. At the same time the drag due to more momentum at the internal walls related to initial spread of the jet is more severe the further the ejector is displaced. Obviously a distance where those effects balance each other resulting in peak thrust gain has to be present. It is the understanding of this paper that further investigation of the phenomena in the jet spread region and to deliver a closed analysis for displaced cases of jet augmentation can shed additional light into the process and can deliver an extension of the theory for predicting the augmentation ratio in those practical application cases of thrust augmenting ejectors.

Regarding the application to the SR-30 MiniLab, a practical way of attaching a simple thrust augmenting device to the existing engine setup was achieved and the ease of theoretical analysis and the appointment of the basic flow phenomena resulting in the thrust gain makes this ejector configuration a valuable addition in the educational framework of the MiniLab's use at OSU.

Nevertheless the outlined reduction of thrust gain due to pressure forces acting on the backside of the engine also limits the practical application of displaced ejector cases of the classical approach (i.e. without enhanced mixing implemented) further emphasized by the fact that the overall dimensions of this ejector configuration also yield comparably high losses in the non-static case due to drag losses on the inlet contour and outside

walls.

Further investigations in this area should address the application of enhanced mixing and thus further reduction of the overall ejector length and subsequently raise of the secondary to primary flow area ratios α. The application of mixer-ejector-diffuser systems can be seen as an improvement to achieve higher thrust gains with shorter ejector lengths [21]. Also the obtained results of a CFD calculation [38] can be considered further for refinement of the ejector design and evaluation of the effects of ejector displacement on any design applied to the small scale jet engine under practical conditions.

References

[1] Morton Alperin and Jiunn-Jenq Wu. Thrust Augmenting Ejectors, Part I. *AIAA Journal*, 21(10):1428–1436, October 1983.

[2] Morton Alperin and Jiunn-Jenq Wu. Thrust Augmenting Ejectors, Part II. *AIAA Journal*, 21(12):1698–1706, December 1983.

[3] Balla, Benton, Busch, Clum, Lawrence, Long, McQuaide, Watsek, and Whitaker. AFRLPROJECT - Afterburner Research Project. conversations with the team members and observation of the experimental results, January - June 2010.

[4] M. P. Boyce. *Gas Turbine Engineering Handbook, Second Edition*. Gulf Professional Publishing, 2nd edition, 2002.

[5] William S. Campbell and Hans von Ohain. Thrust Augmentation For V/STOL. Technical report, Aerospace Research Laboratories, US Air Force, 1967.

[6] Gregory W. Davis. Modifications of the SR-30 Gas Turbine Experimental Apparatus to Improve Data Accuracy. In *Proceedings of the 2004 American society for engineering education annual conference and exposition*. American Society for Engineering Education, 2004.

[7] N. L. Efremov and A. N. Kraiko. Theory of an Ideal Jet Thrust Augmenter. *Fluid Dynamics*, 39(4):621–632, 2004.

[8] Richard B. Fancher. Low-Area Ratio, Thrust-Augmenting Ejectors. *Journal of Aircraft*, 9(3):243–248, March 1972.

[9] Ken French. Recycled Fuel Performance in the SR-30 Gas Turbine. In *Proceedings of the 2003 American society for engineering education annual conference and exposition*. American Society for Engineering Education, 2003.

[10] E. L. Goldsmith and J. Seddon. *Practical Intake Aerodynamic Design (AIAA Education Series)*. AIAA (American Institute of Aeronautics & Astronautics), 1993.

[11] Gary L. Hackaday. Thrust Augmentation for a small Turbojet Engine, March 1999.

[12] Joseph H. Haritonidis. Advisory Council. Advisory progress reports, Thesis Mentoring, 2009-2010.

[13] W. H. Heiser. Thrust Augmentation. *Journal of Engineering for Power*, 89(1):75–82, 1967.

[14] Patrick Hendrick and Frank Buysschaert. RESEARCH ON SMALL TURBOJET ENGINES. Technical report, Royal Military Academy of Belgium, Dept. of Applied Mechanics, NA NA.

[15] G. Hikiss and J. Callinan. Operating Experience with the Turbine Technologies SR-30 Turbojet Test System. In *Proceedings of the 2002 American Society for Engineering Education Annual Conference and Exposition*. The American Society for Engineering Education, Nashville, TN., 2002.

[16] K.P. Huang and E. Kisielowski. An Investigation of the Thrust Augmentation Characteristics of Jet Ejectors. Technical report, U.S. Army Aviation Materiel Laboratories (USAAVLABS), Fort Eustis, Virginia, April 1967.

[17] Hu Hui, Toshio Kobayashi, Tatsuo Saga, Nobuyuki Taniguchi, Sigeki Segawa, and Akira Ono. Research on the Mixing Enhancement Performance of Lobed Nozzles by using PIV and LIF. In *Proceedings of the 1998 ASME Fluids Engineering Devision Summer Meeting, Washington, DC*. American Society Of Mechanical Engineers, 1998.

[18] James A. Ierardi. Specific heat of air vs. temperature. Website, 2010. Available online at `http://users.wpi.edu/~ierardi/PDF/air_cp_plot.PDF`; visited on May 20th 2010.

[19] C. N. Jones. Ejector Thrust Augmentation - Fact or Fiction? In *Thermofluids Conference 1974, Melbourne*, volume 74/7, pages 91–95. Institution of Engineers, Australia, 1974.

[20] W. Presz Jr. Mixer/ Ejector Noise Suppressors. In *AIAA/ SAE/ ASME 27th Joint Propulsion Conference, Sacramento, CA*. American Institute of Aeronautics & Astronautics, 1991.

[21] W. Presz Jr. Thrust Augmentation Using Mixer-Ejector-Diffuser Systems. In *AIAA Aerospace Sciences Meeting & Exhibit, 32nd, Reno, NV*. American Institute of Aeronautics & Astronautics, 1994.

[22] W. Presz Jr., B. Morin, and R. F. Blinn. Short Efficient Ejector Systems. In *AIAA/ SAE/ ASME/ ASEE 23rd Joint Propulsion Conference*. American Institute of Aeronautics & Astronautics, 1987.

[23] W. Presz Jr., B. Morin, and R. G. Gousy. Forced Mixer Lobes in Ejector Designs. *Journal of Propulsion*, 4(4):350–355, 1986.

[24] W. Presz Jr., G. Reynolds, and C. Hunter. Thrust Augmentation with Mixer/Ejector Systems. In *AIAA Aerospace Sciences Meeting & Exhibit, 40th, Reno, NV*. American Institute of Aeronautics & Astronautics, 2002.

[25] Eli Kedem. An experimental study of static thrust augmentation using a 2D variable ejector, December 1979.

[26] A. L. King and S. T. Bonnington, editors. *Jet Pumps and Ejectors: A State of the Art Review and Bibliography*. Air Science Company, 2nd revised edition edition, 1977.

[27] R. Ramesh Kumar and J. Kurian. Studies on freejets from radially lobed nozzles. *Experiments in Fluids*, 19:95–102, 1995.

[28] William D. Lewis. An Experimental Study of Thrust Augmenting Ejectors, December 1983.

[29] O. Léonard, J. P. Thomas, and S. Borguet. Ten Years of Experience With a Small Jet Engine as a Support for Education. *Journal of Engineering for Gas Turbines and Power*, 2009.

[30] J. Mattingly. *Elements of Gas Turbine Propulsion w/ IBM 3.5' Disk*. McGraw-Hill Science/Engineering/Math, 1st edition, 1996.

[31] Emmanuel Chima Okpara. *Numerical Simulation of Steady and Pulsed Flows Through Thrust Augmenting Ejectors*. PhD thesis, Washington University, December 2008.

[32] H. Perez-Blanco. Activities around the SR-30 Minilab at PSU. In *Proceedings of the 2003 American Society for Engineering Education Annual Conference and Exposition*. The American Society for Engineering Education, Nashville, TN., 2003.

[33] John David Phillips. Temperature and Pressure Effects on Thrust Augmentation, 1974.

[34] A. Pourmovahed, C. M. Jeruzal, and K. D. Brinker. Development of a Jet Engine Experiment for the Energy Systems Laboratory. In *Proceedings of ASME International Mechanical Engineering Congress and Exposition*. American Society of Mechanical Engineers, 2003.

[35] Brian Quinn. Compact Ejector Thrust AUgmentation. *Journal of Aircraft*, 10(8):481–486, August 1973.

[36] Brian Quinn. Ejector Performance at High Temperatures and Pressures. *Journal of Aircraft*, 13(12):948–954, December 1976.

[37] S. G. Reznick and M. E. Franke. Inlet and Diffuser Effects on Thrust Augmenting Ejectors. In *Ejector Workshop for Aerospace Applications, Dayton, Ohio*. Air Force Office of Scientific Research, Flight Dynamics and Aeropropulsion Laboratories of the Air Force Wright Aeronautical Laboratorie, 1982.

[38] Donald Riedeberger, Tessa McAnally, Deena Dembrosky, and Rick Marshall. Passive Thrust Augmentation Using Jet Ejectors - A Study of Heat and Geometry Influences. Poster concluding the CFD analysis undertaken in the course AAE 514 - SPring 2010 at the Department of Aeronautical and Aerospace Engineering of The Ohio State University, June 2010.

[39] Tetsuo Saga, Hui Hu, and Toshio Kobayashi. Mixing Process in the Jet Flow of Lobed Nozzle. In *Proceeding of the 1999 Korea-Japan Joint Seminar on Particle Image Velocimetry*. American Society Of Mechanical Engineers, 1999.

[40] J. C. Sanders and V. L. Brightwell. Analysis of Ejector Thrust by Integration of Calculated Surface Pressures. Technical report, National Advisory Committee for Aeronautics, 1958.

[41] H. I. H. Saravanamuttoo, editor. *Gas Turbine Theory*. Pearson Prentice Hall, 6th edition, 2009.

[42] B. M. Spee, editor. *Technical Evaluation Report on the AGARD Fluid Dynamics Panel Symposium on Fluid Dynamics of Jets with Applications to V/STOL*. NATO, Advisory Group for Aerospace Research & Development - AGARD, 1982.

[43] P. Strykowski and S. White. Characterizing the Performance of the SR-30 Turbojet Engine. In *Proceedings of the 2003 American Society for Engineering Education Annual Conference and Exposition*. The American Society for Engineering Education, Nashville, TN., 2003.

[44] Tah teh Yang, Francois Ntone, Tong Jiang, and D. R. Pitts. An Investigation of High Performance, Short Thrust Augmenting Ejectors. *Journal of Fluids Engineering*, 107:23–30, March 1985.

[45] LTD Turbine Technologies. Sr-30 cross sectional flow areas. Perry A. Kuznar, written conversation.

[46] LTD Turbine Technologies. Contact with manufacturer support. Tom Kutrieb, e-mail conversation, February 2010.

[47] Turbine Technologies, LTD. *Gas Turbine Power System Operator's Manual*, 2005. REVISION 9.05 (1.00).

[48] Gregory Unnever. An Experimental Study of Rectangular and Circular Thrust AUgmenting Ejectors, December 1981.

[49] T. von Karman. Theoretical Remarks on Thrust Augmentation. In *Reissner Anniversary Volume: Contributions to Applied Mechanics*, pages 461–468. J. W. Edwards, Ann Arbor, Michigan, 1949.

[50] Michael J. Werle and Walter M. Presz. New Developments in Shrouds and Augmentors for Subsonic Propulsion Systems. In *Proceeding of the 44th AIAA/ASME/SAE/ASEE Joint Propulsion Conference and Exhibit, Hartford, CT*. American Institute of Aeronautics and Astronautics, 2008.

[51] N. Whitley, A. Krothapalli, and L. Van Dommelen. A Determinate Model of Thrust-Augmenting Ejectors. *Theoretical and Computational Fluid Dynamics*, 8:37–55, 1996.

A. Analytical solution to the engine performance

To determine the performance of the jet engine, the measured data at the key points of the engine needs to be used in a step-by-step calculation of the engine parameters at each stage.
In general, we assume the following things during our calculations:

- air entering the engine is behaving like a perfect gas, $R_\mathrm{s} = 287 \frac{\mathrm{J}}{\mathrm{kgK}}$
- incompressible flow

As with those assumptions we compute the necessary calculations to obtain the engine performance stage by stage as follows.

Ambient condition (Stage 0):
It is assumed that the ambient conditions are known from a measurement of both pressure p_0 and Temperature T_0 in the environment of the engine before its run. Therefore, taken from the ideal gas law

$$\rho_0 = \frac{p_0}{R_\mathrm{s} T_0}. \tag{A.1}$$

Furthermore the relation between the pressure components for a fluid is noted as

$$p_t = p_\mathrm{static} + p_\mathrm{dynamic} = p_\mathrm{static} + \frac{1}{2}\rho u^2 \tag{A.2}$$

and the relation between the values of temperature follows as

$$T_t = T + \frac{u^2}{2c_p}. \tag{A.3}$$

It is noted here that the specific heat capacity c_p is considered to be a function of temperature only for the range of operation in which our working gas is air. Distinct values can either be obtained by referring to charts of $c_p(T)$ or by looking up equivalent polynomial fits of this functional relationship. With the ambient fluid resting at infinity, i.e. $u_0 = 0$ it follows

$$p_{t0} = p_{\mathrm{static}\ 0} = p_0 \tag{A.4}$$

$$T_{t0} = T_0. \tag{A.5}$$

Engine inlet (Stages 1 - 2):
No work is done at the inlet therefore

$$T_{t2} = T_{t1} = T_{t0}. \tag{A.6}$$

Nevertheless, the pressure changes over the inlet and is subject to an efficiency of the inlet namely

$$\eta_\mathrm{inlet} = \frac{p_{t2}}{p_{t1}}. \tag{A.7}$$

Here we will assume the inlet to work ideally, meaning $\eta_{\text{inlet}} = 1$ - a suitable simplification for the testbed environment with no forward movement. So together with the assumption that the total pressure does not change from ambient conditions (0) to the inlet section (1) we get

$$p_{t2} = p_{t1} = p_{t0} \tag{A.8}$$
$$p_{t2} = p_0. \tag{A.9}$$

Compressor inlet (Stage 2):
It follows at the entrance of the compressor using the measured dynamic pressure $p_{\text{static 2}}$ at stage 2

$$p_{t2} = p_0 = p_{\text{static 2}} + p_{\text{dynamic 2}} \tag{A.10}$$
$$p_{\text{static 2}} = p_0 - p_{\text{dynamic 2}}. \tag{A.11}$$

As with this we also get knowledge about the velocity, namely

$$p_{t2} = p_0 = p_{\text{static 2}} + \frac{1}{2}\rho_0 u_2^2 \tag{A.12}$$
$$u_2 = \sqrt{\frac{2\, p_{\text{dynamic 2}}}{\rho_0}}. \tag{A.13}$$

Formulating the sonic velocity as

$$a_2 = \sqrt{\gamma R_{\text{s}} T_2}. \tag{A.14}$$

In the above equation the heat capacity ratio γ has been introduced which can be taken from a relationship between the specific gas constant R_{s} and heat capacity c_p, namely

$$\gamma = \frac{1}{1 - \frac{R_{\text{s}}}{c_p}}. \tag{A.15}$$

We get the Mach number at the compressor inlet

$$M_2 = \frac{u_2}{a_2}. \tag{A.16}$$

The steps to evaluate the volume flow out of the knowledge of the cross section A_2 are

$$\dot{V}_2 = A_2 u_2, \tag{A.17}$$

and the mass flow accordingly with

$$\dot{m}_2 = \rho_0 A_2 u_2 = \rho_0 \dot{V}_2. \tag{A.18}$$

As the thrust of the engine will later be calculated, knowledge about the inlet momentum is necessary and given as

$$F_2 = \dot{m}_2 u_2. \tag{A.19}$$

Concluding calculations for the inlet to the compressor we can note down the enthalpy at this stage by

$$h_2 = c_p T_2. \tag{A.20}$$

Compressor exit (Stage 3):
In addition to the assumptions mentioned before we will continue the analysis inside the engine by neglecting the kinetic energy that the fluid is containing which basically suggests to assume comparably low velocities of the fluid inside of the engine (at the respective stages, not inside the compressor or turbine stator-rotor interaction) so that at each stage the equations for both pressure and temperature, using the assumption of $u \approx 0$, come down to be

$$p_t = p_{\text{static}} + p_{\text{dynamic}} = p_{\text{static}} + \frac{1}{2}\rho_0 u_0^2 \approx p_{\text{static}} \tag{A.21}$$

$$T_t = T + \frac{u^2}{2c_p} \approx T. \tag{A.22}$$

The only known values at the compressor exit are total pressure p_{t3} and Temperature T_3 which can be used to obtain the enthalpy as

$$h_3 = c_p T_3. \tag{A.23}$$

As for the further calculation for the isentropic efficiency of the compressor $\eta_{\text{is,comp}}$ the value of the enthalpy that would be reached if the compressor would work on an ideal isentropic way is needed. Therefore the temperature at the end of such an isentropic process would come out as

$$T_{3,is} = T_2 \left(\frac{p_3}{p_2}\right)^{\left(\frac{\gamma-1}{\gamma}\right)} \tag{A.24}$$

and this will provide the enthalpy at this isentropic state we need for comparative reasons

$$h_{3,is} = c_p T_{3,is}. \tag{A.25}$$

Compressor (Stages 2 - 3):
The calculations before enable us to obtain the work done by the compressor as

$$w_{\text{comp}} = h_3 - h_2, \tag{A.26}$$

as well as the efficiency of the compressor stage that is

$$\eta_{\text{is,comp}} = \frac{w_{\text{comp,is}}}{w_{\text{comp}}} \tag{A.27}$$

$$= \frac{h_{3,is} - h_2}{h_3 - h_2}. \tag{A.28}$$

Turbine inlet (Stage 4):
Similar to calculations before we get the enthalpy as

$$h_4 = c_p T_4. \tag{A.29}$$

Combustion chamber (Stages 3 - 4):
Looking at the combustion chamber as a control volume the balance of enthalpies obviously delivers the efficiency of the combustion process (eqt. (10-1) [4])

$$\eta_{\text{comb.ch.}} = \frac{\Delta h_{\text{actual}}}{\Delta h_{\text{theoretical}}} = \frac{\left(\dot{m}_2 + \dot{m}_{\text{fuel}}\right) h_4 - \dot{m}_2 h_3}{\dot{m}_{\text{fuel}} H_i}. \tag{A.30}$$

Using the measured total pressures the total pressure drop in the combustion chamber can also be calculated as

$$\frac{\Delta p_{\text{comb.ch.}}}{p_{t3}} = \frac{p_{t3} - p_{t4}}{p_{t3}}. \tag{A.31}$$

As it is known the processes relating to this pressure drop are both aerodynamic and thermodynamic in origin.
Turbine exit (Stage 5):
Similar to calculations before we get the enthalpy

$$h_5 = c_p T_5. \tag{A.32}$$

As it has been with evaluating the compressor efficiency also the efficiency of the turbine will be calculated using an isentropic comparison process for which the temperature of the isentropic expansion $T_{5,is}$ needs to be found with

$$T_{5,is} = T_4 \left(\frac{p_5}{p_4}\right)^{\left(\frac{\gamma-1}{\gamma}\right)} \tag{A.33}$$

and this will provide the enthalpy at this isentropic state we need for comparative reasons

$$h_{5,is} = c_p T_{5,is}. \tag{A.34}$$

Turbine (Stages 4 - 5):
The calculations before lead to similar calculations as for the compressor for both work and isentropic efficiency as

$$-w_{\text{turb}} = h_5 - h_4 \tag{A.35}$$

$$\eta_{\text{is,turb}} = \frac{w_{\text{turb}}}{w_{\text{turb,is}}} \tag{A.36}$$

$$= \frac{h_5 - h_4}{h_{5,is} - h_4}. \tag{A.37}$$

Nozzle (Stages 5 - 9):

Regarding the flow through the nozzle with constant mass flow the governing enthalpy relation is

$$h_5 + \frac{1}{2}u_5^2 = h_9 + \frac{1}{2}u_9^2. \tag{A.38}$$

Assuming a dominating velocity at the nozzle exit and therefore $u_5 << u_9$ we rearrange the above to deliver the velocity at the nozzle exit

$$u_9 = \sqrt{2(h_5 - h_9)}. \tag{A.39}$$

Apart from the assumptions inside the engine that the velocity and therefore kinetic energy can be neglected during the calculations, this obviously is not the fact here so we need to find a way to calculate h_9. As the measured sensor data only delivers the stagnation value of the Temperature of the exhaust gas stream we come up with the assumption of *isentropic expansion* in the nozzle to an *ambient pressure* meaning $p_9 = p_0$. This enables as to calculate the temperature following an isentropic process within the nozzle as

$$T_{9,is} = T_5 \left(\frac{p_0}{p_5}\right)^{\left(\frac{\gamma-1}{\gamma}\right)} \tag{A.40}$$

and consequently

$$h_{9,is} = c_p T_{9,is} \tag{A.41}$$

which leads to

$$u_9 = \sqrt{2(h_5 - h_{9,is})}. \tag{A.42}$$

As with the inlet the following equations can be processed

$$a_9 = \sqrt{\gamma R_s T_{9,is}}, \tag{A.43}$$

$$M_9 = \frac{u_9}{a_9}. \tag{A.44}$$

As for the mass flow the solution is taken simply from the summarized flow of air and fuel as

$$\dot{m}_9 = \dot{m}_2 + \dot{m}_{\text{fuel}}. \tag{A.45}$$

This finally enables us to calculate the momentum the exhaust gas delivers as

$$F_9 = \dot{m}_9 u_9. \tag{A.46}$$

And so the net thrust of the engine will be

$$F_{net} = F_9 - F_2 \tag{A.47}$$

$$= \dot{m}_9 u_9 - \dot{m}_2 u_2. \tag{A.48}$$

It is mentioned here that the nozzle is working adapted to ambient pressure - therefore no additional term counts into the thrust equation. Furthermore, as for the whole scope of this paper, the drag losses of any installed setup of the engine in a nacell will just be neglected as no distinct value can be assigned for an unknown configuration.

B. Matlab code for the performance calculation

This section gives the Matlab code that was created for the performance analysis of the SR-30 engine based on the calculation procedure given before.

```
% SR30_05
%
% This program evaluates the data stream coming from the SR-30 Turbojet
% engine.
% Calculations are used NEGLECTING KINETIC ENERGIES
% After the data is read from the input data file PDAQ.MAT the user can set
% the amount of datasets to be extracted from the program by selecting them
% on a graphics output of the temperature plot.
% In the end all results are put out to a tex filecal led result.txt.
%
clear             % clears workspace
close all         % clears all figures
% first some given data as assumed
R = 287; % J/KgK
H_u = 43.15*10^6; %J/Kg for Jet A-1 fuel
roh_fuel = 0.81; % kg/l
% ambient conditions
% subject to adaption regarding values at date of experiment
T0  = input ('ambient temperature in °C');% °C
p0 = input('ambient pressure in inHg');%  inHg
% conversion of ambient conditions
T0  = T0 + 273.15; % K
p0 = p0 * 3386.389; % Pa
% engine cross sections
A_2 = 5.94 * 0.00064516; % m^2 (was 4.75 in^2 before)
A_9 = 3.88 * 0.00064516; % m^2
% loading the measurement data
path = 'PDAQ.mat';
open (path);    % opens the data where the measurents are saved
A=ans.A;        % get out Matrix A from the loaded data
Pressures(:,1:5)=A(:,1:5);      % extract all data to separate matrices
Temperatures (:,1:5)=A(:,9:13);
Fuel(:,1)=A(:,6);
RPM(:,1)=A(:,7);
Thrust(:,1)=A(:,8);
% frequency of data aquisiton
freq=0.72; % in Hz
x_end=numel(RPM);
x=[1:1:x_end];
x=x*freq;
% plot  the temperature
figure
plot(x,Temperatures(:,1),'b',x, Temperatures(:,2),'g',x, Temperatures(:,3),'r',x,↩
    Temperatures(:,4),'m',x,Temperatures(:,5),'k')
title('Temperatures')
legend('T_{t2}','T_{t3}','T_{t4}', 'T_{t5}', 'T_{t9}')
xlabel('t [s]')
ylabel('T [°C]')
% input
intervals = input('How many intervals? ');   % number of intervals to evaluate
offset = input('Is there an offset (Yes 1/ No 0)?');
intervals = intervals +offset;
% allocating the arrays
RPM_mean = zeros(intervals,1);
T_t2 = zeros(intervals,1);
T_t3 = zeros(intervals,1);
```

```
T_t4 = zeros(intervals,1);
T_t5 = zeros(intervals,1);
T_t9 = zeros(intervals,1);
p_d2 = zeros(intervals,1);
p_t3 = zeros(intervals,1);
p_t4 = zeros(intervals,1);
p_t5 = zeros(intervals,1);
p_t9 = zeros(intervals,1);
ff = zeros(intervals,1);
F_measure = zeros(intervals,1);
for i=1:intervals
    I=ginput(2);
    a = round(I(1,1)/freq);  % start of the respective interval i
    b = round(I(2,1)/freq);  % end of interval i
    % calculating the mean values of all necessary measurements
    RPM_mean(i,1)=mean(RPM(a:b));
    % using international notation of engine stages
    % T_amb = T0, T_inlet = T1, T_comp_inlet = T2, ...
    % also converted in Kelvin (0 C = 273.15 K)
    T_t2(i,1)=mean(Temperatures(a:b,1))+273.15;
    T_t3(i,1)=mean(Temperatures(a:b,2))+273.15;
    T_t4(i,1)=mean(Temperatures(a:b,3))+273.15;
    T_t5(i,1)=mean(Temperatures(a:b,4))+273.15;
    T_t9(i,1)=mean(Temperatures(a:b,5))+273.15;
    % assume pressures to be stagnation exept for:
    % p2=pitot-static=dynamic, p4=static
    % pressures are also converted from psig to psi and then to Pa
    % psi = psig + psi(atm), 1 psi = 6.8948*10^3 Pa
    p_d2(i,1) = mean(Pressures(a:b,1))*6.8948*10^3;
    p_t3(i,1) = mean(Pressures(a:b,2))*6.8948*10^3+p0;
    p_t4(i,1) = mean(Pressures(a:b,3))*6.8948*10^3+p0;
    p_t5(i,1) = mean(Pressures(a:b,4))*6.8948*10^3+p0;
    p_t9(i,1) = mean(Pressures(a:b,5))*6.8948*10^3+p0;
    ff(i,1) = mean(Fuel(a:b))*3.78541178 * 0.81 /(60*60); % kg/s
    % 1 lbs = 4.448222 N
    F_measure(i,1)=mean(Thrust(a:b))*4.448222; % in N
end
close;
% deleting offset
if offset >0;
for i=2:intervals
    RPM_mean(i,1)=RPM_mean(i,1)-RPM_mean(1,1);
%     T_t2(i,1)=T_t2(i,1)-T_t2(1,1);
%     T_t3(i,1)= T_t3(i,1)- T_t3(1,1);
%     T_t4(i,1)= T_t4(i,1)-  T_t4(1,1);
%     T_t5(i,1)= T_t5(i,1) - T_t5(1,1);
%     T_t9(i,1)= T_t9(i,1)- T_t9(1,1);
%     p_d2(i,1) = p_d2(i,1)-p_d2(1,1);
%     p_t3(i,1) = p_t3(i,1)- p_t3(1,1);
%     p_t4(i,1) = p_t4(i,1)- p_t4(1,1);
%     p_t5(i,1) = p_t5(i,1)- p_t5(1,1);
%     p_t9(i,1) = p_t9(i,1)- p_t9(1,1);
    ff(i,1) = ff(i,1)-ff(1,1);
    F_measure(i,1)=F_measure(i,1)-F_measure(1,1);
end
end
% calculations at each stage
% ambient
roh_0 = p0 /(R*T0); % kg/m^3
p_t0 = p0;
% inlet
eta_inlet = 1;
p_t2= p0;
```

```
% comp inlet
p_s2 = p_t2 - p_d2;
v_2 = sqrt(2*p_d2/roh_0);
c_p2=1.9327E-10*T_t2.^4 - 7.9999E-07*T_t2.^3 + 1.1407E-03*T_t2.^2 - 4.4890E-01*T_t2 +↩
     1.0575E+03;
gamma_2 = 1./(1-R./c_p2);
T_2 = T_t2 - v_2.^2./(2*c_p2);
a_2 = sqrt(gamma_2 * R .* T_2);
Ma_2 = v_2./a_2;
vol_flow_2 = A_2 .* v_2;
m_flow_2 = roh_0 .* vol_flow_2;
F_2 = m_flow_2 .* v_2;
h_t2= c_p2 .* T_t2;
%%%%%
% alternative approach to v_2 via enthalpy
% c_p0=1.9327E-10*T0^4 - 7.9999E-07*T0^3 + 1.1407E-03*T0^2 - 4.4890E-01*T0 + 1.0575E↩
    +03;
% h_0 = c_p0*T0;
% v_2_alt = sqrt(2*(h_0-h_t2));
%%%%%
% comp exit
c_p3=1.9327E-10*T_t3.^4 - 7.9999E-07*T_t3.^3 + 1.1407E-03*T_t3.^2 - 4.4890E-01*T_t3 +↩
     1.0575E+03;
h_t3 = c_p3 .* T_t3;
T_t23 = (T_t2+T_t3)/2;
c_p23=1.9327E-10*T_t23.^4 - 7.9999E-07*T_t23.^3 + 1.1407E-03*T_t23.^2 - 4.4890E-01*↩
    T_t23 + 1.0575E+03;
gamma_23 = 1./(1-R./c_p23);
T_t3s = T_t2 .* (p_t3./p_s2).^((gamma_23-1)./gamma_23);
c_p3s=1.9327E-10*T_t3s.^4 - 7.9999E-07*T_t3s.^3 + 1.1407E-03*T_t3s.^2 - 4.4890E-01*↩
    T_t3s + 1.0575E+03;
h_t3s = c_p3s .* T_t3s;
% compressor
eta_comp = (h_t3s - h_t2)./(h_t3-h_t2);
%turbine inlet
% now fuel is added, but for simplicity, we keep the cp calues for pure air
c_p4=1.9327E-10*T_t4.^4 - 7.9999E-07*T_t4.^3 + 1.1407E-03*T_t4.^2 - 4.4890E-01*T_t4 +↩
     1.0575E+03;
h_t4 = c_p4 .* T_t4;
% combustion chamber
q_cc = ff * H_u;
dp_cc = (p_t3-p_t4)./p_t3;
% turb exit
c_p5=1.9327E-10*T_t5.^4 - 7.9999E-07*T_t5.^3 + 1.1407E-03*T_t5.^2 - 4.4890E-01*T_t5 +↩
     1.0575E+03;
h_t5 = c_p5 .* T_t5;
T_t45 = (T_t4+T_t5)/2;
c_p45=1.9327E-10*T_t45.^4 - 7.9999E-07*T_t45.^3 + 1.1407E-03*T_t45.^2 - 4.4890E-01*↩
    T_t45 + 1.0575E+03;
gamma_45 = 1./(1-R./c_p45);
T_t5s = T_t4 .* (p_t5./p_t4).^((gamma_45-1)./gamma_45);
c_p5s=1.9327E-10*T_t5s.^4 - 7.9999E-07*T_t5s.^3 + 1.1407E-03*T_t5s.^2 - 4.4890E-01*↩
    T_t5s + 1.0575E+03;
h_t5s = c_p5s .* T_t5s;
% turbine
eta_turb = (h_t5-h_t4)./(h_t5s-h_t4);
% nozzle exit
p_s9 = p0;
p_d9 = p_t9 - p_s9;
% assume adiabatic expansion in nozzle to p_s9=p0
T_t59 = (T_t5+T_t9)/2;
c_p59=1.9327E-10*T_t59.^4 - 7.9999E-07*T_t59.^3 + 1.1407E-03*T_t59.^2 - 4.4890E-01*↩
    T_t59 + 1.0575E+03;
```

```
gamma_59 = 1./(1-R./c_p59);
T_9s = T_t5.*(p_s9./p_t5).^((gamma_59-1)./gamma_59);
c_p9s=1.9327E-10*T_9s.^4 - 7.9999E-07*T_9s.^3 + 1.1407E-03*T_9s.^2 - 4.4890E-01*T_9s ↩
    + 1.0575E+03;
h_9s = c_p9s .* T_9s;
v_9 = sqrt(2*(h_t5-h_9s));
m_flow_9 = m_flow_2 + ff;
F_9 = m_flow_9 .* v_9;
F_net = F_9 - F_2;
c_p9=1.9327E-10*T_t9.^4 - 7.9999E-07*T_t9.^3 + 1.1407E-03*T_t9.^2 - 4.4890E-01*T_t9 +↩
     1.0575E+03;
gamma_2 = 1./(1-R./c_p9);
T_9 = T_t9 - v_9.^2./(2*c_p9);
a_9 = sqrt(gamma_2 * R .* T_9);
Ma_9 = v_9./a_9;
%%%%%
% alternatively you can use the massflow at the exit and the assumed static
% Temperature T_9s to get the same velocity
% v_9_alt = (m_flow_9*R.*T_9s)./(A_9*p_s9);
% roh_9 = (2*p_d9./v_9.^2);
% roh_9_alt = (2*p_d9./v_9_alt.^2);
%%%%%
% cycle calculations
a_comp = h_t3-h_t2;
a_turb = h_t5-h_t4;
W_comp = (m_flow_2).*a_comp;
W_turb = (m_flow_9).*a_turb;
W_cycle = abs((m_flow_9).*a_turb) - (m_flow_2).*a_comp ;
eta_th_cycle = W_cycle./((m_flow_9).*h_t4-m_flow_2.*h_t3);
eta_th_cycle_v = (0.5*v_9.^2)./(q_cc);
eta_carnot = 1-T0./T_t4;
% combustion chamber efficiency
eta_cc = ((m_flow_9).*h_t4-m_flow_2.*h_t3)./(q_cc);
% various calculations
Pi_c=p_t3./p_t2;
Pi_t=p_t4./p_t5;
f=ff./m_flow_2;
TSFC = ff./F_measure;
% Exporting results to a text file
f_id = fopen('result.txt', 'w+');
% Print data to file
if offset>0
    a=2;
else
    a=1;
end
fprintf(f_id,'--- Results ---\r\n');
fprintf(f_id,'-------------------------------------------------------------------\r\n');
fprintf(f_id,'%11s\t%11s\t%13s\t%8s\r\n', 'RPM [1/min]', 'm_air [kg/s]', 'm_fuel [kg/↩
    s]', 'f [-]');
for i = a:intervals
fprintf(f_id,'%11.0f\t%11.4f\t%13.5f\t%8.5f\r\n', RPM_mean(i,1), m_flow_2(i,1), ff(i↩
    ,1), f(i,1));
end
fprintf(f_id,'-------------------------------------------------------------------\r\n');
fprintf(f_id,'%8s\t%9s\t%8s\r\n', 'Pi_c [-]', 'dp_cc [-]', 'Pi_t [-]');
for i = a:intervals
fprintf(f_id,'%8.2f\t%9.4f\t%8.2f\r\n', Pi_c(i,1), dp_cc(i,1), Pi_t(i,1));
end
fprintf(f_id,'-------------------------------------------------------------------\r\n');
fprintf(f_id,'%9s\t%9s\t%9s\r\n', 'eta_c [-]', 'eta_cc [-]', 'eta_t [-]');
for i = a:intervals
fprintf(f_id,'%9.2f\t%9.2f\t%9.2f\r\n', eta_comp(i,1), eta_cc(i,1), eta_turb(i,1));
```

```
end
fprintf(f_id,'-------------------------------------------------------------------\r\n');
fprintf(f_id,'%8s\t%8s\t%20s\r\n', 'F_net [N]', 'F_msr [N]', 'TSFC [(kg fuel/s)/N]');
for i = a:intervals
fprintf(f_id,'%8.2f\t%8.2f\t%20.3E\r\n', F_net(i,1), F_measure(i,1), TSFC(i,1));
end
fprintf(f_id,'-------------------------------------------------------------------\r\n');
fprintf(f_id,'%8s\t%8s\t%8s\r\n', 'W_c', 'W_t', 'eta_th');
for i = a:intervals
fprintf(f_id,'%8.0f\t%8.0f\t%8.4f\r\n', W_comp(i,1), W_turb(i,1), eta_th_cycle(i,1));
end
fprintf(f_id,'-------------------------------------------------------------------\r\n');
fprintf(f_id,'%8s\t%8s\t%8s\t%8s\r\n', 'v_2', 'M_2', 'v_9', 'M_9');
for i = a:intervals
fprintf(f_id,'%8.2f\t%8.2f\t%8.2f\t%8.2f\r\n', v_2(i,1), Ma_2(i,1), v_9(i,1), Ma_9(i↩
    ,1));
end
fprintf(f_id,'\r\n--- Measurements ---\r\n');
fprintf(f_id,'-------------------------------------------------------------------\r\n');
fprintf(f_id,'%8s\t%13s\t%10s\r\n', 'RPM [1/min]', 'm_fuel [kg/s]', 'F_net [N]');
for i = a:intervals
fprintf(f_id,'%8.0f\t%13.5f\t%10.2f\r\n', RPM_mean(i,1), ff(i,1), F_measure(i,1));
end
fprintf(f_id,'-------------------------------------------------------------------\r\n');
fprintf(f_id,'%8s\t%8s\t%8s\t%8s\t%8s\r\n', 'T_t2 [K]', 'T_t3 [K]', 'T_t4 [K]', 'T_t5↩
    [K]', 'T_t9 [K]');
for i = a:intervals
fprintf(f_id,'%8.2f\t%8.2f\t%8.2f\t%8.2f\t%8.2f\r\n', T_t2(i,1), T_t3(i,1), T_t4(i,1)↩
    , T_t5(i,1), T_t9(i,1));
end
fprintf(f_id,'-------------------------------------------------------------------\r\n');
fprintf(f_id,'%8s\t%8s\t%8s\t%8s\t%8s\r\n', 'p_d2 [Pa]', 'p_t3 [Pa]', 'p_t4 [Pa]', '↩
    p_t5 [Pa]', 'p_t9 [Pa]');
for i = a:intervals
fprintf(f_id,'%8.1f\t%8.1f\t%8.1f\t%8.1f\t%8.1f\r\n', p_d2(i,1), p_t3(i,1), p_t4(i,1)↩
    , p_t5(i,1), p_t9(i,1));
end
fprintf(f_id,'\r\n--- Input Values ---\r\n');
fprintf(f_id,'-------------------------------------------------------------------\r\n');
fprintf(f_id,'%9s\t%7s\t%8s\t%15s\t%10s\t%9s\t%9s\r\n', 'R [J/kgK]', 'T_0 [K]', 'p_0 ↩
    [Pa]', 'rho_fuel [kg/l]', 'H_u [J/kg]', 'A_2 [m^2]', 'A_9 [m^2]');
fprintf(f_id,'%9.3f\t%7.2f\t%8.1f\t%15.4f\t%10.0f\t%9.8f\t%9.8f\r\n', R, T0, p0, ↩
    roh_fuel, H_u, A_2, A_9);
% Close a file:
fclose(f_id);
% ask for plotting graphs
plotting = input('Should the graphs be plotted?');
if plotting>0
figure
subplot(3,1,1)
plot(x,RPM)
title('RPM')
xlabel('t [s]')
ylabel('RPM [1/min]')
axis ([x(1) x(x_end) 0 85000])
subplot(3,1,2)
plot(x,Fuel)
title('Fuel Flow')
xlabel('t [s]')
ylabel('m_{fuel} [gal/h]')
axis ([x(1) x(x_end) 0 5])
subplot(3,1,3)
plot(x,Thrust)
```

```
title('Thrust')
xlabel('t [s]')
ylabel('F_{net} [Lbs.]')
axis ([x(1) x(x_end) 0 20])
figure
subplot(2,1,1)
plot(x,Temperatures(:,1),'b-',x,Temperatures(:,2),'g-',x,Temperatures(:,3),'r-',x,↩
    Temperatures(:,4),'m-',x,Temperatures(:,5),'k-')
title('Temperatures')
legend('T_{t2}','T_{t3}','T_{t4}', 'T_{t5}', 'T_{t9}')
xlabel('t [s]')
ylabel('T [°C]')
axis ([x(1) x(x_end) 0 700])
subplot(2,1,2)
plot(x,Pressures(:,1),'b-',x,Pressures(:,2),'g-',x,Pressures(:,3),'r-',x,Pressures↩
    (:,4),'m-',x,Pressures(:,5),'k-')
title('Pressures')
legend('p_{d2}','p_{t3}','p_{t4}', 'p_{t5}', 'p_{t9}')
xlabel('t [s]')
ylabel('p [psig]')
axis ([x(1) x(x_end) 0 30])
end
```

C. Senior student laboratory experiment

The gas turbine has revolutionized both the way nowadays energy is converted and aircrafts are propelled. Its high power-to-weight density as well as its intermittent work cycle are reasons for this. Although the performance of an engine can be evaluated approaching from the geometry of the component level (during the design stage) the necessity to measure the actual capabilities of a built engine by test runs is essential to obtain data of the real engine performance.

With the necessity to assure a pressure level above ambient within the engine that can be expanded to gain work the most simple gas turbine cycle can be constructed by the components of a compressor, a combustion chamber and a turbine. Those three components, put together in a Brayton (or Joule) cycle - figure 22 - follow a simple scheme: isentropic compression, isobaric heat addition, isentropic expansion, isobaric heat rejection which are outlined in the As the ideal cycle is an assumption the processes

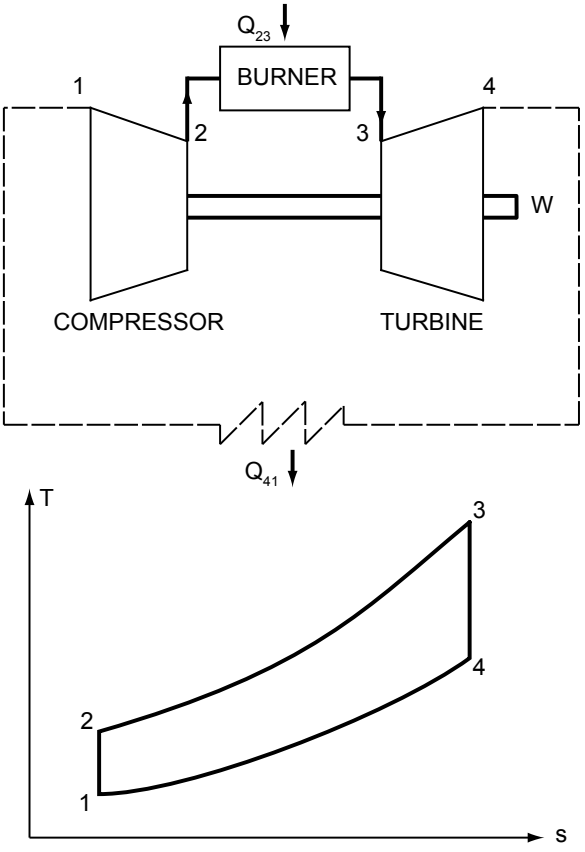

Figure 22: Standard Brayton cycle

of compression (adiabatic), combustion (pressure drop) and expansion (adiabatic) will be subject to losses. Depending on the purpose of usage of the gas turbine, e.g. creating

a high velocity exhaust gas stream, the components (exhaust nozzle) can be adapted to assure this. Taking into consideration the equations of conservation of mass and energy over specified control volumes (e.g. over the compressor) an energy balance can be specified and thus efficiencies can be calculated as outlined in the calculations of the previous chapter.

C.1. Objective of the laboratory

The aim of this laboratory is to get familiar with the basic Brayton-Cycle that a single-spool jet engine uses to create a high velocity exhaust gas jet for propulsion needs. The outlined ideas and procedures build a solid base for an implementation of the SR-30 jet engine into the laboratories undertaken in the course work of senior students in aerospace engineering at the respective department at The Ohio State University.

In their theoretical preparation the students should become familiar with what they can expect during the experiment. Within the laboratory itself they will face the real data that, together with calculations of performance, show them what limitations exist when the assumptions and idealizations made in theoretical analysis meet real engine behavior. The tasks as outlined in this section aim for creating awareness of the following topics:

- To understand the process of a Brayton-Cycle and the application of the necessary equations to analyze it.
- To familiarize the students with ho a single spool turbo jet engine is operated.
- To theoretically determine the values of net thrust, component efficiencies and overall cycle efficiency.
- To visualize the effect that spool speed has on net thrust, TSFC and fuel to air ratio as well as on component efficiencies.

To achieve those aims the following chapters contains the suggested tasks for students to prepare, work and summarize the experiment and also a laboratory guideline for operation through the teaching personal is given.

C.2. Preparations, experiment, analysis

To evaluate the performance the student needs to be familiar with the Brayton-Cycle and the equations that describe it. To assure this, some preparation can be based on the following tasks and questions that the students should answer and prepare prior to the experiment:

- Draw a schematic of a single-spool engine with the international notation of stages (0 to 9).

- Sketch an ideal Brayton-Cycle (T,s-diagram) for a single-spool jet engine (stages 0 to 9) similar to the SR30.
- Show, in a sketch of a Brayton-Cycle with losses, which parts of the cycle will look different from ideal behavior.
- Determine the fuel you are using to power the system. (energy content per unit volume, density)
- Compare this fuel to other fuels used in the aerospace industry.
- How can the mass flow be measured using the pressure measurements at the inlet (pitot-static probe) and the exhaust (pitot probe)? Prepare the equations.
- What is the present barometric pressure in your area?
- Why would barometric pressure be important when planning to operate the Gas Turbine System?
- What is another possible reliable source for accurate barometric pressure readings?
- Other than time, what is another measured variable that would be useful to plot the other measured values against?

With those questions answered the awareness of the topics necessary to understand the experiment should be well risen to assure that the students benefit from the laboratory.

During the laboratory experiment the students need to carefully follow the instructions of the teaching personal. To deliver all data necessary for later analysis the following steps should be taken by the students:

- Find the barometric pressure and room temperature (necessary to calculate ambient conditions).
- Get familiar with the SR-30 MiniLab setup and its operation - told by the instructor.
- Observe the run of the engine (approx. 5 min data, intervals for different RPM < 80,000).
- Observe the recorded data after the recording (program automatically collects data stream to ascii, .dat, or .m files).
- Discuss the observations (net thrust, engine speed, pressure levels, temperatures).
- Copy the data set for later analysis.

Later on, after the experiment has been done the students need to analyze the data they obtained by mainly following the given steps below.

- Plot the data (by choice either with Matlab code or Excel).
- Analyze steady state data interval. Pick three intervals of a steady RPM to analyze and mark analysis points in the plots.
- Use charts and tables to evaluate the value of c_p for each point in the turbine (note: there is a dependency on both Temperature and fuel-air-ratio)
- Analyze the system: Enthalpies, specific works, net work, thermal efficiency of cycle.
- Calculate the specific works and efficiencies of compressor and turbine
- Calculate the exit velocity, mass flow rate and thrust as well as the overall efficiency
- Draw a conclusion. Comment on any offset between expected theoretical and measured/calculated values)

With this post processing of the data the experiences of the laboratory experiment are well complemented and together with the preparations the students get a good understanding on how the basic jet engine cycle works, what the offset of the real cycle performance is and how nowadays propulsion systems are working.

C.3. Utilizing the SR-30 MiniLab

The SR-30 jet engine as equipped in the MiniLab at the department at OSU is a self contained jet engine test bed that can be operated from the main panel. In addition it has data acquisition possibility streaming to a PC via USB connection and the post-processing delivering the sensor data plots, performance calculations and result printouts using a Matlab procedure is also given. The following outline presents what steps have to be taken to assure a successful and secure run of the SR-30 MiniLab.

The procedure given here should also be seen as an addition to the instructions as given in the manual to the MiniLab [47] that are also made available as laminated print outs in the laboratory area. Furthermore the occurrence of any not normal events should immediately be answered by a shut down of the engine using the red push button on the operator panel and the key master switch turned off.

Preparations
Before a start of the engine can be facilitated the following things need to be done and no start should be undertaken without clearly proceeding through this list:

1. Control area, turn on exhaust fan.
2. Control availability of fire extinguisher.
3. Check level of fuel in reservoir of the MiniLab
4. Check level of oil in the reservoir.
5. Inspect the MiniLab components visually and control the wheel brakes.
6. Clean the spark plug (soothing particles).
7. Connect the MiniLab to the external air compressor (Porter Cable).
8. Connect air compressor to power, close draining valve and switch on the compressor.
9. Check the valve of the compressor to be set to at least 120 psi.
10. Connect the power supply to the MiniLab.
11. Connect the USB cable to the MiniLab and to the Computer
12. Switch on the MiniLab using the Key.
13. Control that all displays are reading properly.
14. Start the computer. Open the Program personal DAQ-View.

Note that the compressor will automatically shut down as soon as the chosen pressure at the valve is reached. Any person within range of the engine needs to be briefed on safety procedures. Before the engine is started is also the right moment to note down ambient pressure and temperature for the post-processing calculations (they are necessary to obtain the ambient air density from the ideal gas law).

Start, Running, Stop
Given the previous preparations the engine is now in operational status ready to be started. Immediately prior to the run the following things should be done.

1. Check if the air pressure indicator on the MiniLab operation panel reads a value greater or equal to $120psi$ - do not attempt a start with lower pressure supply.
2. Start the data recording by pressing the play button and the manual trigger on the main window. Wait for calibration and then activate all graphical panels by pushing their play button.
3. Apply ear and other personal protection.

Only with all of the previous things checked and done a successful start can be undertaken with the following steps of operation.

1. Push the green start button.
2. Check that engine speed goes up fast as air pressure drops.
3. Observe ignition flame.
4. If engine does not ignite within 10 - 25 seconds stop procedure.
5. If engine reaches idle (45,000 -48,000 RPM) the engine can be operated using the thrust lever as necessary.
6. When the engine run is about to be ended, put thrust lever back to idle.
7. Wait for RPM to return to 45,000 - 48,000 and for turbine inlet temperatures to drop visibly.
8. To shut down, press the red button.

After shut down the engine should be further observed and caution needs to be taken as components are still hot - danger of injury. The data acquisition procedure can be ended after the engine shut down doing the following:

1. Click the stop button on the main window of the software.
2. Answer any possible prompt with YES.
3. Close the program.
4. Open the folder DATA (link on desktop) and create a new folder named with the current data and run number. Move all folders and data previously recorded (i.e. of recent date) into your created folder.

The last given step assures a clear data archiving structure and prevent the overwriting of previously taken data by a next run of the acquisition program.

After run procedure
To view the data recorded the program ez-post-acquisition viewer can be used or the Matlab procedure can directly be called - both shortcuts are on the desktop of the laboratory computer. The following steps show how a typical data post processing can be done with the given programs.

1. Copy the PDAQ.mat file from the folder of the recorded data you want to analyze to the desktop.

2. Open the the Matlab program *SR-30 performance* with the link on the desktop.
3. Execute the Matlab routine.
4. Enter ambient pressure and temperature as prompted.
5. Observe how many steady intervals there are (other than the pre-start plateau) in the plotted temperature sensor data.
6. Enter how many steady intervals there are and if an offset should be taken from the pre-startup phase of the data recorded (1 or 0).
7. In the plot mark each interval's start and end point by a single left click on each respective point. If an off-set should be taken, mark the offset region first.
8. If you want to plot the sensor data, answer the prompted question with 1, if not, answer 0.
9. Observe the results from the results text file saved on the desktop.

After all necessary runs have been done and the data acquisition is completed the Mini-Lab needs to be treated as follows to assure a safe rest until a next restart.

1. Switch off the MiniLab, detach the maser key.
2. Disconnect the power supply and the USB connection from the MiniLab.
3. Shut off and disconnect the air compressor from the power supply.
4. Drain the Compressor reservoir by opening the valve on the bottom. If the valve does not open easily, release main pressure using the pulling valve on top of the reservoir.
5. Disconnect the air pressure hose from the MiniLab.
6. Shut down the PC and close the Laboratory test cell.

The engine is now out of operational status and can securely rest in the test cell until a next start following the procedure list from the very top.

D. Technical drawings

This sections holds the technical drawings needed to produce the support mechnism.

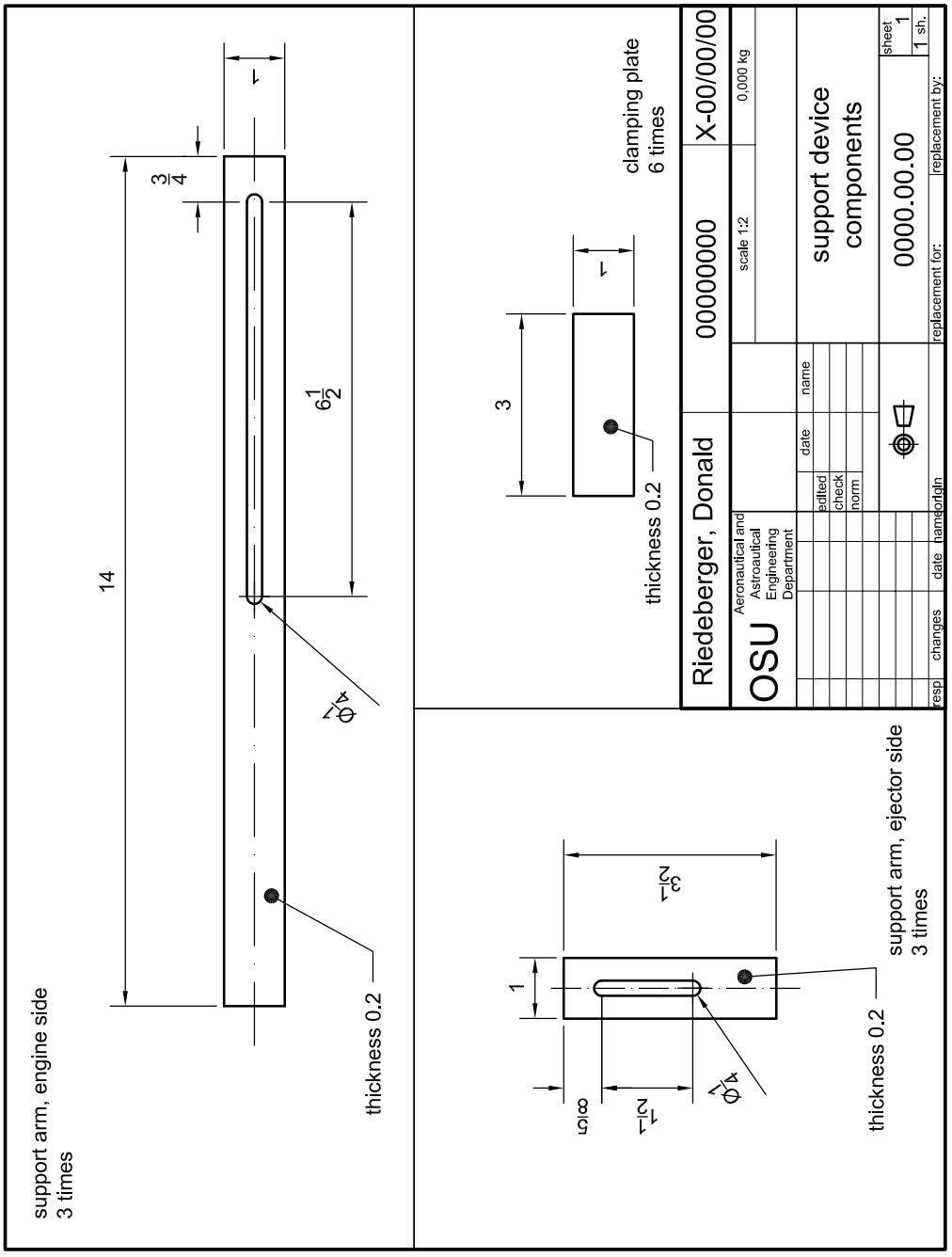

Figure 23: Support mechanism parts - technical drawing not to scale

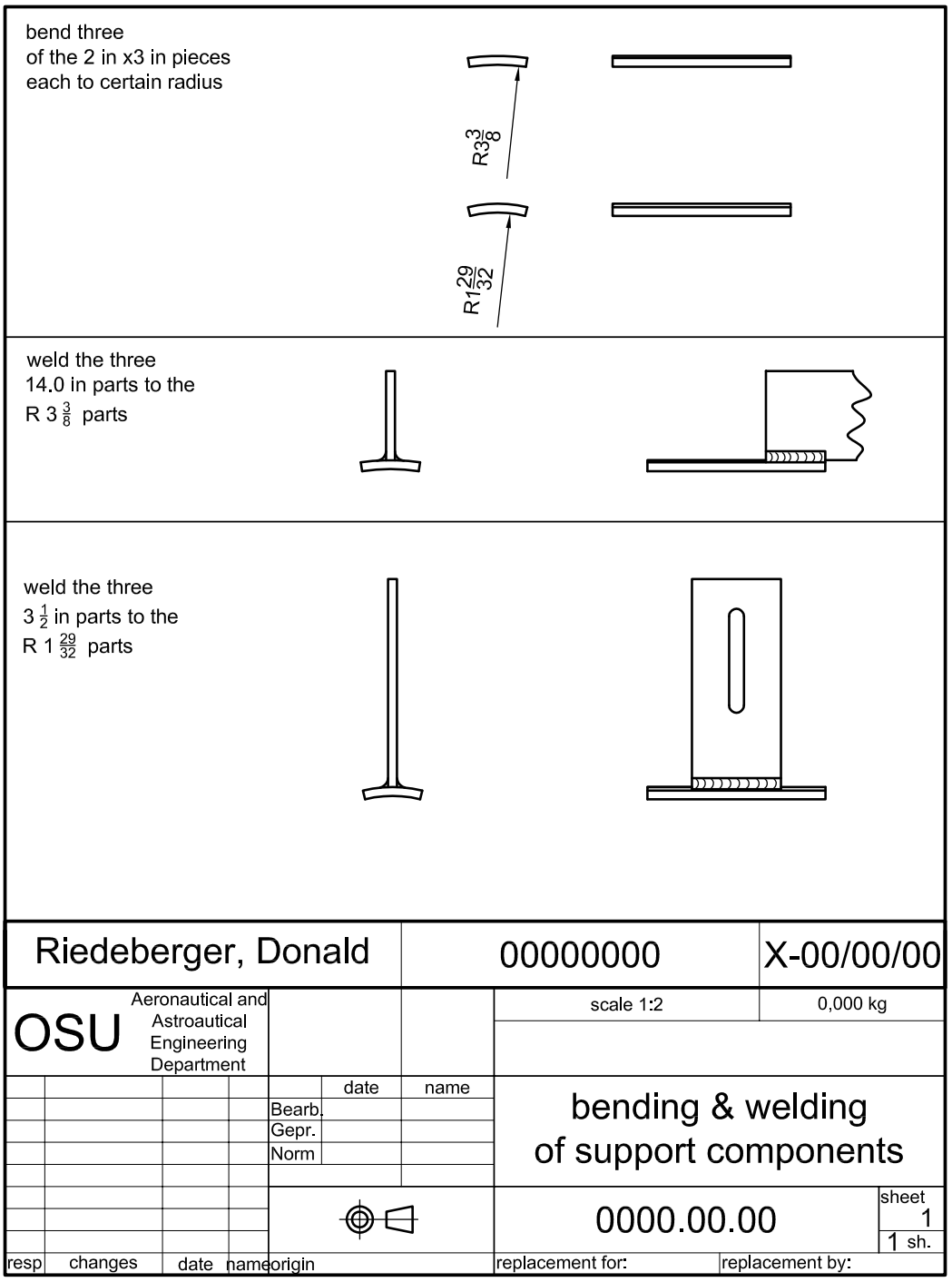

Figure 24: Support mechanism bending and welding instructions - technical drawing not to scale

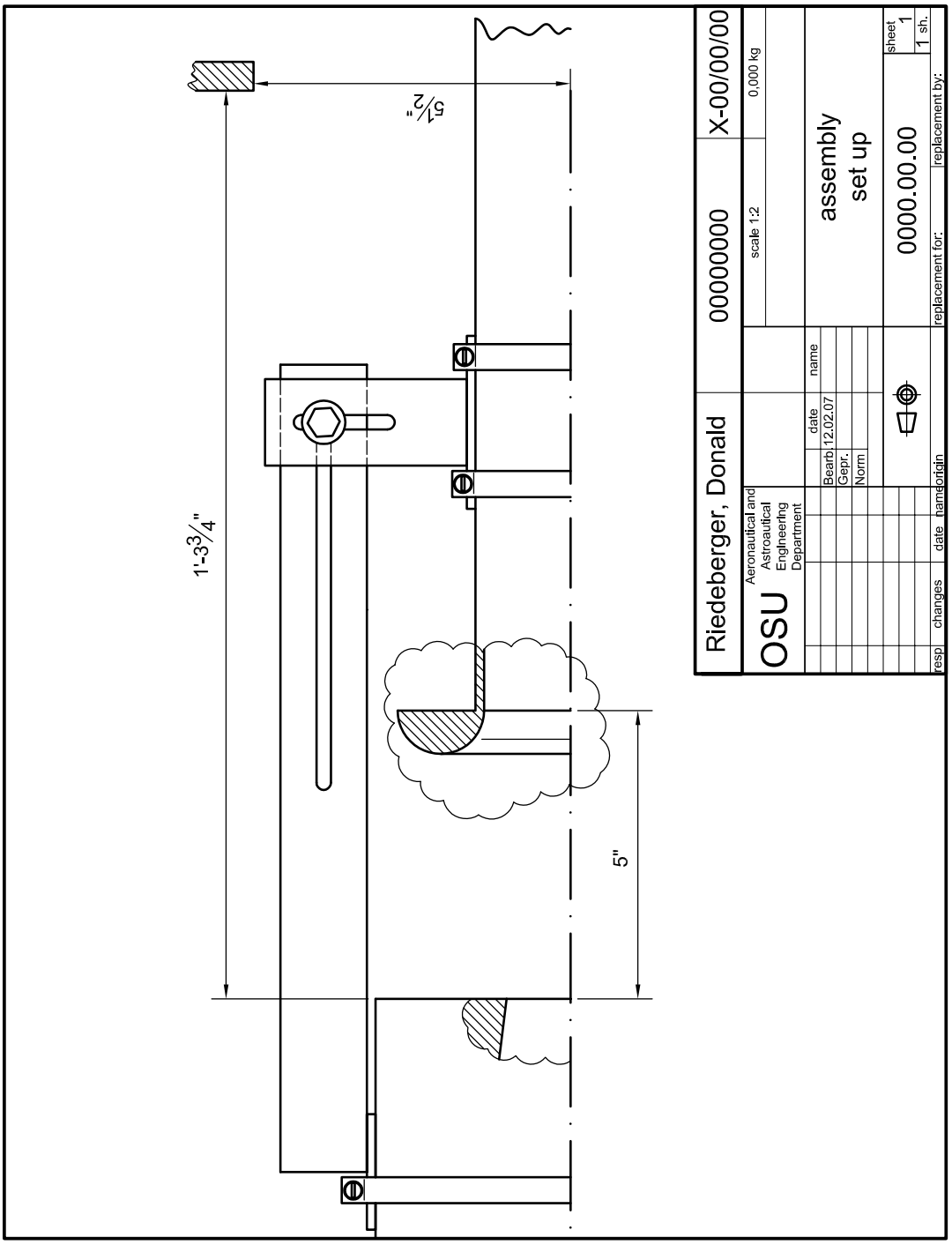

Figure 25: Support mechanism assembly - technical drawing not to scale

E. Data records

This section presents the various data sets collected from runs of the SR-30 MiniLab at The Ohio State University during the research done during this documentation. The data presented includes the temperature and pressure of the ambient air as well as the averaged values for the steady states for the engine.

January 22, 2010

```
T_0 = 290.65 [K] p_0 = 98222.2 [Pa]

-----------------------------------------------------
RPM [1/min] m_fuel [kg/s]  F_net [N]
   60580       0.00176      27.34
   70100       0.00246      41.36
   75317       0.00292      52.34
-----------------------------------------------------
T_t2 [K] T_t3 [K] T_t4 [K] T_t5 [K] T_t9 [K]
  292.25   386.00   717.20   669.24   660.46
  291.94   410.92   782.27   681.49   674.59
  291.93   424.85   809.93   701.24   690.70
-----------------------------------------------------
p_d2 [Pa] p_t3 [Pa] p_t4 [Pa] p_t5 [Pa] p_t9 [Pa]
  2443.7 180265.4 178549.0 105104.5 103499.5
  3528.5 216863.5 215401.7 109046.8 106207.6
  4286.0 241123.6 239967.7 111626.0 108483.6
```

February 8, 2010

```
T_0 = 283.15 [K] p_0 = 9509.0 [Pa]

-----------------------------------------------------
RPM [1/min] m_fuel [kg/s]  F_net [N]
   48305       0.00130      16.67
   60802       0.00181      29.97
   69694       0.00243      43.14
   80549       0.00344      70.59
-----------------------------------------------------
T_t2 [K] T_t3 [K] T_t4 [K] T_t5 [K] T_t9 [K]
  292.23   357.48   666.47   672.46   639.26
  292.18   389.81   706.40   661.80   660.33
  291.83   414.88   774.87   678.60   673.80
  291.52   455.80   880.67   728.62   720.15
```

```
-----------------------------------------------------
p_d2 [Pa] p_t3 [Pa] p_t4 [Pa] p_t5 [Pa] p_t9 [Pa]
  1464.2 147282.4 145846.3 103291.6 102553.1
  2511.4 183088.1 181294.8 106478.8 104914.5
  3527.5 217924.4 216363.1 110289.7 107535.3
  5251.7 273522.0 272431.6 116781.0 112642.1
```

February 22, 2010

```
T_0 = 292.65 [K] p_0 = 97646.5 [Pa]

-----------------------------------------------------
RPM [1/min] m_fuel [kg/s]  F_net [N]
   46349       0.00129      14.78
   60084       0.00183      29.14
-----------------------------------------------------
T_t2 [K] T_t3 [K] T_t4 [K] T_t5 [K] T_t9 [K]
  295.96   356.00   696.46   678.87   647.60
  295.73   392.09   732.84   670.96   665.09
-----------------------------------------------------
p_d2 [Pa] p_t3 [Pa] p_t4 [Pa] p_t5 [Pa] p_t9 [Pa]
  1303.5 140680.9 139474.1 101132.1 100300.9
  2412.3 177592.8 175869.5 104398.2 102634.7
```

May 20, 2010 (baseline)

```
T_0 = 291.15 [K] p_0 = 99204.3 [Pa]

-----------------------------------------------------
RPM [1/min] m_fuel [kg/s]  F_net [N]
   46625       0.00131      16.84
   60656       0.00192      32.28
   70057       0.00259      48.90
   80496       0.00348      76.62
-----------------------------------------------------
T_t2 [K] T_t3 [K] T_t4 [K] T_t5 [K] T_t9 [K]
  295.89   358.12   694.20   667.83   643.63
  295.50   393.30   734.86   671.81   668.32
  295.08   421.93   806.60   689.51   679.44
  294.69   458.72   895.92   727.92   724.70
-----------------------------------------------------
p_d2 [Pa] p_t3 [Pa] p_t4 [Pa] p_t5 [Pa] p_t9 [Pa]
  1304.9 143054.7 141894.5 102867.2 101905.2
```

```
  2463.7 181728.8 180137.1 106119.0 104420.9
  3533.4 217714.6 216277.4 109737.3 107004.3
  5168.6 270304.2 269269.9 116146.3 112116.9
```

May 20, 2010 (3.5 OD augmenter, 24 in long, 5 in displaced)

```
T_0 = 291.15 [K] p_0 = 99204.3 [Pa]

-----------------------------------------------------
RPM [1/min] m_fuel [kg/s]  F_net [N]
   45479       0.00129      15.76
   59700       0.00183      30.89
   70286       0.00258      47.66
   80076       0.00343      74.88
-----------------------------------------------------
T_t2 [K] T_t3 [K] T_t4 [K] T_t5 [K] T_t9 [K]
  294.24   347.75   700.99   674.76   638.82
  295.23   387.99   732.38   682.39   657.80
  296.00   423.08   799.73   690.10   678.46
  295.45   457.04   877.09   723.47   722.58
-----------------------------------------------------
p_d2 [Pa] p_t3 [Pa] p_t4 [Pa] p_t5 [Pa] p_t9 [Pa]
  1238.5 141197.3 139984.9 102689.6 101910.9
  2389.0 178611.5 177066.9 105683.8 104272.0
  3567.1 218698.6 217330.7 109752.0 107168.3
  5117.7 267770.0 266734.8 115700.9 111855.7
```

May 21, 2010 (3.5 OD augmenter, 12 in long, 5 in displaced)

```
T_0 = 292.15 [K] p_0 = 99051.9 [Pa]

-----------------------------------------------------
RPM [1/min] m_fuel [kg/s]  F_net [N]
   46113       0.00130      16.67
   60569       0.00192      33.62
   70156       0.00258      50.08
   79878       0.00341      77.20
-----------------------------------------------------
T_t2 [K] T_t3 [K] T_t4 [K] T_t5 [K] T_t9 [K]
  296.31   347.26   688.36   656.27   636.62
  296.32   391.77   727.07   676.46   667.98
  296.42   422.87   801.71   689.33   680.17
  296.10   457.27   879.68   726.02   719.71
```

```
-----------------------------------------------------
p_d2 [Pa] p_t3 [Pa] p_t4 [Pa] p_t5 [Pa] p_t9 [Pa]
  1295.0 142168.2 140915.7 102609.6 101844.8
  2458.3 180807.1 179125.3 105845.2 104279.1
  3522.5 217211.1 215717.5 109567.0 106871.3
  5012.7 265129.7 263982.4 115221.0 111488.2
```

May 21, 2010 (3.5 OD augmenter, 6 in long, 5 in displaced)

```
T_0 = 292.15 [K] p_0 = 99051.9 [Pa]

-----------------------------------------------------
RPM [1/min] m_fuel [kg/s]  F_net [N]
   45795       0.00129      15.75
   60333       0.00195      32.33
   70294       0.00263      48.89
   80345       0.00347      76.68
-----------------------------------------------------
T_t2 [K] T_t3 [K] T_t4 [K] T_t5 [K] T_t9 [K]
  296.41   346.45   675.45   647.83   634.90
  296.60   392.33   723.93   677.84   667.58
  296.72   424.77   803.80   693.15   680.18
  296.25   460.29   887.60   727.65   721.89
-----------------------------------------------------
p_d2 [Pa] p_t3 [Pa] p_t4 [Pa] p_t5 [Pa] p_t9 [Pa]
  1267.3 141493.1 140427.1 102563.1 101785.8
  2424.3 180155.5 178595.9 105747.1 104213.4
  3527.3 217975.2 216578.5 109588.8 106889.6
  5076.2 268082.2 267093.4 115620.5 111854.6
```

F. Literature research

The literature research in this project can be divided into two subcategories. One is about publications on research and university usage of the SR-30 jet engine within the MiniLab, the other is focusing on the previous research done in the field of passive thrust augmentation through jet ejectors. Reviewing the activities of other research institutions on the SR-30 jet engine is necessary for evaluating the performance whereas the publications of previous achievements in the field of jet ejectors actually build the basis for the design and implementation of the passive thrust augmenting device as undertaken in this project. In addition to the previous publications also the results of a CFD study undertaken parallel to this work is given in this section.

F.1. Literature on university usage of the SR-30

In outlining some important activities of other research universities using the SR-30 engine a valuable amount of information was included into the work of this paper. To set the different articles into perspective it has to be mentioned that the turbine lab as used at OSU was bought in 200 and although the test bed has been updated in later years the engine mounted on it stayed the same improved with more measurement probes and a direct thrust measurement via load cell (rather than a correlation with combustion chamber pressure as done in the first beginning[9]). Therefor the engine at OSU is still considered to be of the first generation whereas the measurement capabilities (e.g. for net thrust) are to some extend updated.

University of Liege
As outlined in their report on ten consecutive years of work on the SR-30 engine [29] the University of Liege touched different topics. Amongst other things they adapted the measurement hardware (thrust, fuel flow, mass flow), equipped a variable area nozzle and also set up an aerothermodynamic (0D) model to analytically simulate the engine behavior to a resolution of component level. Especially the evaluation of the cycle performance is a valuable example of applying the theoretical equations in a complex manor - an objective also for the project undertaken by this paper. As a remark they also emphasize that the one-dimensional instrumentation puts severe constraints on obtaining accurate results in performance analysis. As Liege acquired the SR-30 engine in 1997 it is assumed to be of the similar generation as the turbine running in the OSU lab although sensor equipment and measurement technique (especially in respect to the undertaken hardware changes at Liege) is not the same . Nevertheless the given information will be taken as one solid reference.

Pennsylvania State University (PSU)
At the PSU an SR-30 lab was acquired in 1999 and offered similar instrumentation as the one at OSU therefore the report [32] delivers helpful information for purposes of

comparison. In a simple calculation of enthalpy and thus energy balances over the components of the engine the PSU obtained data for various RPM which is given in table 8.

Loyola Marymount University (LMU)
The Mechanical Engineering Department of LMU delivered several healthy information towards the evaluation of accuracy of the measurement data from the SR-30 engine that they acquired in 1999 - similarly equipped in measurement capabilities as the version in use at OSU. The report [15] states clearly what performance parameters can be calculated out of the measurements: $\eta_{\mathrm{n,comp}}$, $\eta_{\mathrm{n,turb}}$, $\eta_{\mathrm{n,nozzle}}$, $\dot{m}_{air}$, $f = \frac{\dot{m}_{fuel}}{\dot{m}_{air}}$, exit gas velocity u, η_{thermal}, specific thrust F; and thrust specific fuel consumption TSFC.
A typical test result for one engine run at constant RPM is given in table 9. In addition to this the LMU ran the engine in a speed range of $60,000$ RPM to $85,000$ RPM and obtained measured thrust of 25 N to 120 N with $\eta_{\mathrm{n,comp}}$ with an average of 0.60 going slightly down in high speed ranges. The given results matched similar published data (Appendix B [30]) for comparable small-scale jet engines with respect to TSFC and specific thrust.

Concerning the results of experiments the LMU reports too high turbine and nozzle efficiencies as well as disagreement of measured to calculated values of the thrust. The report calls measurement errors in the force measurement setup as well as the unshielded thermocouples to account for those off-sets. The unshielded temperature probe at the exit results in lower temperatures and therefore higher exit velocities and too large calculated thrust and nozzle efficiencies - the same is stated for the turbine efficiency. The presence of mechanical hysteresis in the bearings of the engine mount for thrust measurement as well as a faultily mounted or not optimally designed pitot-static probe is also mentioned as reason for errors due to their point of analysis.

University of Minnesota
Although it is not mentioned explicitly in the report [43] the given data suggests that the University of Minnesota operates a comparable version of the SR-30 engine. Pursuing a 0D analysis a dataset was created and is given for comparison in table 10.

Next to the performance data the report outlines three other important things.

1. The time needed for the engine to reach a steady state in which no major temperature variations occur takes between 10 to 20 minutes and therefore a pre-measurement run time of at least 10 minutes is suggested before any actual data is recorded. (Temperature variations tend from around 10 K at the compressor inlet to around 80 K at the turbine inlet and the reader is refered to the report [43] for further details.)

2. The temperature recordings of the movable probe at the position after the compressor exit are very sensitive. In the available radial range of movement into the engine (10 mm) between the outer wall and the inner wall, later one being the combustion chamber boundary, a temperature variation of 50 K or even up to 70

n [1/min]	Π [-]	$f = \frac{\dot{m}_{\text{fuel}}}{\dot{m}_{\text{air}}}$ [-]	$\eta_{\text{n,comp}}$ [-]	$\eta_{\text{n,turb}}$ [-]
55,000	1.72	0.0162	0.68	0.75
55,000	1.73	0.0160	0.68	0.74
55,000	1.72	0.0159	0.64	0.75
60,000	1.9	0.0164	0.70	0.73
60,000	1.9	0.0165	0.66	0.75
60,000	1.89	0.0164	0.67	0.73
65,000	2.06	0.0135	0.69	0.75
71,600	2.33	0.0161	0.64	0.94
75,000	2.51	0.0177	0.76	0.91
75,000	2.53	0.0178	0.74	0.88
78,000	2.61	0.0161	0.75	0.88

Table 8: Performance parameters for SR-30 at various RPM reported from laboratory at PSU [32]

Parameter	Value	Dimension
n	85,040	[1/min]
$\eta_{\text{n,comp}}$	0.576	[-]
$\eta_{\text{n,turb}}$	1.11	[-]
$f = \frac{\dot{m}_{\text{fuel}}}{\dot{m}_{\text{air}}}$	0.016	[-]
$\dot{m}_{\text{air}}$	0.296	[kg/s]
u	463	[m/s]
$\eta_{\text{n,nozzle}}$	2.11	[-]
η_{th}	0.159	[-]
TSFC	$3.95 \cdot 10^{-5}$	$[(\text{kg}_{\text{fuel}}/\text{s})/\text{N}]$
Specific Thrust	405	$[\text{N}/(\text{kg}_{\text{air}}/\text{s})]$
F_{measure}	120	[N]
F_{calc}	139	[N]

Table 9: Performance parameters for SR-30 at constant RPM reported from laboratory at LMU [15]

K (depending on engine speed) was noticed. This lead to the advice to make sure the temperature probe is placed mid-way at the position of compressor exit.

3. The variation of measurement values at the exit plane should best be evaluated with a traversion and integration process spanning the diameter of the nozzle.

In addition to this the report also shows some insight into the way how the lab setup uses the manifold pressure in the fuel return system (reflux coming from the engine depending on the throttle lever position) to calculate the fuel flow. The appendix of this report closes with a detailed component analysis based on the geometry of both the radial compressor and axial turbine stage. A discussion on predicted losses is undertaken and results are presented matching expectations of a small-scale turbo jet engine.

Kettering University
The Kettering University also undertakes a 0D analysis in their report [34] on the SR-30 engine. Although their test stand did not deliver straight forward measurement of fuel flow and thrust they added those capabilities through hardware changes. The results of their experiments and analytical evaluation results in the data as presented in table 11 (which is approximately taken from the graphs given in their report [34]). As part of the analysis of the exhaust gas composition the Kettering University also evaluated the change in the specific gas constant in the exhaust gas stream. The reported increase with respect to the fuel-to-air ratio is of negligible amount ($\Delta R_\mathrm{s} < 0.5\mathrm{J/Kg}$) in the specified range of f from 0 to 0.02. The offset of the measured and calculated Thrust F was assigned to be caused by measurement errors.

In another report [6] the Kettering University explains to more detail in what way they have adapted the SR-30 engine test stand to end up with the result in their previous publication on the engine performence [34]. They implemented an inflow nozzle to measure mass flow more precisely, a different thrust load arrangement was created and they switched to a gravimetric fuel flow measurement using a scale for stationary runs. Their update of the thrust force measurement system from a highly constrained, error-prone first version of factory set-up enabled them to improve their offset between theoretical calculations and measurements from 50 % to under 10% (which is about the precision the OSU measurements show). The remaining offset of continuously higher measured thrust compared to calculated values from the momentum equation was accounted to unprecise readings of either the pressure or temperature probes involved in this calculation across the engine exhaust and inlet.

Royal Military Academy of Belgium
At the Department of Applied Mechanics of RMA in Belgium the influence of inlet pre-cooling has been investigated [14]. The pictures of their SR-30 MiniLab allow to consider it as of similar version as the one at OSU and their basic performance analysis of the captured engine data amounts to the component values at design point as given in

Parameter	Value	Dimension
n	70,000	[1/min]
$\eta_{\mathrm{n,comp}}$	0.5444	[-]
$\eta_{\mathrm{n,turb}}$	0.7285	[-]
W_{comp}	28.27	[kW]
W_{turb}	28.33	[kW]
$\eta_{\mathrm{comb.ch.}}$	0.9834	[-]
$\mathrm{Air-Fuel-Ratio}$	68.58	[-]
$f = \frac{\dot{m}_{\mathrm{fuel}}}{\dot{m}_{\mathrm{air}}}$	0.01458	[-]
$\dot{m}_{\mathrm{air}}$	0.206	[kg/s]
η_{th}	0.0365	[-]
F	44	[N]

Table 10: Performance parameters for SR-30 at constant RPM reported from laboratory at University of Minnesota [43]

n [1/min]	$\dot{m}_{\mathrm{air}}$ [kg/s]	$f = \frac{\dot{m}_{\mathrm{fuel}}}{\dot{m}_{\mathrm{air}}}$ [-]	TSFC $[(\mathrm{kg_{fuel}/s})/\mathrm{N}]$
48,830	0.14	0.0168	$12.2 \cdot 10^{-5}$
60,043	0.18	0.0156	$8.75 \cdot 10^{-5}$
67,291	0.21	0.0157	$7.50 \cdot 10^{-5}$
76,848	0.24	0.0161	$6.25 \cdot 10^{-5}$
	$\eta_{\mathrm{n,comp}}$ [-]	$\eta_{\mathrm{n,turb}}$ [-]	$\eta_{\mathrm{comb.ch.}}$ [-]
48,830	0.46	0.91	0.70
60,043	0.52	0.83	0.79
67,291	0.56	0.88	0.74
76,848	0.59	0.80	0.74
	F_{measure} [N]	F_{calc} [N]	
48,830	19.0	16.5	
60,043	31.0	28.5	
67,291	41.5	39.0	
76,848	62.5	58.5	

Table 11: Performance parameters for SR-30 reported from the Kettering University (approximately taken from graphs) [34]

table 12. Next to this data and their analysis of precooling effects only the spool speed

Parameter	Value	Dimension
$\eta_{\mathrm{n,comp}}$	0.70	[-]
$\eta_{\mathrm{n,turb}}$	0.95	[-]
$\eta_{\mathrm{comb.ch.}}$	0.99	[-]

Table 12: Performance parameters for SR-30 at design point reported from Royal Military Academy of Belgium [14]

dependent compressor efficiency $\eta_{\mathrm{n,comp}}$ is of interest to this report and it ranges from 0.62 to 0.65 between RPM of 50,000 and 65,000.

F.2. Literature on passive thrust augmenters

The information, research and data published in reports on the field of passive thrust augmentation devices, focusing on jet ejectors is quite different in approach (theoretical or experimental) and primary objective (jet ejectors, thrust augmenters, applications to V/STOL). Most appropriately a time line can be described in the focus of research being outlined as follows.

Since the first applications of jet engine propulsion the idea of augmenting the possible thrust has been evaluated. As the literature research in this paper was processed an interesting theoretical starting point can be given in the middle of the 20th century. A theoretical analysis of the basic principle of thrust augmenting ejectors was mentioned by von Kármán [49] after that Sanders rooted the thrust gain to a low pressure region along the inlet contour [40] in 1958. In the sixties a thorough analytical approach was undertaken to relate the augmentation by jet ejectors (and ideal augmenters) to the pumping rate (i.e. the secondary mass flow) by Heiser [13] and Huang related the augmentation ratio to the ejector area ratio of primary to secondary flow [16]. The paper by Huang also gives a detailed preliminary design procedure for jet ejectors including an augmentation prediction addressing the major loss effects and its results match most of the published experimental data. The Aerospace Research Laboratories also published an elaborate report [5] in 1967 yielding similar results and focusing on the modification and application of passive thrust augmenters to V/STOL aircrafts - one particular field in which jet ejectors have been the primary focus to reach a breakthrough in effective application.

Publications on the theoretical and experimental work on the topic continued in the 1970s. Low-Area Ratio, Thrust-Augmenting Ejectors were reviewed by Fancher in 1972 [8]. Brian Quinn reviewed the possibilities of shortening the ejector length by using hypermixing nozzles [35] and also evaluated the effect of pressure and temperature values during real operational conditions [36] - a topic also adressed by Phillips masterthesis:Phillips. The review and bibliography given by Bonnington and King in 1976 [26] sheds some light into several topics on jet ejectors encountered by several scientists of the time. Next to emphasizing the comprehensiveness of Huang's work [16] the conference proceedings by Jones [19] are mentioned here in particular. As Jones [19] outlines, the propulsion application of jet ejectors as thrust augmenters has to be carefully evaluated due to inlet design and diffuser setup. Otherwise the results for augmentation in the real case will be far off the expected theoretical values. Turning to the 1980s several authors addressed various flow phenomena of ejectors during experiments in their master thesis at Wright-Patterson AFB [25] [48] [37]. As result there was more knowledge gained about the factors that significantly increase losses in diffusers, inlet shrouds and various nozzle setups. Two articles by Morton Alperin and Jiunn-Jenq Wut in 1982 [1] [2] address a variety of ejector designs and comment also on sub- and supersonic flight behavior. In 1982 Quinn gave a review on the application of Jet Ejectors to V/STOL in an AGARD advisory report [42] summarizing that the approaches of

one-dimensional analysis of ejector flow still leaves the knowledge about the flow phenomenon on a rather poor level. It is stated that even though lots of experimental data exists the design of effective augmenters using jet ejectors can not be pursued without deep understanding of the flow patterns. It is also outlined that time depended pulsing of the primary jet can be advantageous. Further research on diffuser loss influence by Yang in 1985 [44] was done and the topic of forced mixing with lobes on the primary flow nozzle [23] leading to shorter ejector systems [22] was addressed by Presz.

In the 1990s noise suppression by shorter, efficient ejector configurations incorporating hypermixing nozzles was further reviewed by Presz [20] and diffusers further optimized [21] even leading to implementation to the Gulfstream GII by the turn of the century as documente by Presz in 2001 [24].

The last decade brought further insight of the flow patterns by a determinate model by Whitley [51] and a theoretical analysis of ideal augmentation incorporating heat exchange by Efremov and Kraiko in 2003 [7]. Also new practical applications have been arising like application to propeller driven subsonic propulsion systems by Werle in 2007 [50]. Furthermore the numerical study of pulsed flow in ejectors by Okpara in 2008 [31] - together with recent theoretical studies as mentioned before - shows two things that happen in recent years: First, the deep aero- and thermodynamic basics as foundation of the complex phenomena in jet ejectors are still subject in research and second, the numerical approach to unsteady (pulsed) primary jets open an additional possibility to develop higher thrust augmentation in short ejector dimensions by more accurate simulation of the flow phenomena.

The most important content of the reviewed literature is given in chronological order in the following paragraphs.

Theoretical remarks on thrust augmentation - von Kármán - 1949
In his report [49] von Kármán outlines the basic analysis of an ideal, incompressible flow through a cylindrical jet ejector without a diffuser. A comparison between achievable augmentation ratio for either uniform or non-uniform velocity profile of the entering secondary flow is given. Von Kármán reasons the theoretical possibility for a higher augmentation at non-uniform secondary flow (the Coanda-Nozzle with annular primary nozzle in particular) with an assumption (same mass entrainment in uniform and non-uniform case) that is questioned in correctness by Huang [16, p. 6].

Analysis of Ejector Thrust by Integration of Calculated Surface Pressures - Sanders - 1958
Looking for the basic cause of the augmented thrust by jet ejectors Sanders [40] is calculating the resulting forces out of pressure measurements along the contour of the ejector and inlet walls. Prior published, experimental data to that point was inconsistent to the benefits of ejectors for thrust augmentation and to weather forward speed would have adverse effects on the overall thrust gain. Within the evaluation Sanders assumed

mixing to be done to completion and necessary pressures were computed out of one dimensional flow analysis. Focussing on incompressible flow (with some outlook to compressible phenomenon) the results shows that the main cause for thrust increase is created by pressure forces acting on the inlet contour due to acceleration of the ambient fluid, secondary flow prior to the mixing chamber. This effect and thus thrust gain is seen to reduce with increase of secondary flow speed, i.e. forward motion.

An investigation of the thrust augmentation characteristics of jet ejectors - Huang - 1967

As also outlined by King and Bonnington in their review on jet ejectors [26] the technical report by Huang and Kisielowskj [16] is a valuable reference due to the two main objectives of the paper[16, p. 1]: extend existing theories for jet ejector performance to account for more real flow phenomena (compressibility, losses, geometry) thus finding an explicit solution and evaluate the published data on the topic. First, they extend the basic one dimensional analysis of von Kármán [49] for different nozzle set-up and derive the thrust augmentation ratio as a function of secondary inlet to primary flow cross section ratio for both a constant area mixing and constant pressure mixing geometry. Parameters are introduced to account for various losses (due to non-uniform secondary flow velocity profile, wall friction, etc) to adapt the ideal calculation to real circumstances. Also the necessary mixing-chamber length and demands for possible diffusers are analyzed. Second, the report delivers a bibliography of 585 elements and uses the collected experimental data of 34 of those references to cross-match their theoretical analysis with reality which delivers - in most cases - a satisfactory match. In the end the preliminary design procedure using nomographs is given to calculate mixing chamber length as a function of secondary-primary area ratio and losses. As the paper also suggests empirical correction factors, e.g. for the assumption of uniform velocity distribution of the secondary flow that would limit the theory to small entrance area ratios, the given design procedure and augmentation prediction is based on a compulsory and sound theoretical foundation.

Thrust Augmentation for V/STOL - Campbell - 1967

Regarding especially applications to V/STOL, reviewing previously unshrouded and purely external ejectors to be extremely dissatisfying, the report by Campbell [5] is following a similar explanation and analysis of the fundamental ejector principle as Huang [16]. It outlines the driving parameters of a one-dimensional ejector analysis, addresses constant and variable mixing chamber geometries and focuses on air breathing propulsion applications - i.e. considering incompressible flow and similar fluid properties for primary and secondary flow. The conclusion that complete mixing (and longer ejector dimensions) and reduced friction (i.e. short ejector lengths) are counteracting each other is drawn just as by Huang [16]. Some more insight is shed into forward speed impact on the overall efficiency of the ejector with the bottom line of basically vanishing augmentation (and even negating) with increasing velocity due to arising drag forces. The

research outlook is drawn to specifically address further understanding of the mixing process through nozzle adaptations as well as the nature of flow losses to eventually assure complete flow mixing with shorter ejector lengths and thus achieve superior performance.

Thrust Augmentation - Heiser - 1967
The article of Heiser [13] theoretically analyses the possibility of augmenting devices and divides them into two categories: Ideal Augmenters that exert a net force on the fluid but do not allow exchange of heat or work and Ideal Ejectors that allow heat- and work-exchange but apply no forces. The non-isentropic nature of the viscous mixing process of the momentum exchange of ejector systems is mentioned to limit the augmentation ratio drastically (between 1 and 2) compared to the ideal augmenter. Although Heiser's analysis is quite comprehensive (also the negligibility of compressibility effects is discussed) the augmentation ratio with respect to the mass entrainment ratio a formulation that does not account for any geometrical information. Thus the report remains rather superficial concerning actual design possibilities and has to be seen as an overview of augmenting technique.

Low-Area Ratio, Thrust-Augmenting Ejectors - Fancher - 1972
Addressing the topic of enhanced mixing facilitated by a hyper mixing primary nozzle the article [8] concentrates on low secondary to primary flow area ratios - close to actual V/STOL, in-wing applications. Applying flow analysis of an Inlet-Mixer-Diffuser set-up yielded similar results for augmentation ratio as Huang [16] and Campbell [5] reported. Issues of Mixing-Losses due to a gradient between secondary and primary flow velocity, non-uniform velocity profiles and flow losses are addressed. The necessity of achieving complete mixing and keeping the ejector short is reasoned and a hyper mixing nozzle is suggested to increase the spread rate of the primary jet. The experimental test produced results that matched with the undertaken theoretical analysis. An approximate equation for thrust augmentation for the area range of ejectors analyzed is given and the focus for future research is emphasized to be on hyper mixing and diffuser efficiency as main sources of improoving the ejector process for practical thrust augmentation.

Compact Ejector Thrust Augmentation - Quinn - 1973
To offer practical solutions to the design compromise between short, light design and assured complete mixing of the two interacting flows in an ejector is the purpose of the article by Quinn [35]. Including primary nozzle, inlet, mixing and diffuser losses to van Kármán's analysis [49] Quinn proceeds in investigating experimentally different ejector, nozzle and diffuser set-ups. Energizing the diffuser wall-boundary by blowing out fluid as well as diffusing the fluid improved augmentation ratios up to around a value of 2. Quinn picked long ejectors in the magnitude of what Huang [16] proposes. An investigation of pressure ratio of the primary flow to ambient proved that the augmentation of thrust is independent of pressure. In conclusion Quinn emphasizes that the sensitivity to

component losses of ejectors in thrust augmenting applications is crucial - as his paper obviously proved.

Ejector Trust Augmentation - Fact or Fiction? - Jones - 1974
In his article [19] Jones addresses the necessity to have a clear definition of thrust augmentation ratio in order to accurately compare data for jet thrust augmentation especially at very low or zero forward speeds. After giving a very brief recapitulation of Newtons third law applied to the subject twelve possible formulations of augmentation are analyzed and two are picked to be representative. In comparing those with experimental data from various resources a clear difference is seen in the maximum achievable augmentation. This leads to the conclusion that the geometry of the inlet as well as the diffuser efficiencies are crucial for the achievable augmentation and that the use of an ejector - being inferior to plain jets - is limited to special cases. The suggesting to rather not use a diffuser than to use a poor one as well as the urge to have further research in inlet geometry and flow patterns is drawn.

Temperature and Pressure Effects on Thrust Augmentation - Phillips - 1974
In the master thesis by Phillips [33] the influences on pressure and temperature of the primary flow on the mass flow entrainment are investigated. Applying a 1D analysis similar to other reports of this time [16] [13] the augmentation ratio of a rectangular ejector of secondary to primary flow area ratio of 32 and a length of 16 in is predicted theoretically and certified through experiments. A hyper mixing, centered nozzle configuration is used. The results show that no variation in entrainment of secondary flow is visible by varying the nozzle total to static pressure ratio $p_{0,\mathrm{p}}/p_{\mathrm{amb}}$ between values of 1.35 and 2.06. A 15% increase in entrained air is seen for adapting the primary to secondary flow static Temperature ratio T_P/T_S from 0.8 to 1.7. As opposed to the mass entrainment the augmentation ratio of the overall ejector configuration was seen to decrease 10% with the temperature adaptations. The reson for this is that the kinetic energy ratios within the mixing process adapt accordingly and thus reduce the benefit of more entrained flow.

Ejector Performance at High Temperatures and Pressures - Quinn - 1976
To analyze the short coming of previous research on ejectors Quinn [36] investigates to what extend the prior research changes when the ejector is working under real conditions - i.e. with a heated primary jet under flight atmosphere. His experiments are necessary due to the lack in analytical understanding how a heated primary jet and higher viscosity would influence the turbulent mixing principle within the ejector (as turbulent mixing is the key driver of this application). As a first result the ejector length influence on augmentation as reported by Huang [16] are reproduced as the augmentation ratio peaks at length to diameter ratios of 6 to 9 and decreases significantly for higher values due to frictional losses. The influence of heating of the primary fluid was found to be of slightly improving nature for short ejectors as the larger viscosities reduce the skewness

of the flow. For long ejectors, the effect showed negative trends. Mass entrainment decreased with increasing primary pressure.

An experimental study of static thrust augmentation using a 2D variable ejector - Kedem - 1979
Defining the cause for thrust augmentation in the exact same way as outlined by Huang [16] the masterthesis by Kedem [25] is investigating a rectangular ejector of secondary to primary flow area ratios of the order of 10. Applying annular as well as coanda nozzles and varying the ejection angle the results were superior for the coanda nozzle, varying under ejection angle. The necessity of 3D inlet shrouds is mentioned to assure unseparated flow and also advantages of axisymmetric ejectors (minimized flow losses) are presented.

An Experimental Study of Rectangular and Circular Thrust Augmenting Ejectors - Unnever - 1981
Continuing the research and using the same experimental setup as Kedem [25] the report by Unnever [48] starts with investigating Coanda type flow at the diffuser walls with different set ups - from discrete nozzles along increasing percentages of the perimeter up to full circular ingestion of primary fluid around the whole wall surface. The achieved Coanda type flow by descrete nozzles at approximately 60 % of the circumference was superior resulting in augmentatzion ratios up to a value of 2.

Inlet and Diffuser Effects on Thrust Augmenting Ejectors - Reznick - 1982
Additional research to the reports by Unnever [48] and Kedem [25] was done by Reznick [37]. Investigating rectangular and circular ejectors with inlet contours and diffusers the effect of circumferential injection of primary flow close to the walls were observed. Discrete nozzles (rather than annular) close to but not on the walls of the circumference of the beginning of the mixing chamber lead to superior results in thrust augmentation. Separation and stall within the diffuser was seen to be favored by centered nozzle set up whereas peripheral or wall ingestion of the primary flow hindered the occurrence of this disadvantageous phenomenon. Circular ejectors where found to be superior to rectangular one of the same primary to secondary flow area ratio and the importance of inlet primary nozzle configurations was emphasized. In the work done by Lewis [28] in 1983 who applied an automatic data acquisition system to the setup the results of Reznick were again confirmed leading to similar conclusions.

Thrust Augmenting Ejectors I + II - Alperin - 1983
In the comprehensive articles by Alperin [1] [2] the ejectors utilization for thrust augmentation is addressed as opposed to ejector use as a jet pump or blow-in-doors. Applying a detailed analysis of the equations governing the flow in and around the ejector of constant cross section complete mixing is assumed, skin friction is neglected and a compressible calculation is done. For a mixing chamber to primary flow area ratio

of 25 the solutions are presented and split into first and second solution ejectors. A good amount of detail into different geometry set-ups of various ideal ejectors is given. The analysis proofs that there is one optimal design for any flight and primary flow condition and that efficient augmentation can be reached in low subsonic and high supersonic conditions of free stream. The comparison of first and second solution ejectors also proved that the conventional converging-constant-diverging set-up of ejectors was very suitable for subsonic conditions but adaption and caution needs to be taken in the supersonic regime where two solutions to the equations exist - a problem similar to the chocking at supersonic wind tunnel starts is encountered then and needs to be addressed.

An Investigation of High Performance, Short Thrust Augmenting Ejectors - Yang - 1985
Looking into ejector performance of ejectors with rather large secondary to primary flow area ratios (20 - 40) Yang [44] is applying a reversed design method using with vorticity at the diffuser inlet as a major flow parameter. Along with outlining the importance of ejectort legth (they picket a Length to Diameter ratio of 6) the results indicate that high differences in mixing chamber diameter and diffuser exit diameter cause separation and decrease augmentation - a traceable conclusion. A comparison of momentum calculations with measured thrust resulted in an almost perfect match (except for very high flow ratios) with the result that the anticipated static pressure at both inlet and end of the ejector can be assumed to be ambient.

Forced Mixer Lobes in Ejector Designs - Presz - 1986
To adress the enhancement of mixing utilizing lobed primary nozzles is the main focus of the paper by Presz [23]. Investigating different shapes of lobes on the primary nozzle the results were indicating up to a 100% increase in thrust gain capability. This result was accounted to the creation of large-scale streamwise vorticirty by the lobes. This facilitate rapid mixing of the two fluid streams without introducing mayor losses. The vorticities also energize the boundary of the flow at the diffuser thus enabling larger diffusion rates and thus more efficient diffusers. The overall result is increased mixing and higher augmentation with significantly shorter mixing ducts (and thus lower friction). The suggested further investigation of lobe design with application to thrust augmenting ejectors is noted by Presz and later publications are persuing this - representatively the work by Kumar [27], Hui [17] and Saga [39] are mentioned.

Short Efficient Ejector Systems - Presz - 1987
Focusing on the improvement of the mixing process of jet ejectors this paper [22] examines forced mixing lobes in the primary jet to significantly decrease the mixing length and to favor short diffusers. Different forms of the lobes that introduce stream wise vorticity have shown to dramatically increase the energy transfer and thus reduce the necessary length of ejectors as opposed to pure shear layer mixing. It is noted that the reduction of mixing length is favorable not due to the decrease in wall friction (as this

is a minor important source to decrease the possible augmentation ratio compared to incomplete mixing) but to the overall length and weight constraints in aircraft application. Additionally experiments on heated primary jets were conducted resulting in the conclusion that temperature plays no mayor role in low pressure ratio ejectors - a further proof of the publication by Presz [23] one year before where it was shown that a flow parameter modified by Temperature collapses the data and thus cause density and temperature effects to drop out of the problem.

Mixer/ Ejector Noise Suppressors - Presz - 1991
Analyzing the ability of using an ejector for noise suppression purposes (noise correlates to stream velocity by Lighthills power laws) the article [20] deals with an optimal ejector design to assure close to ideal performance. The set up of enhanced mixing by a lobed primary nozzle enables short mixing chamber length (equal or smaller than one diameter) and therefore reduced losses in conjunction with more complete mixing - a key driver for insufficient ejector performance. In introducing the ejector analysis a simple momentum balance is drawn for three control volumes. This gives the reasoning for the fact that the ejector thrust gain only results from the pressure distribution along the inlet walls (lip suction). As the thrust gain is derived as a function depending on the entrained mass flow of secondary air the theoretical conclusion is that thrust gain is a function of area ratio and mixing efficiency alone (given negligible shear stresses in a´mixing chamber of the order of one diameter in length). The experimental data obtained supports this assumption and concludes the result to the possibility to design enhanced mixing jet ejectors that have a compact design and close to ideal performance.

Thrust Augmentation Using Mixer-Ejector-Diffuser Systems - Presz - 1994
Reviewing the effect of diffusers in an ejector and incorporating this in an enforced mixing device the 1994 paper by Presz [21] delivers an up to date set up of a thrust augmenter. A diffuser will force the pressure in the mixing entrance to be below ambient and therefore increase the entrainment velocity of the secondary air (more than it will effect the already high velocity primary jet). Therefore the velocity differences at the entrance will be lower resulting in reduced mixing losses. The downside of decreased mixing rates (thus longer mixing tubes and thus higher friction) due to this is overcome by applying forced mixing lobes in the primary stream exhaust. THis allows a short mixing tube and the combined mixer-ejector-diffuser (MED) can be seen as the up-to-date application of passive thrust augmentation devices.

A Determinate Model of Thrust-Augmenting Ejectors - Whitley - 1996
An ideal mathematical analysis is undertaken by Whitley [51] who aims to find a closed form solution of the governing equations. He approaches this not by specifying certain inlet conditions as did in previous analysis [49] [35] but rather by setting the ratios of some stagnation properties between primary and secondary stream. Following the assumption of complete mixing at the end of the duct and uniform velocity profiles a

1D analysis is done for a constant-area mixerand the result out of perturbation analysis is matching with van Kármán [49]. For incompressible fluid the augmentation ratio is bounded at a value of 2 for increasing the secondary to primary flow area ratios. Furthermore significant reduction in thrust augmentation is observed for forward speed with vanishing augmentation at around Ma 0.6 free stream which is in agreement of prior publications as well [24] [40]. Concerning supersonic freestream conditions the analytical results offer two solutions one of which outlines a possible thrust gain if a carefully designed converging-diverging inlet is applied.

Thrust Augmentation of a small Turbojet Engine - Hackaday - 1999
In part of the masterthesis by Hackaday [11] a small scale turbo jet engine (Sophia J450) was equipped with a sub-optimum ejector to determine thrust augmentation - sub-optimum meaning far too short to assure complete mixing as outlined by Huang [16]. The secondary to primary area ratio of the ejector was approximately 0.92. A 1D-ejector analysis is undertaken close to the process shown by Hung [16] to determine the expected thrust gain. The primary jet data is taken from the nozzle data of an engine simulation in GASTURB based on a previously recorded compressor and turbine map and mass flow rate of the entrained air is determined by static pressure measurements at the secondary stream inlet. The study of ejector area ratio at design point satisfies the trend Hunag [16] presented with an augmentation ratio bounded at approximately 2.0. The test procedure verified a thrust gain of 3 to 10 % depending on design spool speed which is within the expectations of the 1D-ejector analysis that bounded the expected value with 13 %. The 3 % gain at design speed correlates with Huang's predictions for a setup of that kind [16]

Thrust Augmentation with Mixer/Ejector Systems - Presz - 2001
Focusing on the noise suppression system of the Gulfstream GII the paper [24] gives thrust measurement and performance prediction for ejector configurations that use a lobed nozzle tailpipe and therefore consist of a short mixing chamber (order of one diameter in length). Scale model tests are matched with the theoretical prediction and especially the decrease in thrust augmentation with forward speed is addressed.

This article is also one of the few - additionally only Sanders [40] - that particularly mentions the main cause of static thrust gain: the inlet lip suction due to the accelerated secondary flow at the entrance of the ejector. This fact reasons the vanishing or negative thrust gain at high relative speeds where relative acceleration of secondary stream becomes negligible. As the inlet contour also assures the entrainment of secondary air to assure low loss mixing the inlet design has to be of crucial importance.

Theory of an Ideal Jet Thrust Augmentor - Efremov - 2003
The very theoretical analysis of ejector flow especially addressing heat exchange is done by Efremov [7]. The equations derived for optimum ideal augmenters show that heat exchange between primary and secondary fluid favor better augmentation ratios. As

the derivation of the equations assumes preassigned conditions at both primary and secondary inlet the real case phenomenon of an engine jet driving the entrainment of secondary flow is somewhat different than the undertaken ideal conditions. According to Efremov [7] the effort to maximize the entrained mass flow is of first and crucial importance before any heat exchange considerations. Periodic pulsation of the primary flow was especially mentioned to assure higher entrainment.

New Developments in Shrouds and Augmentors for Subsonic Propulsion Systems - Werle - 2007
Within his work Werle [50] applied control volume calculations on a shrouded propeller and matched those with experimental and computational data. His non-empirical control volume approach delivers promising match with experimental data and thus prooves the high applicability of the ejector principle also to propeller driven propulsion devices. The derivation of the augmenting principle from the acting forces out of the momentum principle is also supporting the outlined control volume reasoning that Presz [20] did on his noise suppression ejector.

Numerical Simulation of Steady and Pulsed Flows Through Thrust Augmenting Ejectors - Okpara - 2008
In the dissertation of Okpara [31] a the commercial CFD (Computational Fluid Dynamics) code Fluent is used to simulate the flow field within a axis symmetric jet ejector. Ejector cross section to primary flow area ratios of 7.6 to 12 have been investigated and the primary flow was varied from Ma values of 0.3 to 0.8. Steady cases as well as a set up with pulsed primary jet (220 Hz) were computed and results showed good agreement with previous theoretical and experimental observations. In the conclusion Okpara mentiones that further investigation both experimentally and numerically should be done to especially evaluate the impact on augmentation by different inlet geometries and displacements of the ejector from the primary flow origin.

F.3. Fluent studies

This section presents the results of a computational study that has been done in parallel to the present work. Within the undergraduate coursework of AAE 514 - Systems Integration - in spring 2010 the CFD simulation [38] was undertaken by the author of this paper and three undergraduate students in aerospace engineering at OSU. A meshing process in Gambit was done and Fluent 6.3.26 was used to receive converged solutions to the flow field and to extract flow variables, surface stresses and overall forces to evaluate the thrust gain of three different cases of a thrust augmenting ejector.

F.3.1. Problem cases

The computational study based on the laboratory set up of the thrust augmenting ejector as it is presented in the main part of this documentation (chapter 2.3). A mixing chamber diameter of $D = 3.35$ in was selected and the inlet contour was picked as a semi-circle with $r = 0.8375$ in for simplicity. The primary nozzle diameter was set to $d = 2.22$ in just like the nozzle of the SR-30. The resulting ejector area ratio of the regarded ejecors thus was $\alpha = 1.277$. The investigation focused on three cases:

- A non-displaced case with a primary jet exhausting directly at the entrance plane of a $L = 7D = 23.5$ in ejector.
- A displaced case where the body of the engine ($D = 6.76$ in) has also been taken into account and the whole ejector of $L = 7D = 23.5$ in length has been offset 3 in from the nozzle exit plane.
- A case where the ejector length has been reduced to $L = 3.5D = 12$ in and its entrance was placed directly at the exit plane of the primary nozzle flow.

With those three cases the objective was to address the following things:

- Verify the predicted augmentation ratio based on theory [16] for the given area ratio by the computed result.
- Investigate the influence of downstream displacement of the ejector from the primary nozzle.
- Comment on the influence of the length of the mixing chamber.

Prior to the CFD studies the theory as outlined previously (see chapter 2.3.1) has been used to obtain anticipated augmentation ratio based on the geometry. This was found to be $\Phi = 1.06$ and needed verification using the non-displaced case of the CFD studies.

F.3.2. Meshing, boundary conditions, solver setup

The geometries for the chosen setup as described above was meshed for the various cases and with varying densities of the grid. Three grids have been meshed applying boundary layers along the inlet contour and internal wall of the ejector mixing chamber. Each case was meshed coarse with approximately $300,000$ cells in the domain and with a fine mesh of around 1.5 million cells to comment on grid independence. This relates to at least 400 intervals within the stream wise extend of the pipe internal face and boundary layers that contain 35 rows at a growth rate of 1.1 starting from 0.001 in.

The representative mesh for the non-displaced case of a full length ejector can be seen with the respective boundary conditions in figure 26. Here the primary flow has been modeled as a mass flow inlet of $\dot{m} = 0.311\ \mathrm{kg/s}$, $T_\mathrm{t} = 700\ K$ and a turbulence intensity of $10\ \%$. The solver was set to use pressure based, 2D-axisymmetric equations, steady,

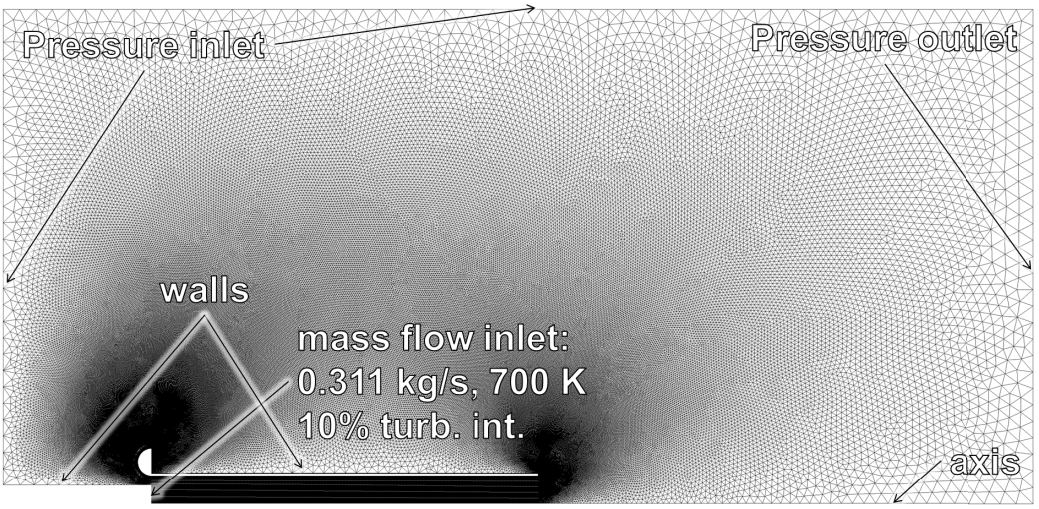

Figure 26: Mesh and boundary conditions representative for the Fluent case studies [38]

implicit with absolute velocity. The viscosity was taken into account and the k-ϵ-Model with standard equations for enhanced wall treatment was used (y^+ was found to be of $O(1)$ along the inside walls for all solutions and thus the used method and mesh are applicable). Air was modeled as fluid acting as ideal gas with energy equation included in the solving process. Residuals converged for each case down to a value of $1 \cdot 10^{-6}$.

F.3.3. Results

The converged solutions of the three outlined cases were used to extract the surface stresses and pressures as well as the mass flows. Those values were used in a control volume calculation to derive the effective restraining force on the ejector and the results are given in table 13.

	non-displaced ($L/D = 7$)	displacement (by 3 in, $L/D = 3.5$)	length influence ($L/D = 3.5$)
primary nozzle thrust	74.48 N	67.07 N	73.76 N
friction force	3.18 N	3.78 N	1.10 N
pressure forces - inlet	4.44 N	3.50 N	4.33 N
pressure forces - engine		-1.56 N	
ejector thrust	75.74 N	65.23 N	76.99 N
thrust gain	1.69 %	-2.74 %	4.47 %

Table 13: Resulting thrust gain calculated from solutions to three CFD cases of thrust augmenting ejectors with $\alpha = 1.277$ [38]

It can be seen that a slight thrust increase of approximately 2 % was obtained for the non-displaced case. This value is trending lower than the 6 % that was predicted from loss incorporating calculations using the analytical procedure (see chapter 2.3.1) [16]. The case where the full length ejector was displaced by 3 in downstream of the nozzle exit shows a decrease in thrust associated to two phenomena. First, the drag increased due to the spread of the jet in the region after the nozzle and prior to the ejector resulting in more turbulent kinetic energy close to the walls internal of the ejector. Second, the entrained ambient air also flows over the engine back to a significant amount, creates a low pressure region whose effective force further reduces the overall forward thrust. Regarding a shortening of the ejector mixing chamber showed a superior thrust gain compared to the full length associated to reduced drag on the shorter internal walls.

F.3.4. Conclusions

The results from the computational studies can be seen beneficial for this work in two ways. First, the theory has been shown to hold but limitations were outlined. Resulting values were trending lower than the analytical results but a dependency of the geometry factor of ejector area ratio α to the overall augmentation ratio was found to be existing. The presence of other flow losses not incorporated in the analytical prediction [16] is understood to be one of the reasons for the results deviating from the prediction. Furthermore the influence of completeness of mixing was found not to be as crucial as previously reported [16] resulting in significant thrust increase for reduced length of mixing chamber - although the computational result needs to be questioned to some extend as the velocity profile at the exit of the half length ejector is far from uniform as it was assumed in the prediction's calculations. A second conclusion impacting the present study is that the displacement after a real engine body has decreasing effect on the augmentation. The reason for this is that the entrained air not only creates a pressure drop over the ejector inlet that leads to the forward thrust but that the same low

pressure region also results in a counter acting force on the back surface of the engine. Furthermore the initial spread of the jet results in a different, more energetic pattern of momentum at the internal walls of the ejector - thus increased drag. Both effects are visible in the velocity magnitude of the respective case as given in figure 27. Any possible thrust gain by an ejector will thus be significantly reduced if the device is applied in practice due to these side effects.

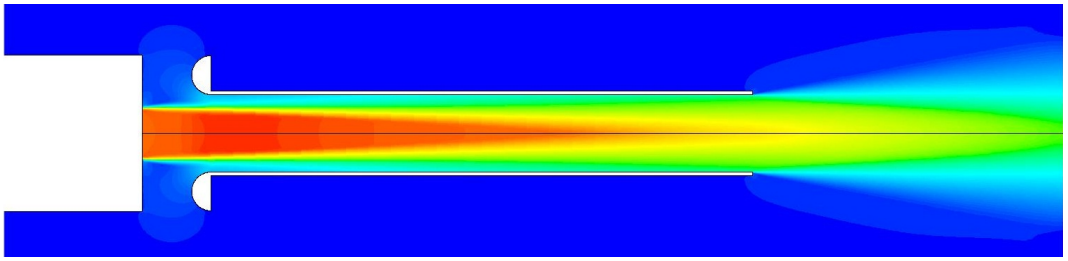

Figure 27: Velocity magnitude contour plot of displaced CFD study of thrust augmenting ejector with $\alpha = 1.277$ (scale: blue = $0\ \mathrm{m/s}$, red = $250\ \mathrm{m/s}$) [38]